"Mathematical Modeling for Drilling Optimization in Pre-salt Sections: a Focus on South Atlantic Ocean Operations"

ANDREAS NASCIMENTO

unesp UNIVERSIDADE ESTADUAL PAULISTA
"JÚLIO DE MESQUITA FILHO"
Campus de Guaratinguetá - SP

ANDREAS NASCIMENTO

MATHEMATICAL MODELING FOR DRILLING OPTIMIZATION IN PRE-SALT SECTIONS: A FOCUS ON SOUTH ATLANTIC OCEAN OPERATIONS

Guaratinguetá-SP

2016

ANDREAS NASCIMENTO

MATHEMATICAL MODELING FOR DRILLING OPTIMIZATION IN PRE-SALT SECTIONS: A FOCUS ON SOUTH ATLANTIC OCEAN OPERATIONS

Thesis presented to the *Faculdade de Engenharia - Campus de Guaratinguetá* (FEG), from the *Universidade Estadual Paulista* (UNESP), as part of the fulfillment to award the degree of Doctor of Engineering (Dr.-Eng.) in Mechanical Engineering with focus in Projects.

Supervisor: Prof. Dr. Mauro Hugo Mathias (Brazil/ UNESP)
Co-supervisor: Prof. Dr.mont. Gerhard Thonhauser (Leoben-Austria/ MUL)

Guaratinguetá-SP
2016

Nascimento, Andreas
N244m Mathematical Modeling for Drilling Optimization in Pre-salt Sections: a Focus on South Atlantic Ocean Operations / Andreas Nascimento - Guaratinguetá, 2016
135 f : il.
Bibliografia: f. 104-109

Tese (doutorado) - Universidade Estadual Paulista, Faculdade de Engenharia de Guaratinguetá, 2016.
Orientador: Prof. Dr. Mauro Hugo Mathias
Coorientador: Gerhard Thonhauser

1. Pré-sal 2. Otimização matemática 3. Perfuração estratigráfica I. Título

CDU 622.323(043)

unesp **UNIVERSIDADE ESTADUAL PAULISTA**
"JÚLIO DE MESQUITA FILHO"
Campus de Guaratinguetá - SP

ANDREAS NASCIMENTO

ESTA TESE FOI JULGADA ADEQUADA PARA A OBTENÇÃO DO TÍTULO DE
"DOUTOR EM ENGENHARIA MECÂNICA"

PROGRAMA: ENGENHARIA MECÂNICA
ÁREA: PROJETOS

APROVADA EM SUA FORMA FINAL PELO PROGRAMA DE PÓS-GRADUAÇÃO

Prof. Dr. Edson Cocchieri Botelho
Coordenador

BANCA EXAMINADORA:

Prof. Dr. MAURO HUGO MATHIAS
Orientador / UNESP-FEG

Prof. Dr. EDSON COCCHIERI BOTELHO
UNESP-FEG

Prof. Dr. JOÃO ANDRADE DE CARVALHO JUNIOR
UNESP-FEG

Prof. Dr. JOSÉ LUIZ GONÇALVES
UNIFEI

Prof. Dr. BEHZAD ELAHIFAR
Enhanced Drilling - Noruega

February 2016

CURRICULUM INFORMATION

ANDREAS NASCIMENTO

BIRTH	-	Date: 30th January 1984;
	-	Place: Seeheim-Jugenheim, Hessen, Germany.
FILIATION	-	Mother: Marta Leite da Silva Nascimento;
	-	Father: Nazem Nascimento.
2000/ 2004	-	Degree: Technician (Tech.) in Industrial Computer Science;
	-	Technical School: Industrial Technical College of Guaratinguetá - *Colégio Técnico Industrial de Guaratinguetá* (CTIG) - Brazil.
2003/ 2008	-	Degree: Engineer (Eng.) in Computer Engineering with focus in Petroleum Engineering and Energy;
	-	University: Federal University of Itajubá - *Universidade Federal de Itajubá* (UNIFEI) - Brazil;
	-	Scholarship: Brazilian National Agency of Petroleum, Natural Gas and Biofuels - *Agência Nacional do Petróleo, Gás Natural e Biocombustíveis* (ANP).
2008/ 2010	-	Degree: Master of Science (M.Sc.) in Energy Engineering with focus in Exploration of Rational Usage of Natural Resources and Energy;
	-	University: Federal University of Itajubá - *Universidade Federal de Itajubá* (UNIFEI) - Brazil;
	-	Scholarship: Brazilian Institute of Petroleum, Gas and Biofuels - *Instituto Brasileiro de Petróleo, Gás e Biocombustíveis* (IBP).
2008/ 2012	-	Degree: Diploma Engineer (Dipl.-Ing.) in International Study in Petroleum Engineering with focus in Drilling Engineering;
	-	University: Mining University of Leoben - *Montanuniversität Leoben* (MUL) - Austria.
2011/ 2014	-	Position: Drilling & Measurement General Field Engineer;
	-	Employer: Schlumberger Oil Field Services - Angola.
2014/ 2016	-	Position: University Assistant/ Visiting Researcher;
	-	Hoster: São Paulo State University - *Universidade Estadual Paulista* (UNESP) - Brazil and Mining University of Leoben - *Montanuniversität Leoben* (MUL) - Austria;
	-	Scholarship: ANP and CAPES BEX 0506/ 15-0.

DEDICATORY

I dedicate this work to my family and to all that have instilled in me trust, confidence and a drive to succeed.

ACKNOWLEDGMENT

To my parents and brother, for the education, love, advice and teachings. To my relatives for their understanding and assistance.

To the Vice-director of the Faculty of Engineering - Campus of Guaratinguetá - *Faculdade de Engenharia - Campus de Guaratinguetá* (FEG) of the São Paulo State University - *Universidade Estadual Paulista* (UNESP) - Brazil and Supervisor, Prof. Dr. Mauro Hugo Mathias, for the guidance, teaching, assistance and patience in developing this research. To Prof. Dr. Luiz Roberto Carrocci, Prof. Dr. Mauro Pedro Peres, Prof. Dr. João Andrade de Carvalho Júnior and to Prof. Dr. José Elias Tomazini for the support, suggestions and discussions.

To Prof. Dr.mont. Gerhard Thonhauser from the Department Petroleum Engineering (DPE) of the Mining University of Leoben - *Montanuniversität Leoben* (MUL) - Austria, who accepted me for a Doctoral exchange, Co-supervising and enabling a greater depth of research.

To the Brazilian National Agency of Petroleum, Natural Gas and Biofuels - *Agência Nacional do Petróleo, Gás Natural e Biocombustíveis* (ANP) by means of the PRH48-ANP program, and to the Brazilian Federal Agency for the Support and Evaluation of Graduate Education - *Coordenação de Aperfeiçoamento de Pessoal de Nível Superior* (CAPES) by means of the BEX 0506/ 15-0 scholarship, for the financing support provided. To the Mechanic Department - *Departamento de Mecânica* (DME) from UNESP and to the Post-graduation technical session of FEG (in special Regina, Maria Cristina, Renata and Rodrigo), for all the assistance provided.

To the Chair of Drilling and Completion Engineering (CDC) from MUL and to the Data Base of Exploration and Production (BDEP) from ANP, for providing information and support in terms of data acquisition and analysis.

To my friends and colleagues from Itajubá - Brazil, including the Student House *Casa Amarela*, (in special Zé, Colombia, Pedrão, Kebrado, Vitim, Santiago, Rafa and Tosco), friends from Guaratinguetá (in special Galão and Cabecinhas), and also friends from Leoben - Austria (Mathias, Danyari, Cohen, Lupo, Asad, Lamik, Daniel, Abbas, Rahman, Roman, Ramsauer, Gunnar and Rita).

And to all colleagues, employees, servants, technicians and professors from MUL and UNESP who supported me throughout this important step of my life.

EPIGRAPH

"The knowledge we learn from the masters and books. The wisdom one learns with life and with the humble..."

Cora Coralina.

"…and strong we have to be in this arduous necessity of proving knowledge…"

NASCIMENTO, A. **Mathematical Modeling for Drilling Optimization in Pre-salt Sections: a Focus on South Atlantic Ocean Operations**. 2016. 135 p. Doctorate Thesis (Doctorate in Mechanical Engineering). Faculdade de Engenharia - Campus de Guaratinguetá, Universidade Estadual Paulista, Guaratinguetá-SP, 2016.

ABSTRACT

Pre-salt basins and their exploration have become more and more frequently mentioned over the years, not just for their potential reserves, but also for the implicit challenges in terms of operations to face in order to make these fields commercially viable. Several research efforts aimed at addressing these related barriers, in which drilling optimization and efficiency are presented as a considerably complex area. The problematic is concentrated in the low drillability and in the high cost involved when drilling the pre-salt carbonates.

The outcome of this research is based in studies performed on top of eight pre-salt wells, addressing drilling operational time savings referenced by benchmarks and drilling mechanics parameters choosiness. The studies were based on simulations performed with penetration rate (ROP) modeling combined with specific energy (SE). The Bourgoyne Jr. and Young Jr. (1974) ROP model was used given the high errors presented for the other models, higher than 40% and, in terms of SE, the formulations from Teale (1965) and Pessier et al. (1992) were used. All these classic literature are still present in the industry and the software Oracle Crystal Ball was used as a supportive tool for the simulations.

This research yielded four important results: 1) the polycrystalline diamond compact (PDC) is the most suitable drill-bit choice for pre-salt, presenting the lowest teeth-cutters wear rate, 0.28 [%/ m]; 2) the possible spare in operational time encountered for the pre-salt operations represent a saving of approximately 13,747,550.00 [USD] for the analyzed pre-salt wells; 3) the final mathematical model developed, after the adjustments for pre-salt, foresee an improvement dropping the relative error from 36.52% to 23.12% in terms of comparing the calculated and modeled ROP with the field measured ROP; 4) the final model yielded from the combination of the ROP and SE formulations is the most adequate to be used in the industry, since it was possible to foresee an improvement by dropping the relative error even more, from 23.12% to 21.2%.

KEYWORDS: Drilling. Optimization. ROP. Efficiency. Energy. Pre-salt.

NASCIMENTO, A. **Modelamento Matemático para Otimização de Perfuração em Seções de Pré-Sal: um Foco em Operações no Oceano Atlântico Sul.** 2016. 135 f. Tese de Doutorado (Doutorado em Engenharia Mecânica). Faculdade de Engenharia - Campus de Guaratinguetá, Universidade Estadual Paulista, Guaratinguetá-SP, 2016.

RESUMO

As bacias do pré-sal e sua exploração se tornaram cada vez mais mencionadas ao longo dos anos, não apenas por seu potencial de reservatório, mas também devido aos grandes desafios implícitos em termos de operações a serem enfrentados para tornar estes campos comercialmente viáveis. Várias pesquisas vêm sendo desenvolvidas visando contornar estas barreiras, das quais a otimização e eficiência de perfuração se apresentam como uma área consideravelmente complexa. A problemática se concentra nas baixas taxas de penetração e no alto custo envolvido ao se perfurar as seções dos carbonatos do pré-sal.

Os resultados da pesquisa apresentados nesta tese baseiam-se em análises com oito poços do pré-sal, abordando economia de tempo operacional com base em análises referenciadas em *benchmarks* e escolhas de parâmetros mecânicos de perfuração. Os estudos foram baseados em simulações realizadas com modelagem de taxa de penetração (ROP) combinadas com energia específica (SE). Utilizou-se o modelo de ROP de Bourgoyne Jr.e Young Jr. (1974) face aos altos erros apresentados pelos outros modelos, superiores a 40% e, em termos de SE, utilizou-se o equacionamento de Teale (1965) e Pessier et al. (1992). Todas estas literaturas classicas ainda estão presentes na indústria e o *software* Oracle Crystal Ball foi utilizado como uma ferramenta de apoio para as simulações.

Os resultados deste trabalho mostraram quatro conclusões importantes: 1) a broca de perfuração do tipo *polycrystalline diamond compact* (PDC) é a mais adequada para o pré-sal, apresentando uma taxa de desgaste de dentes-cortadores de 0.28 [%/ m]; 2) a possível diminuição de tempo de operação encontrada após análises de performance de operação pode resultar em uma economia de aproximadamente 13,747,550.00 [USD] para os poços do pré-sal analisados; 3) o modelo matemático final desenvolvido, após os ajustes para o pré-sal, pode garantir uma melhoria do erro relativo de 36.52% para 23.12% em termos de comparação entre o ROP calculado e o ROP medido durante a atividade no campo; 4) o modelo final como resultado da junção do equacionamento de ROP e SE é o mais adequado para a indústria, uma vez que foi possível garantir uma diminuição ainda maior do erro relative, de 23.12% para 21.2%.

PALAVRAS-CHAVE: Perfuração. Otimização. ROP. Eficiência. Energia. Pré-sal.

LIST OF FIGURES

LIST OF TABLES

LIST OF ABBREVIATIONS AND INITIALS

ANP	Brazilian National Agency of Petroleum, Natural Gas and Biofuels (*Agência Nacional do Petróleo, Gás Natural e Biocombustível*);
BHA	Bottom-hole-assembly;
BHP	Bottom-hole pressure;
BMK	Benchmark;
BYM	Bourgoyne Jr. and Young Jr. model;
CAPES	Brazilian Federal Agency for the Support and Evaluation of Graduate Education (*Coordenação de Aperfeiçoamento de Pessoal de Nível Superior*);
CDC	Chair of Drilling and Completion Engineering;
Connec.	Connection;
CTIG	Technical Industrial College of Guaratinguetá (*Colégio Técnico Industrial de Guaratinguetá*);
D	Deviated;
DME	Mechanic Department (*Departamento de Mecânica*);
DD	Directional drilling;
Diamond impreg.	Diamond impregnated;
DOC	Depth-of-cut;
DR	Drilling rate;
Drill. prog.	Drilling program;
ECD	Equivalent circulating density;
EMW	Equivalent mud weight;
EOR	Enhanced oil recovery;
ESD	Equivalent static density;
FDP	Fast drill program;
FEG	Faculty of Engineering - Campus of Guaratinguetá (*Faculdade de Engenharia - Campus de Guaratinguetá*);
FLOW	Flow-rate;
FIT	Formation integrity test;
FP	Fracturing pressure;
GR	Gamma-ray;
HSE	Health-safety-environment;
HT	High temperature;

IBP	Brazilian Institute of Petroleum, Gas and Biofuels (*Instituto Brasileiro de Petróleo, Gás e Biocombustíveis*);
ILT	Invisible lost time;
IT	Information technology;
LOT	Leak-off test;
LWD	Logging-while-drilling;
MMbbd	Millions of blue barrel per day;
MSE	Mechanical specific energy;
MUL	Mining University of Leoben (*Montanuniversität Leoben*);
MWD	Measuring-while-drilling;
M/U	Making-up;
n/a	Not available;
NPT	Non-productive time;
OIM	Offshore installation manager;
OD	Outer diameter;
OP	Overburden pressure;
Op. c.	Operational counts;
PDM	Positive displacement motors;
PDC	Polycrystalline diamond compact;
POOH	Pull-out-of-the-hole;
PP	Pore pressure;
PU	Pick-up weight;
RAB	Rotary free weight;
RIH	Running-in-hole;
ROP	Rate of penetration;
rpm	Rotation per minute;
RSS	Rotary steerable systems;
S.	Sampling;
SE	Specific energy;
SHT	Shallow-hole-testing;
SO	Slack-off weight;
SPP_off	Stand pipe pressure off bottom;
SPP_on	Stand pipe pressure on bottom;
TBRT	Tool/ drill-bit below rotary table;
TCI	Tungsten-carbide-insert;

Temp.	Temperature;
TH	Tripping-in/ out-of-hole;
TOR_on	Torque on bottom;
TOR_off	Torque off bottom;
UCS	Ultimate compressive strength;
USD	United States dollar;
UNESP	São Paulo State University (*Universidade Estadual Paulista*);
UNIFEI	Federal University of Itajubá (*Universidade Federal de Itajubá*);
USS	Ultimate shear strength;
V	Vertical;
W2W	Weight-to-weight;
WOB	Weight-on-bit.

LIST OF SYMBOLS

$Time_{rotating}$	Total rotating/ drilling time [h];
$Time_{connection}$	Total time spent in connections [h];
$Time_{tripping}$	Total time spent in drill-string tripping [h];
$Cost_{foot}$	Final cost per drilled meter [USD/ m];
$Cost_{bit}$	Drill-bit cost [USD];
$Cost_{rig}$	Drill-rig operational cost per hours [USD/ h];
MD_{final}	Final depth taken into account [m];
$MD_{initial}$	Initial depth taken into account [m];
TVD	True vertical depth [ft];
ROP_{calc}	Rate of penetration [ft/ h];
RPM_{sf}	Rotary speed [rev/ min] [rpm];
WOB_{Sf}	Translational axial force acting in the drill bit [lbf];
OD_{bit}	Outer drill-bit diameter [in];
K	Constant dependent drill-bit dullness, formation and drilling conditions [1];
WOB_{Sf_t}	Translational axial force threshold necessary to initiate rock fracture [lbf];
a_1	Formation strength and drilling fluid properties coefficient [1];
a_2	Normal compaction trend coefficient [1];
a_3	Under-compaction and pore pressure coefficient [1];
a_4	Differential pressure coefficient [1];
a_5	Constant dependent on drilling conditions and WOB behavior [1];
a_6	Constant dependent on drilling conditions and rotary speed behavior [1];
a_7	Teeth-cutters wear coefficient [1];
a_8	Hydraulic coefficient [1];
h	Fractional tooth height that has been worn away [1];
S	Rock drillability or crushing strength [psi];
u_{ap}	Apparent drilling fluid viscosity [cP];
OD_{nozzle}	Drill-bit nozzle diameter [in];
EPP	Formation pore pressure [ppg];
ECD	Equivalent circulating density [ppg];
EMW	Equivalent mud weight [ppg];
ROP_{calc}	Calculated ROP using ROP models [ft/ h];
ROP_{field}	ROP retrieved from field data - observed one [ft/ h];

x_{1-8}	Related temporary parameters;
$R_{squared}$	Regression index correlation [1];
r	Residual error [1];
F_j	Jet impact force used to characterize level of bit hydraulics [lbf];
$F_{j_{adjusted}}$	Jet impact force adjusted by the reduction factor [lbf];
γ_f	Fluid specific gravidity [1];
K_a, K_b, K_c	Drill-bit constants present in the Warren (1987) model [1];
V	Average velocity of jet nozzle [ft/ s];
A_v	Ratio of nozzle jet velocity to return back-flow velocity [1];
k	Junk slot area in percentage of total drill-bit diameter [1];
$V_{back-flow}$	Total return back-flow velocity [ft/ s];
Q_{total}	Nozzle flow-rate [gal/ min] [gpm];
Q_i	Total nozzles flow-rate [ft^3/ s];
Q_f	Total return back-flow flow-rate [ft^3/ s];
$n_{nozzles}$	Number of active bit nozzles [1];
A_{nozzle}	Nozzle cross-section area [in^2];
τ_{total}	Total work performed by the forces acting in the drill bit [in-lbf];
$\tau_{rotational}$	Work performed by rotational force acting in the drill bit [in-lbf];
$\tau_{translational}$	Work performed by translational axial force acting in the drill bit [in-lbf];
F_t	Translational axial force acting in the drill-bit [lbf];
F_r	Rotational force acting in the drill-bit [lbf];
$T_{torque_{sf}}$	Drill-bit torque [in-lbf];
dt	Infinitesimal time range [min];
$d\theta$	Infinitesimal rotary angle [°];
dv	Infinitesimal drill-bit velocity equivalent to the ROP [in/ min];
ds	Infinitesimal drill-bit displacement [in];
N	Total revolution taken into account [1];
$SE_{axial-rotary}$	Drill-bit SE in terms of energy per volume of rock [lbf/ in^2];
A_b	Drill-bit cross section area [in^2];
dV_{dt}	Infinitesimal volume of rock drilled per minute [in^3/ min];
$\frac{N}{d_t}$	Total revolution per time equivalent to the rotary speed [rev/ min];
$SE_{axial-rotary_{field}}$	Drill-bit MSE in terms of energy per volume of rock [lbf/ in^2];
μ	Drill-bit sliding friction factor [1];

$MSE_{adjusted}$	Adjusted MSE to represent down-hole energy [lbf/ in^2];
MSE	Raw MSE in terms of surface energy per volume of rock [lbf/ in^2];
EFF_M	MSE efficiency in terms of percentage transmitted to the drill-bit [1].

TABLE OF CONTENT

1 INTRODUCTION

Pre-salt basins and their exploration have become more and more frequently mentioned over the years, not just for their potential reserves, but also for the implicit challenges in terms of general operations (downstream and upstream) addressed to make these fields commercially viable. Several research efforts aimed at addressing these related barriers, but the known challenges of drilling optimization and efficiency resulted from considerably low drillability throughout the pre-salt carbonates is still present. The pre-salt market trend has been frequently explored over the years in Brazil and in Angola and, considering these countries' potential in terms of oil and natural gas, these reserves have a considerable importance in each country's economy and energy outlook. Moreover, since one of the barriers still faced is the high operational cost and the downside of drilling related events, by boosting directly or indirectly the drilling activities, the possibility of having these fields coming through economically is enhanced. Thus, studies are still under performance in several related research areas in order to model a way to allow reliable forecast and drilling parameters choosiness for efficiency assurance while performing drilling operations.

In this sense, this thesis is based in the analysis of the pre-salt carbonates operations focusing in operations that was carried in the South Atlantic Ocean. Considering the low oil prices and the also Petrobras scandal in Brazil, it is fair to say that any improvements that may result in cost savings can help even more in making these pre-salt fields to come through.

Thus, the originality of this research can be seen firstly by the pre-salt wells statistical study presented, from which an identity was drawn to refer numerically to these layers, allowing analysis to be developed. Subsequently, the research novelty was presented by a new methodology of ROP and SE models combination aiming drilling optimization. From the determination of operational time savings, of the best drill-bit to be used in these regions, of drill-bit teeth-cutters wear rate, up to in-situ geothermal and pressure profiles, a ROP model was modified accordingly, in order to reflect specifically the pre-salt wells. After the ROP model adjustments, it was combined with the SE formulations, yielding as a final result a path for determining the best set of drilling mechanics parameters, aiming to support the industry for an efficient and optimized operation, and so, potentializing costs reduction.

1.1 OBJECTIVES

The main objective of this research is to identify, characterize, and suggest changes in technical exploration of petroleum-related hydrocarbons carried in South Atlantic Ocean. Thus, develop and mold mathematically a drilling optimization model aiming performance improvement and drillability enhancement. This thesis was developed based on the following specific objectives:

- Address the geological similarity of the South Atlantic Ocean's coasts;
- Study techniques and new researches concerning drilling optimization with regard to rate of penetration (ROP) modeling, specific energy (SE) surveillance, and analysis of drilling mechanics parameters;
- Analyze these studies using combined pre-salt field operational information and data sets, proposing performance improvements;
- Suggest possible alternatives to improve drilling efficiency by combining ROP modeling and SE surveillance techniques/
- Dissert a final methodology linked to mathematical modeling, based in the studied literature and suggestions to enhance the drillability and performance in pre-salt sections.

1.2 THESIS STRUCTURE

The thesis is structured in five chapters organized as following:

In this first Chapter - Introduction - relevancies related to the thesis development are addressed, specifying the organization, layout, purpose, and a brief background of the subjects with their relative importance to the present topic under research.

Chapter two - Literature review - presents a literature review of important concepts used throughout the thesis that help understanding the relevancies of the pre-salt to the world energetic scenario, and the methodology used behind the optimization models to develop and gather the data used for the studies.

Chapter three - Pre-salt data analysis - presents the data set used throughout the thesis and its combination results for providing relevant information useful for progressing with the performance analysis and subsequent optimization appliance. It starts addressing the general pre-salt wells information and costs, detailing then the reservoir and hydraulic characterization.

Subsequently, the operational performance analysis is presented, followed by the drilling mechanics and drill-bit performance analysis, respectively.

Chapter four - Optimization modeling - presents the methodology for choosing the best optimization model, the step-by-step of modifications and set-up applied to the best chosen model with the information yielded from chapter three, and the final developed mathematical model for drilling optimization followed by its implementation with help of one pre-salt well data-set as a case study. It starts with the choosiness of the best ROP model to be used, detailed by fitting graphs, findings tables and regression relative error analysis. Subsequently, the step-by-step for modeling the SE based in ROP models is presented, followed by a case study where optimization simulations with the developed mathematical model are run, defining the optimized drilling mechanics parameters by means of best efficiency.

Chapter five presents a consolidation of results in form of conclusion and perspectives for future researches.

2 LITERATURE REVIEW

This chapter covers a literature review of the main topics addressed in the thesis, encompassing information about petroleum-related energy market, drilling operations and related optimization researches.

2.1 THE PRE-SALT

The needs to meet increasing energy demands has allowed room for fossil energy sources to play a very important role within the context of the world energy matrix. Though constantly pitted against renewable energy sources, forecasts have shown that the increase in energy demand has consequently pushed the demand for fossil fuels, even though constantly losing position as a primary energy source versus renewable sources. Figure 1 highlights specific countries and continents, projecting energy source usage in year 2050; oil and natural gas may have their representation decreased in approximately 36% against an increase in more than 200% for renewable energy sources when comparing the scenarios between the years of 2012 and 2050 in a global reference. Figure 2 provides a view of how petroleum will still be in demand in the following years, even if losing space as a primary source of energy (WWF, 2011; EIA, 2015).

Figure 1 - Energy matrix forecast between 2012 and 2050.

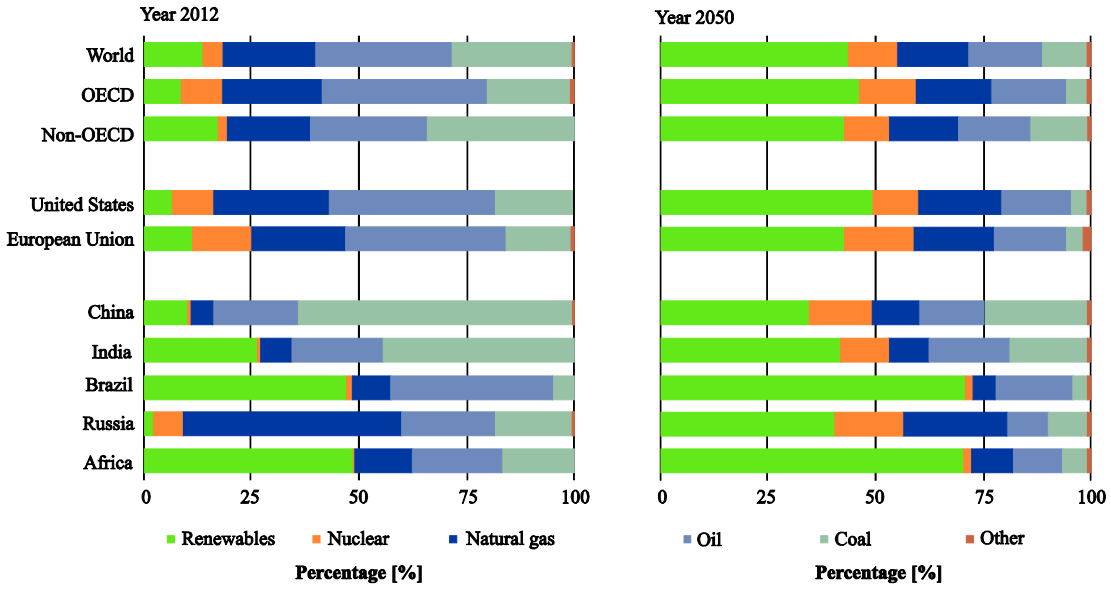

Source: (EIA, 2015).

Figure 2 - Energy demand forecast per energy source till 2050.

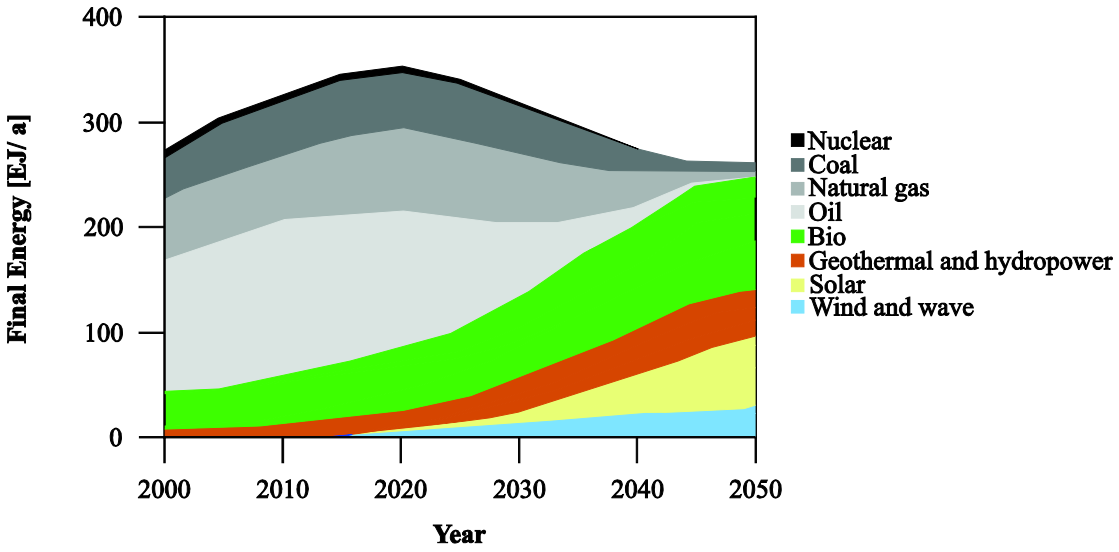

Source: (WWF, 2011).

Since petroleum still have a significant impact on the energetic matrix, it is necessary to guarantee that their production meets expected demand. The actual scenarios and forecasts (Figure 3) show that the industry could face a deficit of petroleum-related hydrocarbon production of about 83 [MMbbd] by 2030 (PETROBRAS, 2009).

Figure 3 - World petroleum-related production and demand forecast to 2030.

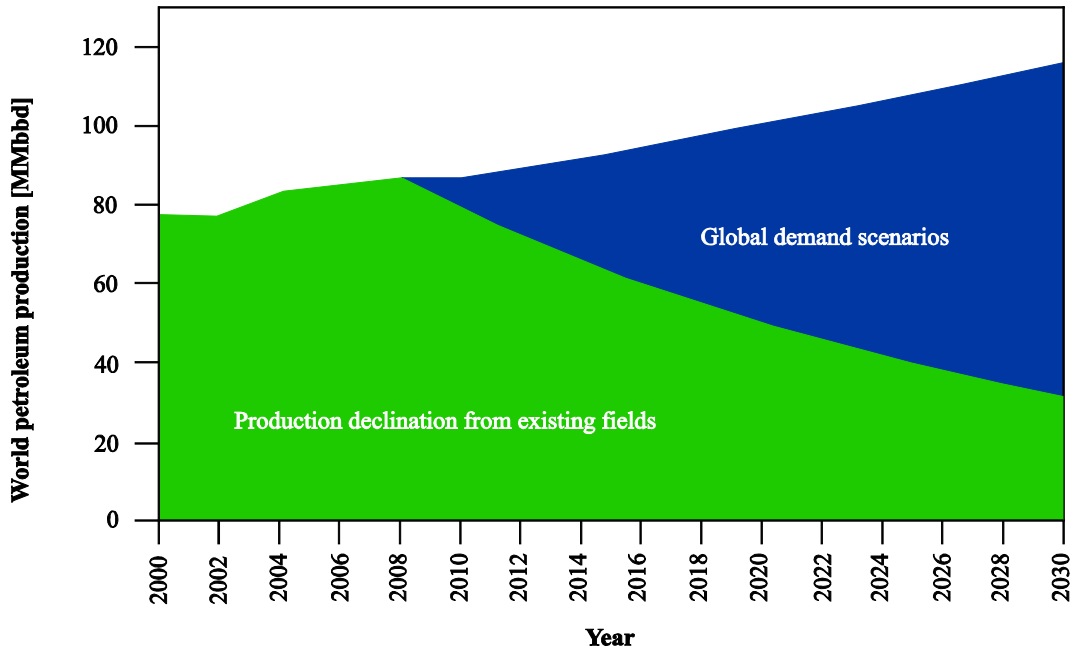

Source: (PETROBRAS, 2009).

Hence, to asses this issue and to be able to meet the world demand, the oil and natural gas industry has to focus on implementing new technologies and incorporating new exploitable reserves. New technologies and techniques include increasing the enhanced oil recovery (EOR) of existing fields (known in the industry as the implementation of various techniques for increasing the amount of oil and natural gas that can be extracted from a reservoir), and reaching unconventional hydrocarbon reservoirs. It is in this scenario that the pre-salt reserves come to play a very important role. These fields are known to be located in remote regions considerable far from the coast, in ultra-deep water environments (known in the industry as water depths greater than 1,500 [m]), where geological and drilling challenges are common (thick salt layer and a very hard and abrasive carbonate rock reservoir). These are schematized in the Figure 4, where the evaporites layer drawn in white are basically a sedimentary rock saline deposit formed by crystallization and chemistry precipitation of salts dissolved in the sea aqueous medium (FRAGA et al., 2015; PINHEIRO et al., 2015). The hydrocarbon reserve discoveries off the Brazilian and Angolan coasts exhibit the potential to help fill this energy deficit based on the considerable supply potential these countries may have in terms of pre-salt reserves (PETROBRAS, 2009; GAFFNEY, 2014).

Figure 4 - Pre-salt layer break-down and details of its remoteness.

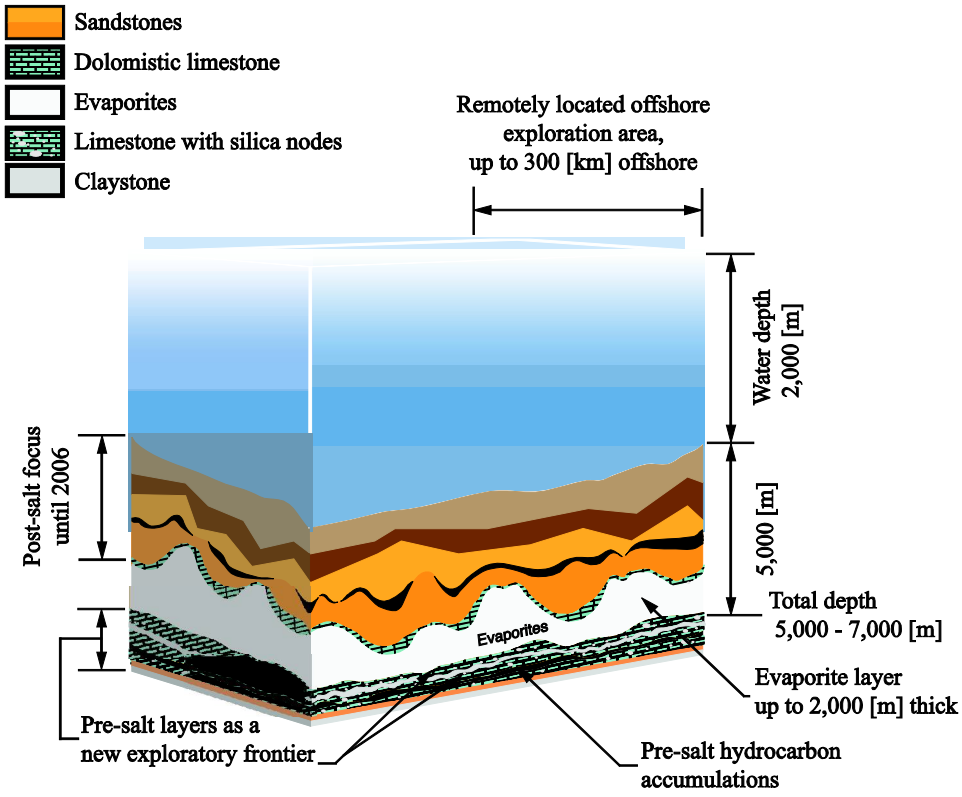

Source: (Adapted from: FRAGA et al., 2015; PINHEIRO et al., 2015).

2.1.1 South Atlantic Ocean coasts similarity

The pre-salt layers are geological formations that were laid down before the evaporites layer (also nicknamed as salt layers in the industry) accumulated above them during the Pangaea supercontinent separation which started around 200 million years ago. More evidenced between the Jurassic and the Cretaceous period (between 150 and 65 millions of years ago), the evaporite layers were formed along the South Atlantic Ocean sides of the now a days known as South American and African continents, as shown in Figure 5 (NASCIMENTO, 2010; KONING, 2015).

Figure 5 - Pre-salt formation details and similarity between Brazil and Angola.

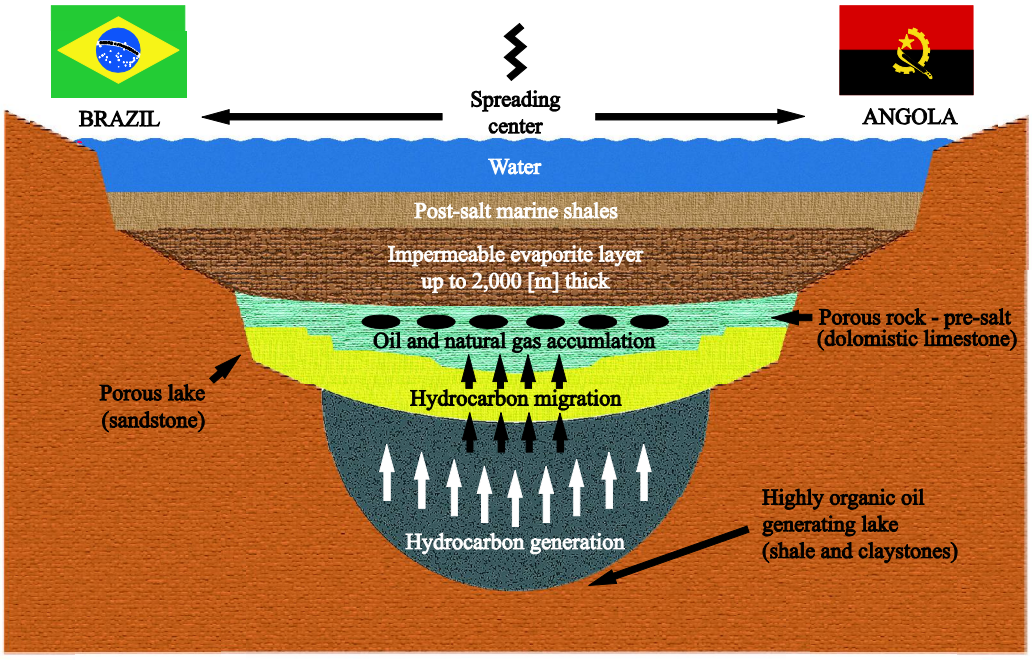

Source: (Adapted from: KONING, 2015).

During the separation of the Gondwanaland (known as the south supercontinent existent between the Jurassic and Cretaceous periods formed after the separation of the Pangea), some gulfs were originated between the continent parts, which, combined with the restricted water fluxes and the climate in the equatorial line, guaranteed favorable conditions for the deposits. And, due to the same origin continental emigration, geological similarity can be to date evidenced in the Brazilian and African coasts, with highlights for Angola, as shown in Figure 6 (NASCIMENTO, 2010; KONING, 2015; PINHEIRO et al., 2015).

Figure 6 - South America and Africa continents early period fitting and main basins.

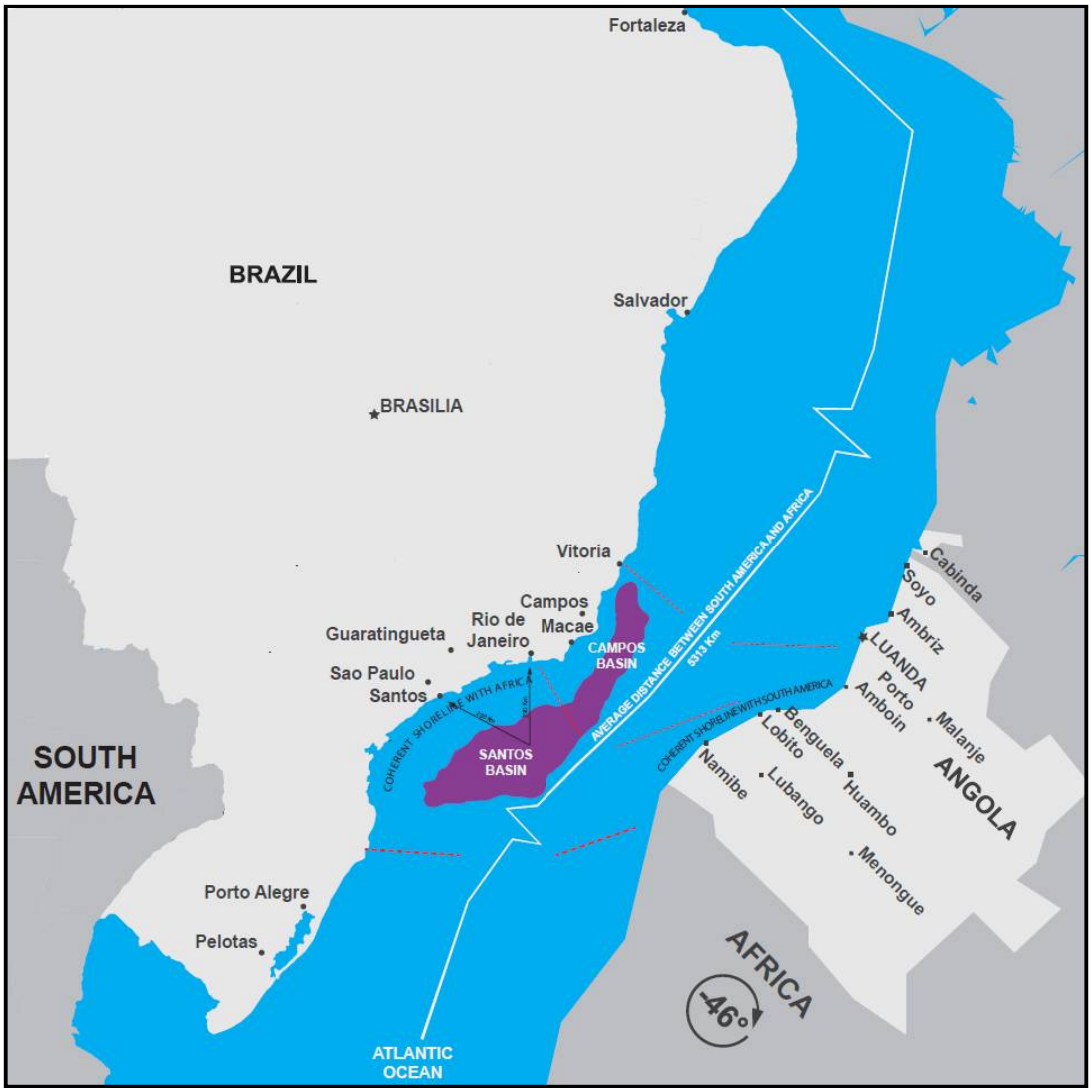

Source: (Adapted from: KONING, 2015).

Thus, the known pre-salt reservoirs and main barriers encountered on the side of one continent are commonly found on the other continent and vice-versa. Generally, the pre-salt explorations have taken place in remote locations in terms of depth and coastal distance. In order to reach these locations in some regions, the activities have to be performed up to 300 [km] from the coast and at a water depth of about 2,000 [m] (classified as ultra-deep water environment, being the depth of 1,500 [m] the boundary). The evaporite layers have shown to be, in some locations, up to 2,000 [m] thick and the pre-salt reservoir to be located up to 7,000 [m] deep, as schematized in Figure 4 (FRAGA et. al., 2015; PINHEIRO et al., 2015).

2.1.2 General geology and drilling information

Mostly of the oil and natural gas accumulations in these pre-salt reserves are trapped in a rock type classified as carbonate. Known as a class of sedimentary rock (formed when particles of materials are deposited from bodies of water in the earth's surface), their primary compound are carbonate minerals; typically encountered and spread within the pre-salt layers are primary the limestones ($CaCO_3$) and secondarily the dolomites, which is chemically represented as $CaMg(CO_3)_2$ (NASCIMENTO, 2010; NASCIMENTO, 2012). The pre-salt has been defined to be heterogeneous in some extensions due to the non-uniform porosity, permeability, and the presence of silica nodes in it (MUNIZ, 2013), resulting in a very hard and abrasive formation (PEIXOTO et al., 2010).

The hardness can be understood, effectively, as the driver for slowing down the ROP, and the abrasiveness, together with the silicate presence (Figure 7), responsible for drill-bit teeth-cutters breakage, dullness, and wear progression, affecting the ROP considerably. A cumulative issue in it is that, at a certain point, not much improvement in terms of excavate hole can be noticed while drilling; activity drops to a low efficiency level, and, in some cases, leads to under-gaged holes (known in the industry as when the hole size diameter is less than the nominal diameter of the drill-bit). These under-gaged end-run edges need to be reamed before allowing the new drill-bit to go straight, to guarantee section gauge and smoothness. But, among several factors that affect drilling efficiency, the downside drilling events can be broken-down into different responsible agents, in which each one has its own degree of influence on the process. Also important to notice are the difficulties faced in spotting the base of the evaporites for optimum casing set linked to some early section drilling fluid (known in the industry as drilling mud) loss events when entering the pre-salt carbonates (PEIXOTO et al., 2010; MUNIZ, 2013; HBAIEB et al., 2013).

Figure 7 - Pre-salt carbonate samples with highlights of silica nodes in dashed red marks.

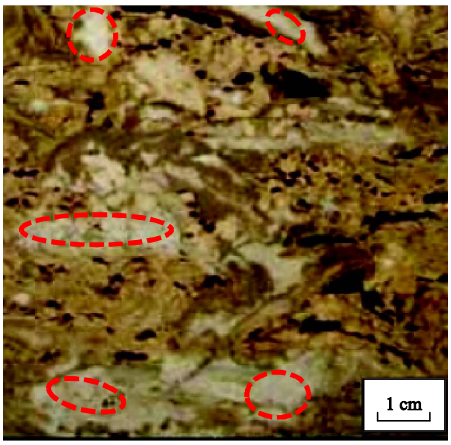

Source: (FORMIGLI, 2008; PEIXOTO et al., 2010).

All these information are important to help understanding the reasons behind the low performance frequently evidenced when drilling pre-salt. Recent researches have shown that the average drilling performance through these formations, historically, has stayed between 0.5 and 6 [m/ h] (HBAIEB et al., 2013).

2.2 DRILLING OPERATIONS

This sub-chapter contextualizes information about drilling operations and how the drilling activities are conducted, linking those to pre-salt operations.

2.2.1 Activities and equipments

The drilling operations conducted in specific regions are accomplished by using different machineries with specific functionalities, combined into several systems working together in a so called drilling platform or drilling-rig (Figure 8). The whole system can be divided into four main parts: the hoisting, the rotary, the power and the circulating system. The power system (composed of generators, engines, and frequency converters) provides power to the drilling

system machineries; the power is transmitted from gas or diesel generators. The hoisting system (composed of drill-lines, draw-works, crown-block, travelling-block, derrick, and the top-drive set) is the key to raising and lowering the whole drill-string, casing, and other subsurface equipment, from and into the wellbore, respectively; this system is responsible for controlling the weight being transmitted to the drill-bit while drilling, also known as weight-on-bit (WOB). The rotary system (composed of top-drive set, drill-string, and other main compounds) is responsible to transmit a clock-wise rotation to the drill-string, and consequently, to the drill-bit, providing the so-called rotary speed and necessary torque to advance the excavating process. The circulating system (composed of mud pumps, flow-lines, drill-string, drill-bit nozzles, mud tanks, mixing equipment, and contaminant removal equipment) has the function of filtrating and cleaning the drilling mud, via a recycling process, for its continuous reusing throughout the drilling operations. The circulating system transmits the drilling mud through the drill-string to the drill-bit. After passing through the drill-bit, the drilling mud transports the cuttings to the surface via the annulus (known as the space formed with the borehole wall outside of the drill pipe) and into the return line. The drilling mud is cleaned of cuttings and then recirculated to provide down-hole equipment cool down and hydraulic energy. Figure 8 summarizes the main components, providing in a schematic view of how drilling-rigs are configured in general, highlighting also the main system's components just detailed.

When a well is being drilled, which happens in stages, it is regularly cased after each drilled section, avoiding possible contaminations and collapse of the just-opened hole (meaning avoid getting closed back up). This casing operation is carried out by lowering a steel pipe (casing) into the hole under its own weight, or pushed down by the hoisting system (mainly in deviated paths) with subsequent cementing outside the casing. The casing has an outer diameter (OD) smaller than the nominal drill-bit diameter (or hole diameter), which basically allows enough room for lowering the casing and pumping cementing slug around it. The cementing fills up the gap in the annulus between the casing OD and the formation, providing support for the axial and vertical loads while maintaining an integral isolation.

Figure 8 - Basic schematic with major components of a drilling-rig.

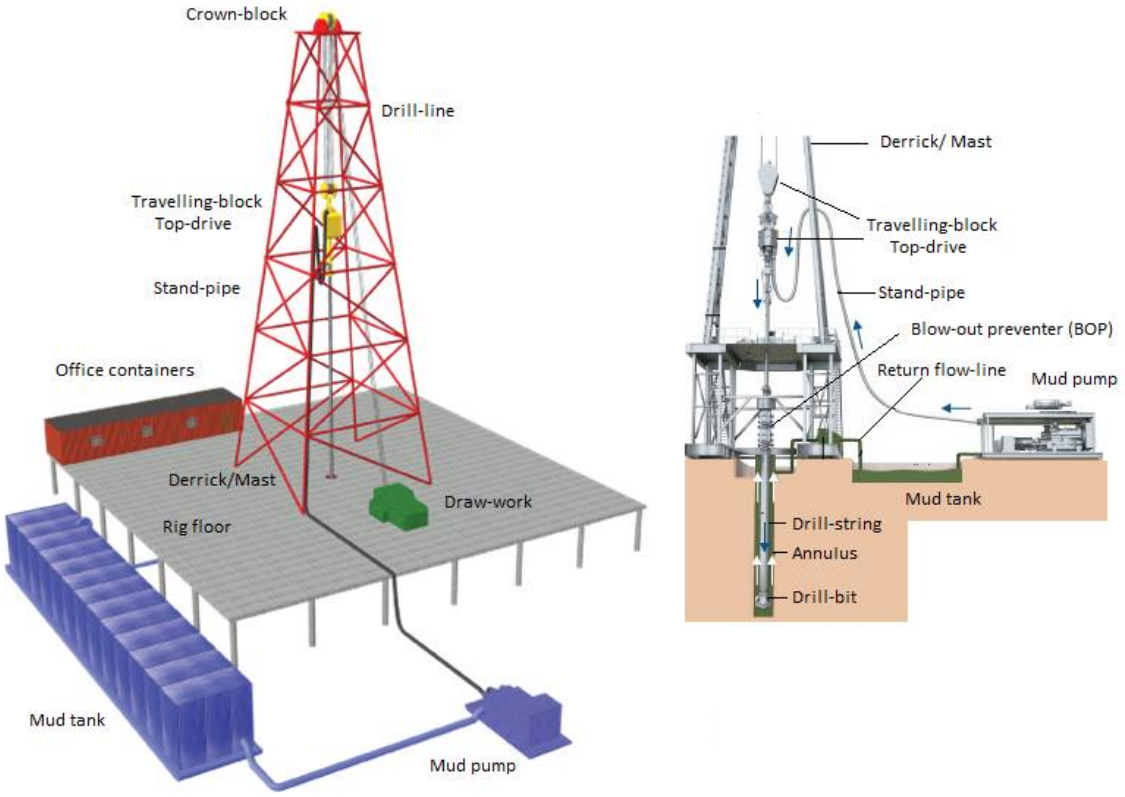

Source: (Adapted from BONITRON, 2015).

Schematically, a well is normally divided into sections, in which the sections' diameter decreases as the well gets deeper. These sections are determined mainly based on an off-set well's formation geology and pressure correlation, specific strategic needs, and unforeseen events arise during the operation. Each section can be accomplished by one or more drill-bit runs; main factors driving the number of drill-bit runs include drill-bit wear, bottom-hole-assembly (BHA) tool failure and operation limitations such as overpressure zones, drill-string sticking, drilling mud losses, and strategic changes governed by the decision maker.

In order to recover underground oil and natural gas, the process requires not just hardware, but also manpower as important drivers. The field personnel (or rig crew), are the main determinant to ensure that operations are carried out safely, correctly, and in a timely manner. The three main groups are the operators crew (block owner), the drilling contractor crew (rig owner and contracted by the operators), and the service companies crew (specialized services and contracted by the operators). The service companies offer services like logging-while-drilling (LWD), measuring-while-drilling (MWD), directional drilling (DD), cementing, fluid

engineering, drilling optimization, among others. The drilling contractor offers the drilling-rig services, sub-contractors and staff, and stays mainly on top of the main drilling-rig operations with the offshore installation manager (OIM), ship captain (when in a floating drilling-rig), engineer supervisors, drilling personnel, information technology (IT) personnel, logistic personnel, health-safety-environment (HSE) personnel and catering services. The operators also have important staff in the drilling-rig to ensure that all is carried out as planned, while supervising activities and operations being performed by drilling contractors and service companies; the main representatives are the company man, the geologist, the fluid engineer, and the drilling engineer.

Details are crucial in all drilling activity such as: how will the drilling mud be designed, how will drill-string BHA be configured, which drill-bit will be used, how will the measuring tools be programmed to provide the desired lithology data, how will the directional drilling tools be adjusted in order to provide desired direction and target, among others. Communication plays a very important role since, for example, service companies have to deliver according to the wishes of the operators, but counting on the drilling contractors in mutual and friendly cooperation. The configuration, designs, and decision have, for the most part, already been defined in the drilling program from the main office or headquarters; however, the operations are always susceptible to adjustments in which responses are expected to be made and implemented as quickly as possible and directly from the field.

The measuring tools allows a close eye on the drill-bit, making possible to known exactly where it is, as well as measure and retrieve information from the down-hole regarding the environment and formation such as: pressure, temperature, formation porosity, formation permeability, drilling mechanics data, among others. This information from the drilling mechanics data is used (consider also surface sensing information) by the field personnel to analyze how the operation is progressing, and evaluate trends; the information are used to determine and adjust drilling mechanics parameters such as flow-rate, rotary speed, WOB and torque, always looking for ways to enhance drilling efficiency by optimizing the rate of penetration (ROP) and improving the operational efficiency.

Still, the details of the configuration and the selection of components to be used in the BHA are extremely important to guarantee optimized operation. For instance, the right placement of the stabilizers and the drill-collars ensure the drill-string will work with less probability of stick-

slip, vibration and buckling. No less important, the drill-bit is the ultimate responsible for making the hole and effectively drill formation.

Different types of drill-bits are offered on the market. The main groups are the drag bits (mostly in use for pre-salt operations) and the roller-cutter bits (HBAIEB et al., 2013). Drag bits consist of fixed cutters blades that are integrated with the body of the drill-bit, rotating as a unit with the drill-string; roller-cutter bits consist of two or more cones (normally three) which have the cutting elements attached to it and rotate about the axis of the cones as the drill-bit rotates at the bottom of the hole. Figure 9 and Figure 10 show these two types of drill-bits, respectively.

Figure 9 - Diamond impregnated (a) and polycrystalline diamond compact (PDC) drill-bit (b).

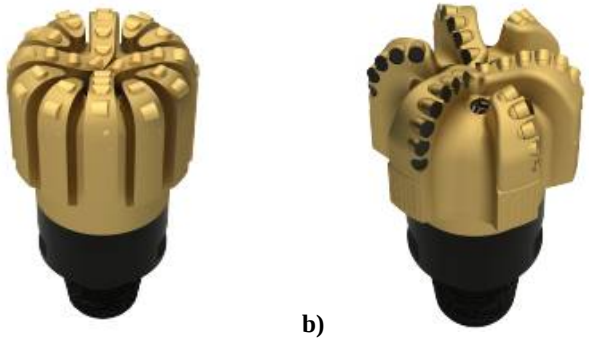

a) **b)**

Source: (BAKER, 2013).

Figure 10 - Milled tooth (a) and tungsten-carbide-insert (TCI) drill-bit (b).

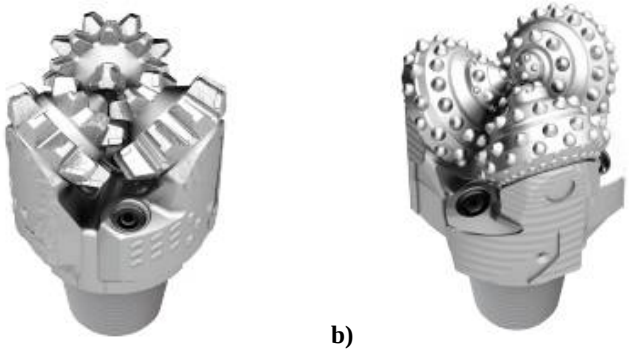

a) **b)**

Source: (BAKER, 2013).

As a new tendency, hybrid bits are being manufactured, showing some improvements in pre-salt drilling (Figure 11). These information are important since statistical analysis will take place in later chapters in a sense of showing which drill-bit allows better performance when drilling pre-salt formation.

Figure 11 - General example of a hybrid drill-bit with PDC and TCI features together.

Source: (BAKER, 2013).

2.2.2 Drilling activity and costs

Going beyond the technical description of the activities, there is an important parameter that has to be taken into account when planning and executing a well; the costs involved in each stage, since the drilling operations of a specific well do not guarantee the existence of petroleum accumulations. If the drilling activity concerns a producing well or an exploratory well in an area with the exploratory activity already advanced, the chances of a dry-hole (known in the industry when no accumulation is found) are considerably diminished. From exploratory wells, studies are performed in order to guarantee a delimitation in which the reserves can be defined as proven. Moreover, a dry-hole may not signify an unsuccessful operation since the geological and drilling information acquired, together with the knowledge gained, are used in subsequent operations as a basis for improving subsequent activities (THOMAS et al., 2002; COOPER et al., 2009).

In general, is common and has been fairly considered in the petroleum industry that the probability of encountering oil and natural gas accumulations from a wild-cat (the first drilled exploratory well from a field) is, in general, 30%. For the development of an entire field, 10 to 20% of the costs can be related to the exploration phase while 50% concerns the development phase. The remaining is related to the production phase and logistics portion necessary to the operations, representing approximately 30 to 40% of the costs. And, from this exploratory phase, 40 to 80% of the costs are specifically related to the drilling itself, representing 4 to 16% of a field's total cost (THOMAS et al., 2002; LEFFLER et al., 2003; THONHAUSER, 2009).

From a historical break-down of drilling activities, it is considered reasonable to say that just 25 to 35% of the operational time is related to effective drilling activity, while the other portion is related to drill-rig movement (approximately 35%), tripping operation, supportive activities and non-productive time (NPT), from which 40% are related to wellbore instability and pressure balance issues, while up to 10% is related to equipment failure (LEFFLER et al., 2003; THONHAUSER, 2009).

In this context, the pre-salt wells do not show to be different. Since the activities are developed in unconventional regions and since the industry considers itself to be still within the learning phase of analog operations, the relative cost of these wells have been considerably high. Table 1 summarizes historical information from the literature in terms of drill-bit performance (considerably low) and costs (considerably high) experienced when drilling pre-salt carbonates in the past years (HBAIEB et al., 2013). This low range necessitates performance improvement and seeks potential value from new surveillance methods and application tools (DUPRIEST et al., 2005).

Table 1 - Historical drill-bit performance and cost for pre-salt sections from the literature.

Drill-bit type	Footage [m/ run]	Average ROP [m/ h]	Cost [USD/ m]
TCI	100 - 250	1 - 3	> 30,000
Diamond impregnated	400 - 500	1 - 3	15,000 - 20,000
PDC	20 - 250	0.5 - 6	long run < 10,000 short run > 50,000

Source: (HBAIEB et al., 2013).

Drilling costs tend to increase considerably with depth; it is a good practice study past data and information from previous wells to address time and costs of future drilling operations in similar regions. When good and reliable data are available for a specific region or location, it is possible to predict the relationship between costs and depth, which are reduced as more successful wells are drilled in nearby regions. This improvement is related to the learning process, mathematically described by learning curves, and, with a minimal amount of gathered data, a curve can be drawn for, e.g., drilling engineers to predict well costs for subsequent wells. A method used in the industry to estimate the cost involved per length drilled (Table 1) considers a calculation accounting for the drill-bit cost per specific run ($Cost_{bit}$), the average drill-rig cost per day ($Cost_{rig}$), the initial and final depth in order to account to the length drilled for the proper cost calculation (MD_{final} and $MD_{initial}$), and the operational time in order to allow estimating the time length and so, the final costs over the time-frame of activity ($Time_{rotating}$,

$Time_{connection}$, $Time_{tripping}$) as per equation (1). Thus, any activity that relates to a more effective drilling operation with less NPT and delivers each well safely and economically is important in all of these contexts, including then also pre-salt wells, the focus of the thesis (RABIA et al., 1985; MITCHELL, 2011).

$$Cost_{foot} = \frac{Cost_{bit} + Cost_{rig} \cdot (Time_{rotating} + Time_{connection} + Time_{tripping})}{MD_{final} - MD_{initial}} \quad (1)$$

2.3 ROP MODELING CONCEPT

Rate of penetration (ROP) modeling has been in use in the industry for decades as a tool to quantitatively reduce drilling costs by drill-bit selection and by determining the optimal combination of mechanical and hydraulic operating parameters to be used while drilling to guarantee optimum activity. This sub-chapter summarizes the main research developments in terms of ROP modeling from 1960 to date, highlighting the main classical literature which are still used as reference in the industry.

2.3.1 ROP Model evolution

Cunningham (1960) addressed a way to represent rate of penetration (ROP) as a function of two specific drilling parameters, running several tests under atmospheric and overbalanced conditions with roller-cutter drill-bits in shale and granite formation types. The drilling conditions applied on the tests were 15 to 50 [psi] hydrostatic pressure, 50 to 400 [rpm] rotary speed, 20 to 700 [lbf] weight-on-bit (WOB), weighted brine and tap water as drilling fluid, with 1.25 and 7.875 [in] OD drill-bits. The final ROP equation relation (ROP_{calc}) was empirically derived from the graphs behaviors, presented in Figure 12, by means of its relation to the WOB over the outer drill-bit diameter $\left(\frac{WOB_{sf}}{OD_{bit}}\right)$ used (directly proportional to it) and to the rotary speed (RPM_{sf}) applied (squarely and directly proportional to it). The constant a_6 was defined, for this specific case and experiments, to be around 0.45 and always less than or equal to 1 (MAURER, 1962). The constant K, regardless of not having been defined, was stated to be a general constant dependent on drill-bit dullness not varying much, since the formations used in the test are considered to be non-abrasive. Equation (2) details the mathematical relationship of these detailed findings (CUNNINGHAM, 1960).

$$ROP_{calc} = K.\frac{WOB_{sf}}{OD_{bit}}.(RPM_{sf})^{a_6} \quad (2)$$

Figure 12 - ROP versus rotary speed in atmospheric (a) and overbalance (b) conditions.

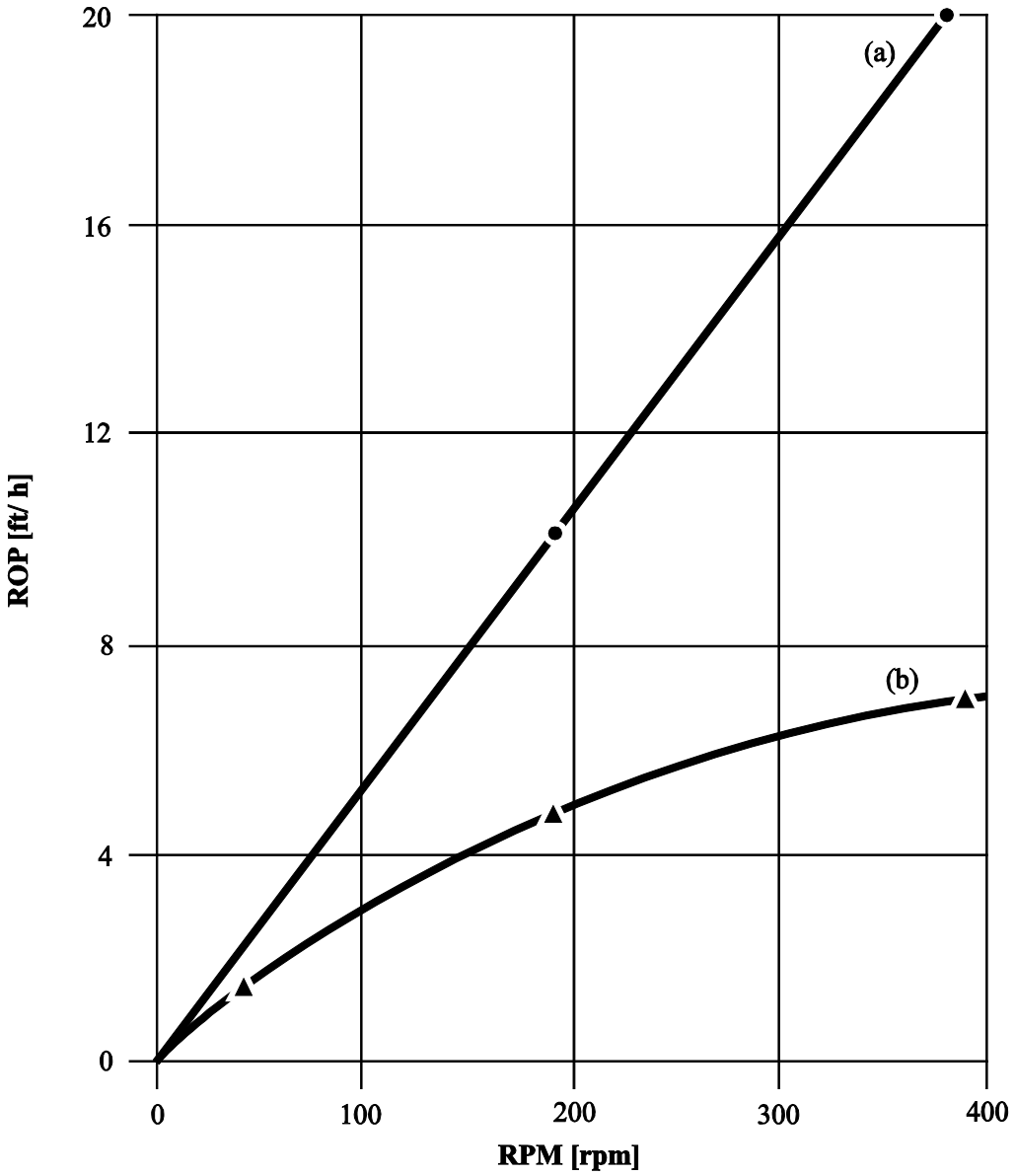

Source: (CUNNINGHAM, 1960).

A few years after, Maurer (1962) derived two equations for ROP as a function of rotary speed, WOB, drill-bit OD and rock drillability strength, accounting also for down-hole cleaning conditions. Was concluded that the rock drillability strength (S) of the rock, has a relation, not simply to the ultimate compressive strengths (UCS) of the rock, but with the ultimate shear strength (USS) as well, being quadratically and inversely proportional to the ROP $\left(ROP \propto \frac{1}{S^2}\right)$.

Also addressed was the fact that the torque may not vary with respect to rotary speed, but just quadratically with respect to the WOB ($Torque \propto WOB^2$) (Figure 13). The tests were performed in sandstone, shale, and concrete formation types with a 4.75 [in] roller-cutter drill-bit with the following parameters: 50 to 200 [rpm] rotary speed, 0 to 30 [klbf] WOB (MAURER, 1962). The mathematical equations developed are representative for perfect drilling conditions (equation (3)) and for imperfect cleaning conditions (equation (4)). They were developed based on the experiment graph outputs presented by Figure 14 and previous researches (Figure 12), defining for this specific experiments a_6 to be positive and a_5 to be less than or equal to 0.5. In Figure 14, the experiment drawn with filled small black spheres represents good borehole cleaning due to higher flow-rate and the one with triangle, borehole with a bad borehole cleaning due to less flow-rate, what directly affects the maximum achievable ROP for given WOBs. The parameter WOB_{sf_t} represents the minimum thrust load necessary to start a rock breakage for initiating the rock fracture.

$$ROP_{calc} = K.\frac{RPM_{Sf}.\left(WOB_{sf} - WOB_{sf_t}\right)^2}{OD_{bit}^2.S^2} \tag{3}$$

$$ROP_{cal} = K.\frac{RPM_{sf}^{a_6}.\left(WOB_{sf} - WOB_{Sf_t}\right)^{a_5}}{OD_{bit}} \tag{4}$$

Figure 13 - Torque relation versus WOB.

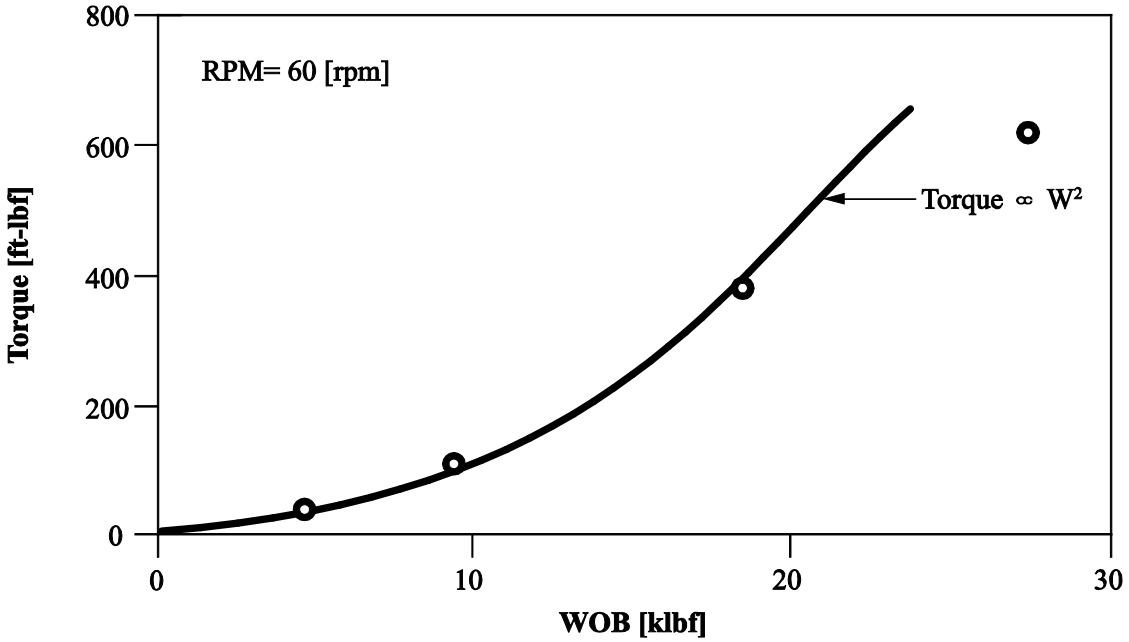

Source: (MAURER, 1962).

Figure 14 - ROP versus WOB (a) and drill-bit OD (b).

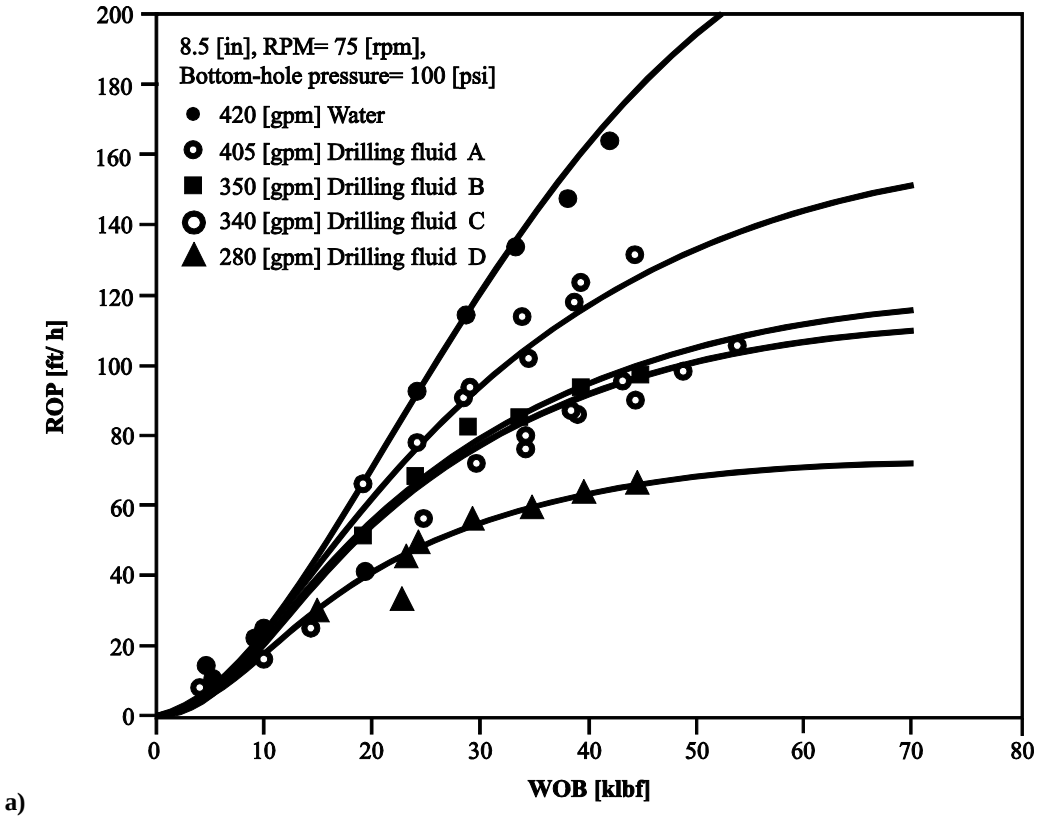

a)

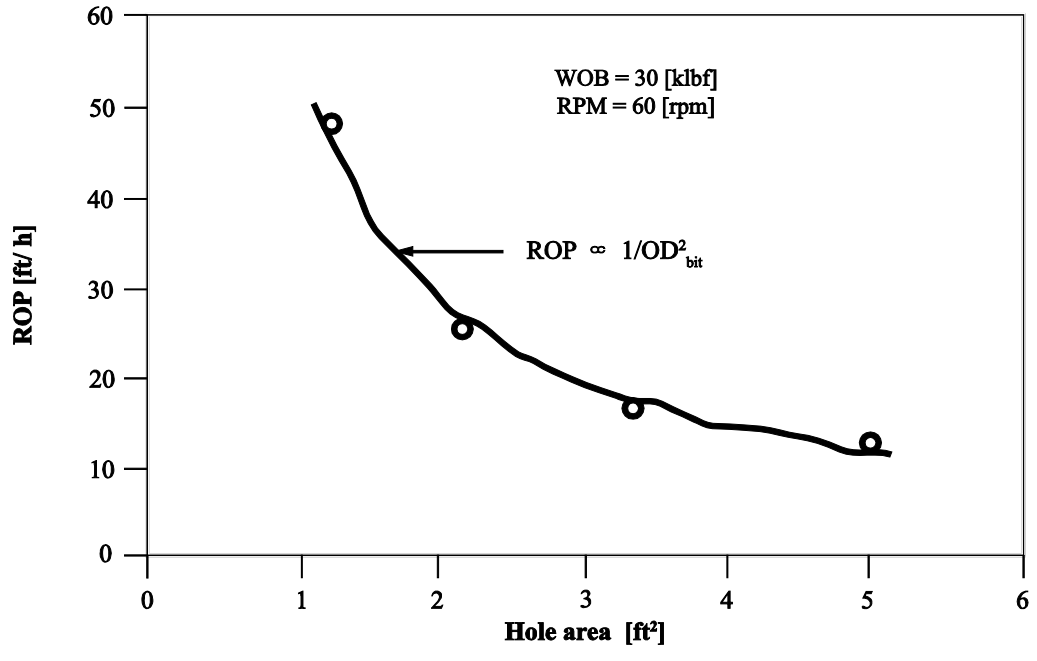

b)

Source: (MAURER, 1962; WARREN, 1987).

But was with some more development and more detailed researches over approximately ten years that a more complete and complex model was put together. Bourgoyne Jr. and Young Jr.

(1974) combined as much parameters as possible that may had influence in the ROP, modeling it into one equation with eight sub-functions addressing many different behaviors, in which the determination of the best fit, with the weighting coefficients (from a_1 to a_8), would be the key in fitting the mathematical model into specific field data. Table 2 summarizes coefficient ranges, related drilling conditions, and equations (equations (5), (6), (7), (8), (9), (10), (11) and (12)), in which TVD represents the true vertical depth, EPP the equivalent *in-situ* pore pressure, ECD the *in-situ* equivalent circulating density, EMW the equivalent mud weight in use, Q the flow-rate of the drilling fluid, u_{ap} the apparent drilling fluid viscosity, OD_{nozzle} the drill-bit nozzle diameter, OD_{bit} the outer drill-bit diameter, WOB_{sf} the surface applied WOB, RPM_{Sf} the surface applied rotary speed, ROP_{calc} the calculated ROP using the model and the ROP_{field} the actual field read ROP while performing the operation. Important to note is that the equation takes into account variables in which when equalized to field data would not affect the original ROP since the sub-functions would be powered by zero and so, the modeled ROP would be multiplied by one. Equation (13), $R_{relative}$represents the residual error, which should be as low as possible, representing the best fit between the modeled calculated ROP (ROP_{calc}) and the field ROP (ROP_{field}). Equation (14), $R_{squared}$, represents the index correlation ($0 \leq R_{squared} \leq 1$) of a regression, having the best fit as it approaches to one (fitting of 100%). The drilling parameters were varied as follows: from 58 to 129 [rpm] rotary speed; 0.81 to 3.76 [klbf/ in] WOB over drill-bit OD; from 9.5 to 17.7 [ppg] equivalent circulating density (ECD); with milled tooth and Tungsten-carbide-insert (TCI) drill-bits varying in OD from 6.125 [in] to 17.5 [in], and all with different types of mud tested in different porous and permeable sandstone formations. The WOB over drill-bit OD threshold necessary to be overcome in order to effectively commence drilling a rock was established to be between 0.6 and 2 [klbf/ in], representing boundary values suitable for soft up to very hard formation (BOURGOYNE Jr. and YOUNG Jr., 1974).

Table 2 - Bourgoyne Jr. and Young Jr. (1974) coefficients and model details.

Sub-functions	Figure	Coefficient	Coefficient range	Affecting representation
n/a	n/a	a_1	2.71 - 3.78	Formation strength and drilling fluid design
Equation (6)	Figure 15-a Figure 15-b	a_2	0.00015 - 0.00028	Formation compaction
Equation (7)	Figure 15-b Figure 15-c	a_3	0.00018 - 0.0009	Formation compaction and pore pressure
Equation (8)	Figure 16-a	a_4	0.00004 - 0.000085	Differential pressure
Equation (9)	Figure 14-a and Figure 14-c	a_5	0.43 - 2	WOB and drill-bit OD
Equation (10)	Figure 14-b	a_6	0.21 - 0.9 (0.21 for hard formations) (0.9 for very soft formations)	rotary speed
Equation (11)	Figure 17	a_7	0.2 - 1.11 (0 for TCI drill-bits)	Fractional teeth-cutters wear (more drill-bit and not much formation dependent)
Equation (12)	Figure 16-b	a_8	0.16 - 0.61	Hydraulics and Reynolds number influence

Source: (BOURGOYNE Jr. and YOUNG Jr., 1974).

$$ROP_{calc} = e^{\left(a_1 + \sum_{j=2}^{8} a_j . x_j\right)} \tag{5}$$

$$x_2 = 10{,}000 - TVD \tag{6}$$

$$x_3 = TVD^{0.69} . (EPP - 9) \tag{7}$$

$$x_4 = TVD . (EPP - ECD) \tag{8}$$

$$x_5 = \ln\left[\frac{\frac{WOB_{Sf}}{OD_{bit}} - \left(\frac{WOB_{sf}}{OD_{bit}}\right)_t}{4 - \left(\frac{WOB_{sf}}{OD_{bit}}\right)_t}\right] \tag{9}$$

$$x_6 = \ln\left(\frac{RPM_{Sf}}{100}\right) \tag{10}$$

$$x_7 = -h \tag{11}$$

$$x_8 = \frac{EMW . Q}{350 . u_{ap} . OD_{nozzle}} \tag{12}$$

$$R_{relative} = \frac{\sum_{i=1}^{n} \overline{|ROP_{field_i} - ROP_{calc_i}|}}{\overline{ROP_{field}}} \tag{13}$$

$$R_{squared}{}^2 = 1 - \frac{\sum_{i=1}^{n} \left[\left(ROP_{field_i}\right) - \left(ROP_{calc_i}\right)\right]^2}{\sum_{i=1}^{n} \left[\left(ROP_{field_i}\right) - \left(\overline{ROP_{calc_i}}\right)\right]^2} \tag{14}$$

The following Figure 15, Figure 16 and Figure 17, represents outputs from experiments run which were also used to derive, empirically, the ROP model defined by Bourgoyne Jr. and Young Jr. (1974). Figure 15 shows that the deeper is drilled, the more compacted a specific geological layer is and the less pore pressure is present at a specific depth, the more negatively would the ROP be influenced. Figure 16, which relates mainly the hydraulics, shows that the less differential pressure is present in the bottom of the hole and the higher the Reynolds Number or the drill-bit jet impact force is, the higher would be the ROP achieved. Figure 17 shows the influence of drill-bit dullness in terms of drillability, where the more worn a drill-bit teeth-cutters are the less would be the maximum achievable ROP.

Figure 15 - ROP versus depth (a), compaction (b) and pore pressure (c).

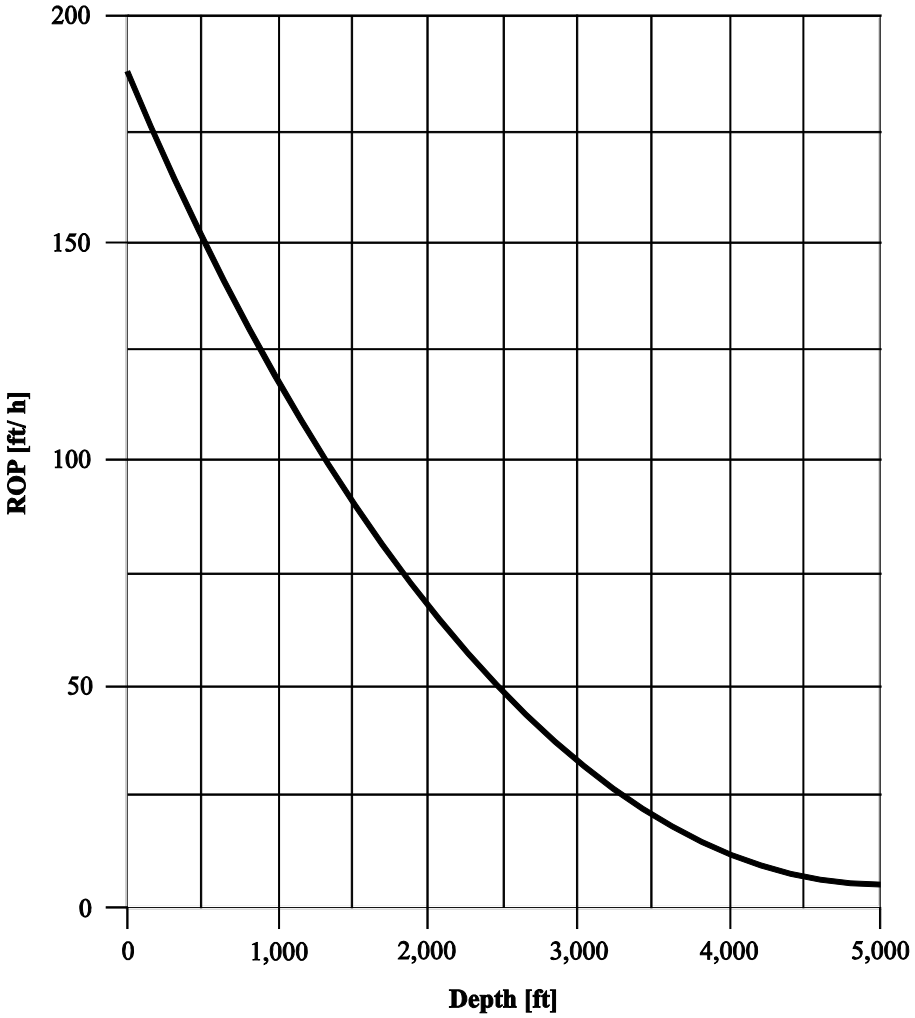

a)

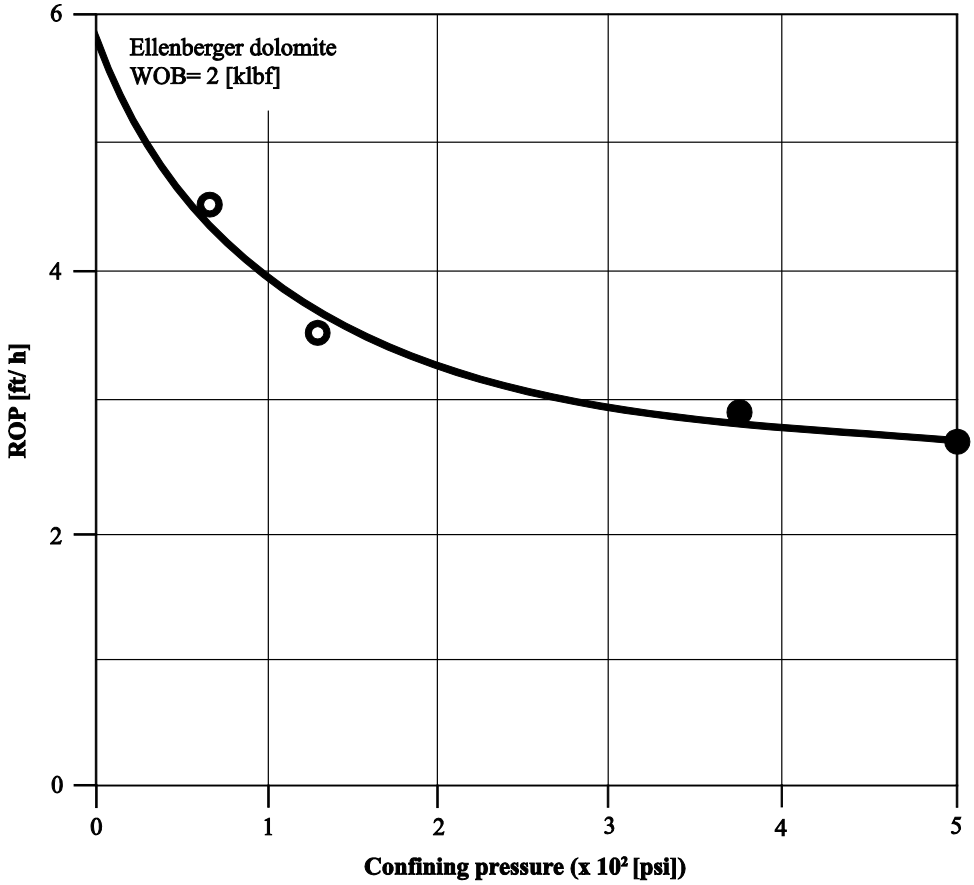

b)

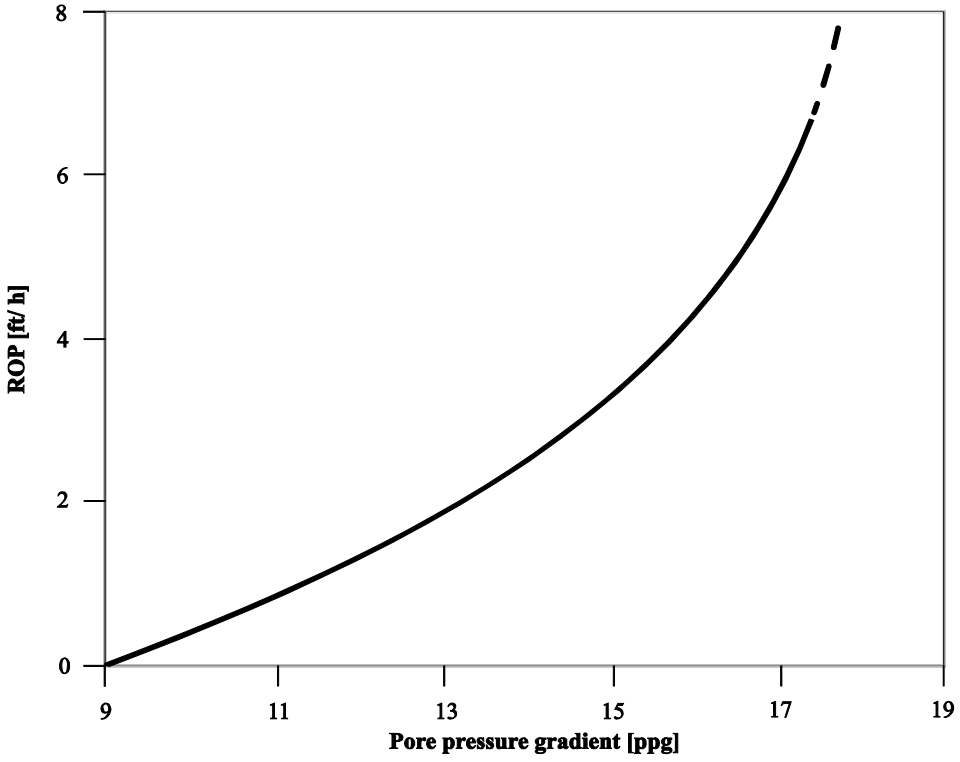

c)

Source: (MURRAY et al., 1955; COMBS, 1968).

Figure 16- ROP versus differential pressure (a) and Reynolds Number (b).

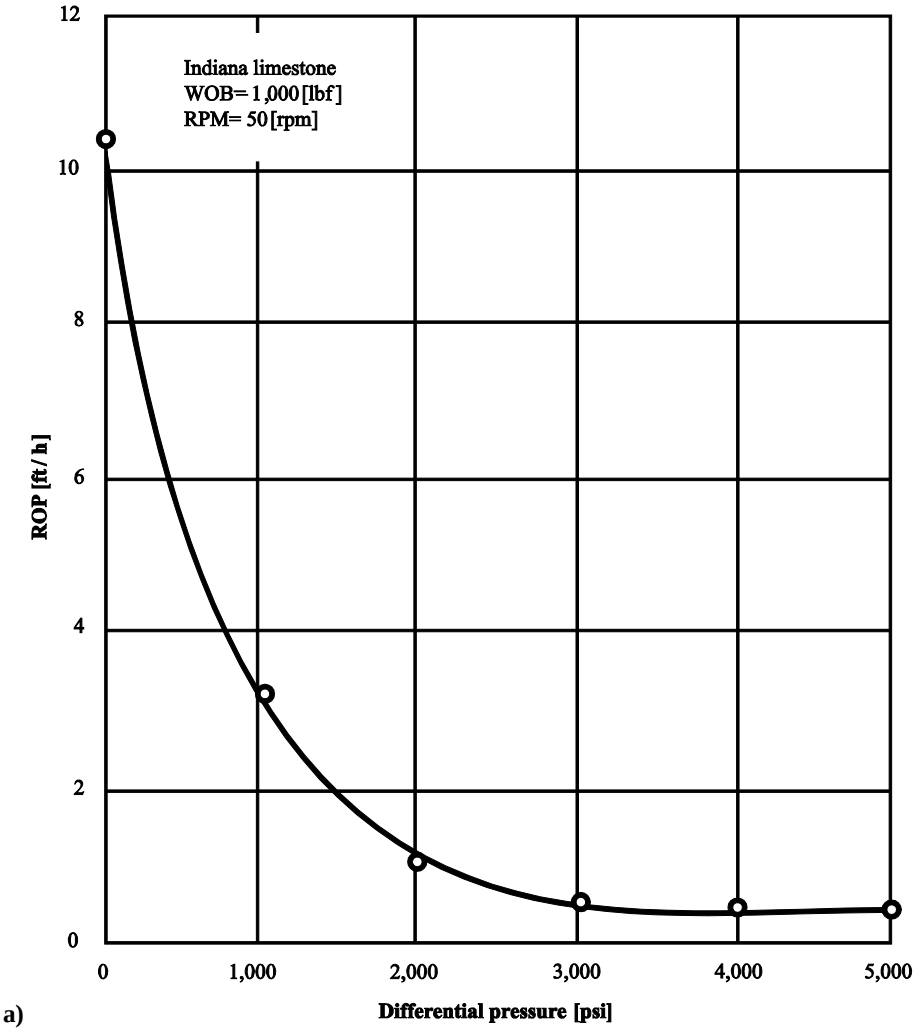

a)

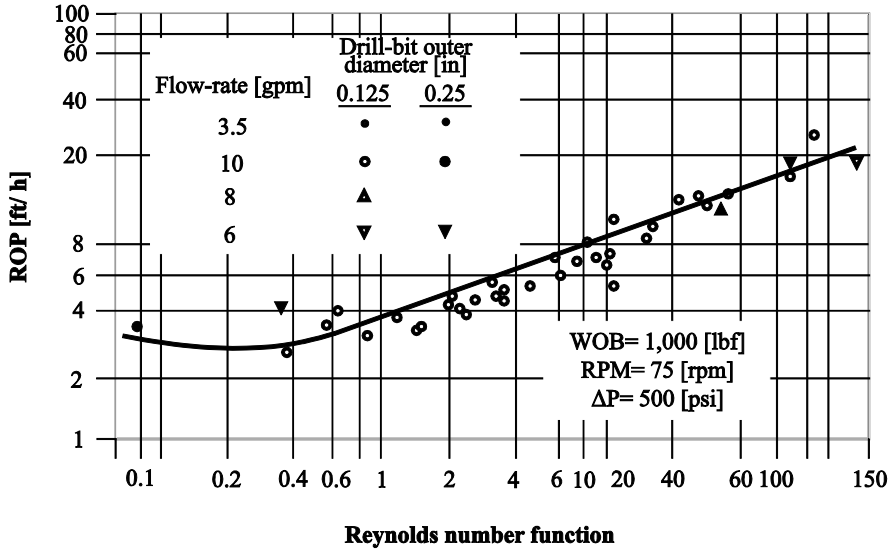

b)

Source: (CUNNINGHAM et al., 1959; ECKEL, 1968).

Figure 17 - ROP versus drill-bit teeth-cutters wear.

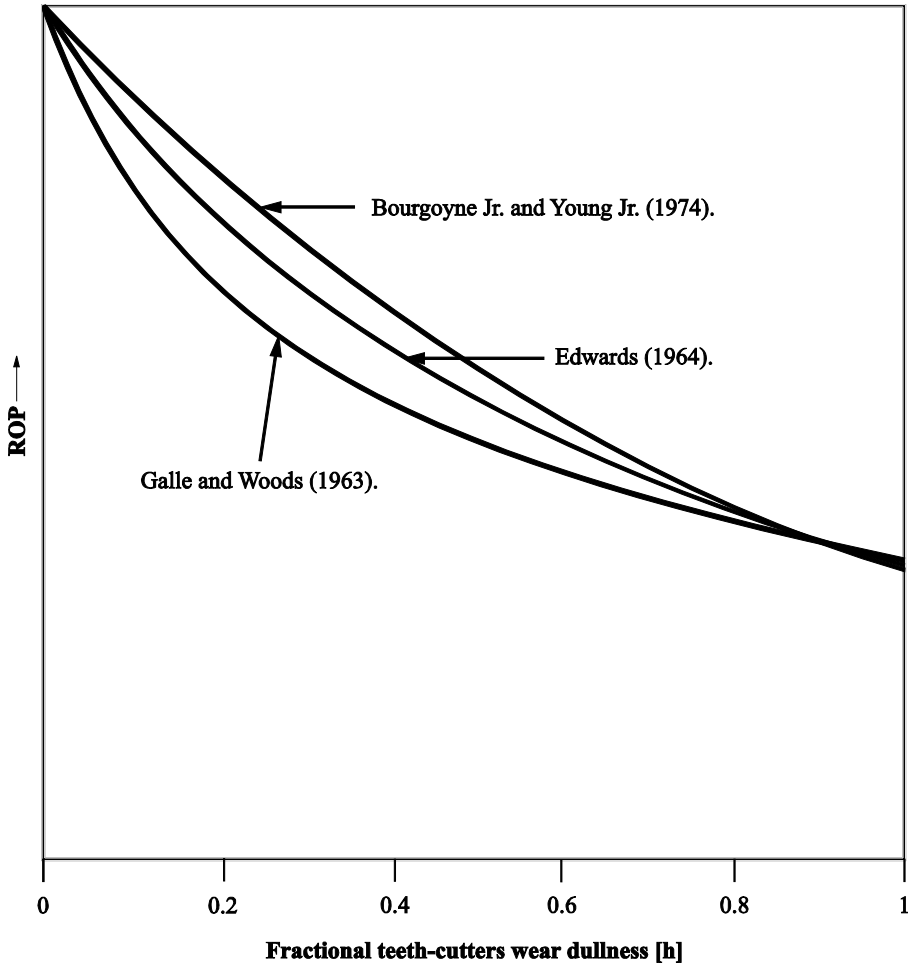

Source: (GALLE and WOODS, 1963; EDWARDS, 1964; BOURGOYNE Jr. and YOUNG Jr., 1974).

As a next step in the evolution of the ROP modeling development, the researchers started focusing themselves on fluid mechanics and the drilling fluid influence in ROP. In this sense, Warren et al. (1984) and Warren (1987) presented a modified mathematical model accounting for different drilling mechanics specifically for soft formations and roller-cutter drill-bits, accounting for the main drilling parameters, as well for the hydraulic jet impact force, conducting tests with 7.875 [in] and 12.25 [in] drill-bit sizes, with the following parameters: 48 to 194 [rpm] rotary speed, 4 to 40 [klbf] WOB, 287 to 460 [gpm] flow-rate, with drilling mud weight ranging from 9 to 13 [ppg], with shale, sandstone, and limestone as formation types. The studies were conducted verifying the effect of the hydraulic jet impact force and the real contribution it may have on rock cutting process. It was determined, through a lot of experiments, some interesting characteristics about the fluid velocity ejecting from the drill-bit nozzles. Separated in three different regions, the fluid flow from the nozzle in zone I (the free

jet zone) is characterized by a cone of moving fluid that expands along the x-axis (the cone angle can vary from 20 to 25 [º]), losing energy as the particles disperse (Figure 18). Zone 2 (the impingement zone) is where maximum pressure is applied against the formation, as defined next. Zone 3 is the radial portion of the fluids and the main driving is the cross flow. It was concluded that energy acting in the bottom of the hole would be higher with a greater number of smaller jets and also the higher the jet impact force (Figure 19), which may positively impact the penetration rate if correctly applied; basically, the greater the nozzle diameter, the lower the energy that would reach the stagnation point (MCLEAN, 1964; WARREN et. al., 1984). In addition, it was formulated an empirical estimation of the effect of jet dispersion in bottom-hole cleaning, so that the final jet impact pressure and force were reduced by a factor driven by the ratio of the nozzle jet velocity and the total back-flow velocity (the return flow upwards and responsible for carrying the cuttings out of the hole). Since the back-flow is dependent on the cross section area of the junk slot of the drill-bit (approximately 15% for roller-cutter drill-bits), the equations (15), (16), and (17) show the development in calculating this influencing factor (WARREN, 1987).

Figure 18 - Schematic of flow and the three definition zones.

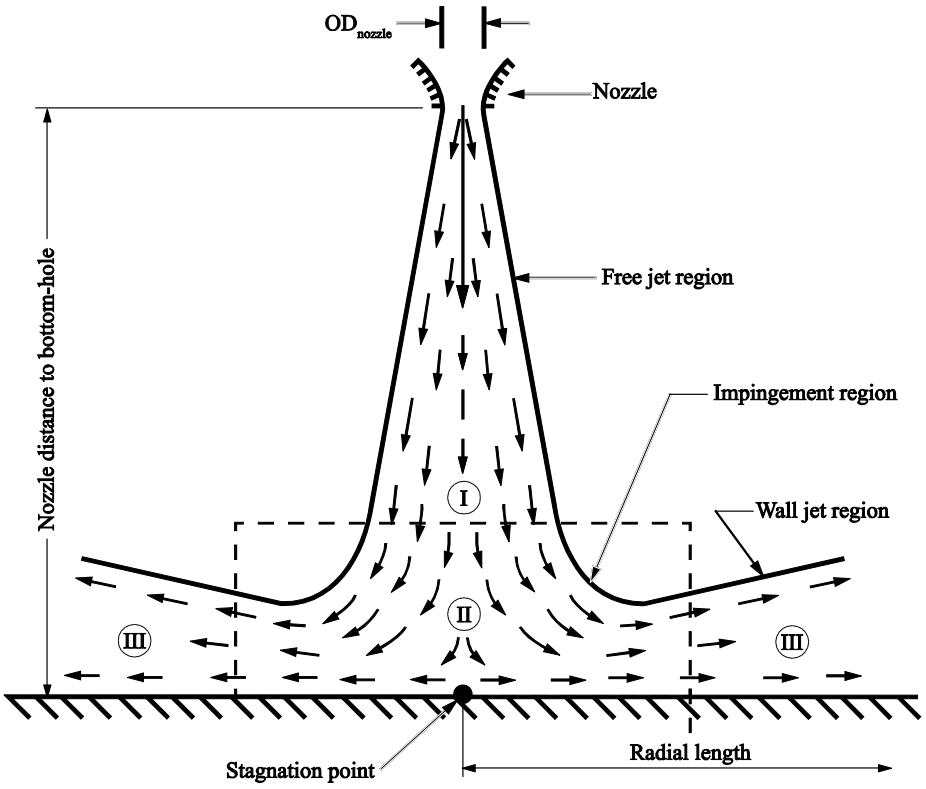

Source: (WARREN et al., 1984).

Figure 19 - Influence of total jet impact force in the ROP.

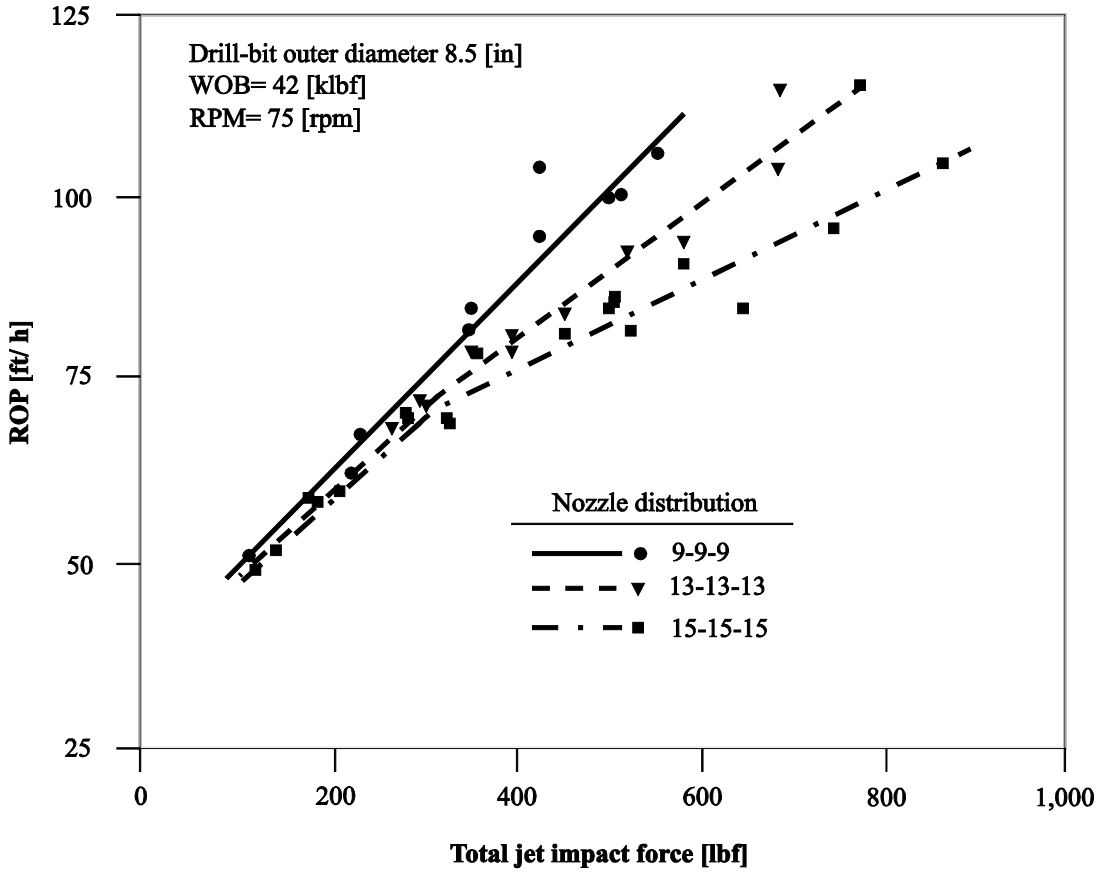

Source: (WARREN et al., 1984).

$$F_j = 0.00126.\rho.OD_{nozzle}{}^2.V^2 = 0.000516.\rho.Q_{total}.V \quad (15)$$

$$A_v = \frac{V}{V_{back-flow}} = \frac{\frac{Q_i}{n_{nozzles}.A_{nozzle}}}{\frac{Q_f}{k.A_{back-flow}}} = \frac{\frac{k}{100}.OD_{bit}^2}{n_{nozzles}.OD_{nozzle}^2} \quad (16)$$

$$F_{j_{adjusted}} = (1 - A_v^{-N}).F_j \quad (17)$$

From additional investigation on the hydraulic jet impact force on the bottom of the hole, Warren (1987) produced a modified ROP model that differed from his initial findings (WARREN et al., 1984), enhancing relationships based on the hydraulics studies performed on the influence of overbalance on the ROP and the flow-rate on the ROP, as per equation (18). In the following equation, the factor K_a has been found to range between 0.0378 and 0.0379, K_b between 0 and 1 and K_c between 2.7 and 2.86. In this context Figure 14-a and Figure 20 details different behavior of the ROP in terms of WOB for different flow and bottom-hole pressure,

where can be seen that the higher the flow-rate and the lower the bottom-hole pressure, the more one let the ROP to be sensitive to changes in WOB.

$$ROP = \left(K_a . \frac{S^2 . OD_{bit}^3}{RPM_{Sf} . WOB_{sf}^2} + K_b . \frac{1}{RPM_{Sf} . OD_{bit}} + K_c . \frac{OD_{bit} . \gamma_f . \mu_p}{F_{j_{adjusted}}} \right)^{-1} \quad (18)$$

Figure 20 - ROP versus WOB for different overbalance pressures.

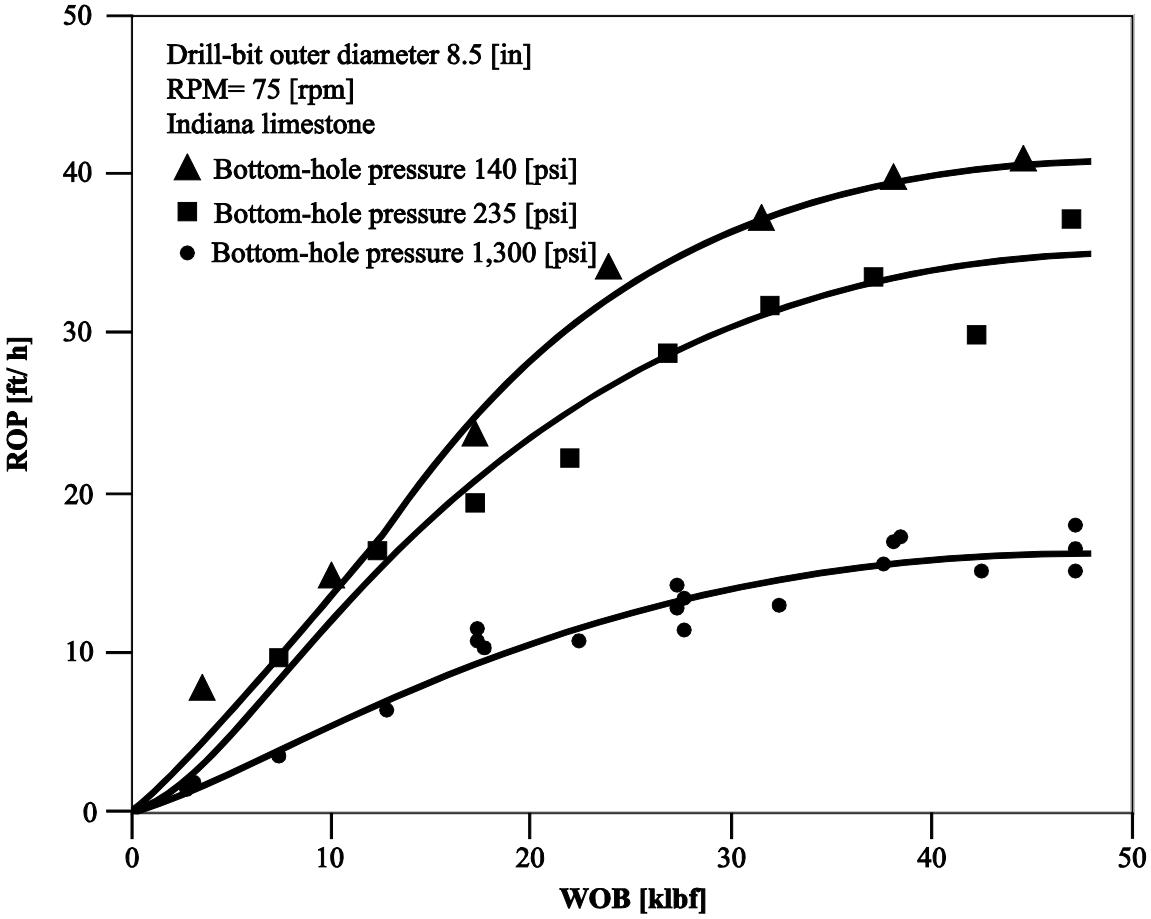

Source: (WARREN, 1987).

Interesting to notice is that the less overbalance is implicit the better the ROP performs and the higher the flow-rate is used for pumping the drilling fluid the better the ROP performs, as a response of bottom-hole cleaning and also of an increased jet impact force, which, as seen previously, influences the ROP positively.

2.3.2 BYM ROP Model applicability

From the presented formulations for ROP modeling, over the years, considering that much drilling operations started to happen in regions and environments where a lot of the drilling mechanics parameters would have a certain degree of directly influence on the ROP, some researches started pointing to simulations using mainly the Bourgoyne Jr. and Young Jr. (1974 and 1986) ROP modeling (BYM) formulation (equation (5)), but still, without proposing any modification to the main equation or improvements, but just directly field application of the methodology for well engineering purposes. Following this idea, from the literature, Table 3 (BOURGOYNE Jr. and YOUNG Jr., 1986), Table 4 (EREN, 2010) and Table 5 IRAWAN et al., 2012), present the BYM applied to specific fields, detailing the normalization factors chosen by the researchers and the best coefficients encountered for driving the ROP model in these specific regions, followed by the estimated error. As known by the skilled in the art, it is not feasible to guarantee a perfect match between the calculated and the field data ROP, so that the best solution would be the one allowing the minimum fitting error (or relative error) between both data when compared to each other. Interesting wise, from the year 1986 up to 2012, as per detailed tables in reference, the BYM has been applied in the industry with minimum changes in it, as can be noticed by the boundary values for the coefficients and the normalization factors. In this sense, by grouping all the information from Table 3, Table 4 and Table 5, it was possible to set a different and wider window for the boundary of the coefficients and also to change the normalization factors accordingly, enhancing the modeling together with a reference of acceptable relative error for modeling set as approximately maximum 38% (BOURGOYNE Jr. and YOUNG Jr., 1986; EREN, 2010; IRAWAN et al., 2012). The abbreviation used in the tables in the tables, in this particular case, stands for not applicable.

All these information detailed in the tables will be used in the final chapter, which details the optimization methodology, for helping developing the final mathematical model proposed throughout this thesis.

Table 3 - BYM ROP model details from Bourgoyne Jr. and Young Jr. (1986).

Parameter	Normalization factors	Coefficients	
		Lower boundary	Upper boundary
$\left(RPM_{sf}\right)_N$	100 [rpm]	n/a	n/a
TVD_N	10,000 [ft]	n/a	n/a
EPP_N	9 [ppg]	n/a	n/a
$\left(\frac{WOB_{sf}}{OD_{bit}}\right)_N$	4 [klbf/ in]	n/a	n/a
$\left(F_j\right)_N$	1,000 [lbf]	n/a	n/a
a_1	n/a	0.5	1.9
a_2	n/a	0.000001	0.0005
a_3	n/a	0.000001	0.0009
a_4	n/a	0.000001	0.0001
a_5	n/a	0.5	2
a_6	n/a	0.4	1
a_7	n/a	0.3	1.5
a_8	n/a	0.3	0.6
Relative error	n/a	n/a	

Source: (BOURGOYNE Jr. and YOUNG Jr., 1986).

Table 4 - BYM ROP model details from Eren (2010).

Parameter	Normalization factor	Coefficients	
		Lower boundary	Upper boundary
$\left(RPM_{sf}\right)_N$	60 [rpm]	n/a	n/a
TVD_N	8,000 [ft]	n/a	n/a
EPP_N	9 [ppg]	n/a	n/a
$\left(\frac{WOB_{sf}}{OD_{bit}}\right)_N$	4 [klbf/ in]	n/a	n/a
$\left(F_j\right)_N$	1,000 [lbf]	n/a	n/a
a_1	n/a	1.0006	3.2914
a_2	n/a	0.0002	0.0048
a_3	n/a	0.0004	0.6589
a_4	n/a	0.0001	0.0003
a_5	n/a	0.1029	0.8529
a_6	n/a	0.48	1.6843
a_7	n/a	0.2843	2.5873
a_8	n/a	-0.6324	1.0805
Relative error	n/a	0.379	0.5395

Source: (EREN, 2010).

Table 5 - BYM ROP model details from Irawan et al. (2012).

Parameter	Normalization factors	Coefficients	
		Lower boundary	Upper boundary
$(RPM_{sf})_N$	100 [rpm]	n/a	n/a
TVD_N	10,000 [ft]	n/a	n/a
EPP_N	9 [ppg]	n/a	n/a
$\left(\frac{WOB_{sf}}{OD_{bit}}\right)_N$	4 [klbf/ in]	n/a	n/a
$(F_j)_N$	1,000 [lbf]	n/a	n/a
a_1	n/a	3.91	
a_2	n/a	0.0001	
a_3	n/a	0.0001	
a_4	n/a	0.0009	
a_5	n/a	0.37	
a_6	n/a	2.23	
a_7	n/a	0.025	
a_8	n/a	0.67	
Relative error	n/a	0.55	

Source: (IRAWAN et al., 2012).

2.4 SPECIFIC ENERGY CONCEPT

Specific energy, in simple words, is represented by energy per unit mass or unit volume. Also known as energy density, it is mainly applied to quantify the amount of stored heat, and in the thesis specific case, to quantify the energy necessary to drill a specific unit of rock volume. It has been stated that the energy per unit volume is a quantity on the order of magnitude of twice the compressive strength of the rock, and that the high energy necessary to advance in drilling a specific rock. This sub-chapter summarizes the main research development in terms of SE from 1965 to date, which interestingly is still present and started to be more evident in the industry for drilling surveillance purposes in the year 2005 (DUPRIEST, 2005).

2.4.1 Specific energy knowledge evolution

Teale et al. (1965) analyzed the work done by a drill bit in order to advance into the rock or formation when excavating an infinitesimal volume of rock, and consequently, the necessary energy in terms of volume removed instead of mass removed, naming it the specific energy (SE) necessary in a rock drilling process. It was then established an equation to address the total

work done by the forces acting on the drill-bit, considering its translational axial and rotational movement within a specific time range, stating also that the maximum mechanical efficiency would occur with a minimum imposed SE. The total work performed by the axial and radial force, in order to allow excavating a specific volume of rock, is represented by equations (19)-(21) (Figure 21) (TEALE et al., 1965).

Figure 21 - Brief schematic of a translational axial and rotational movement of a drill-bit while drilling.

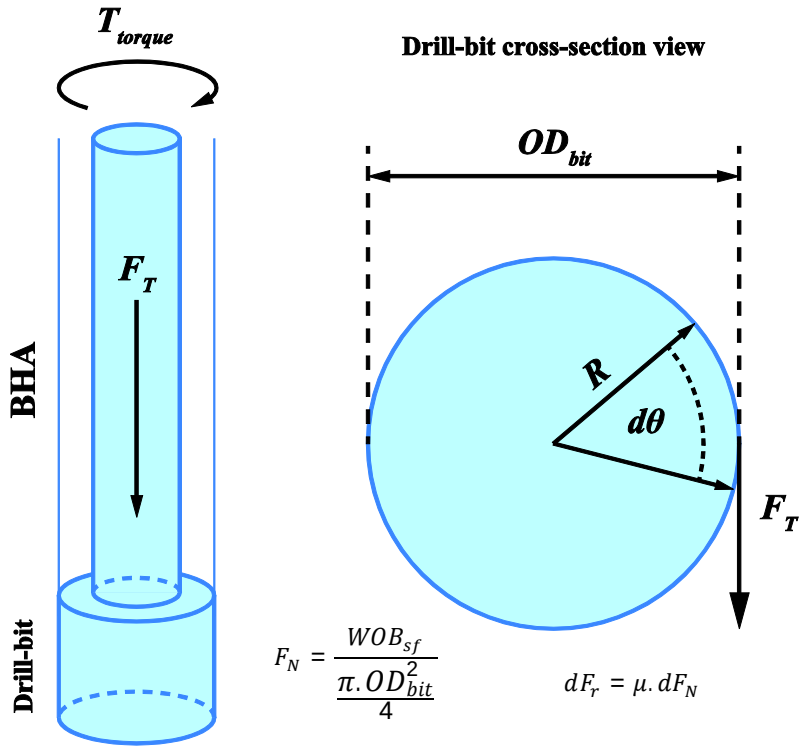

Source: (Adapted from: TEALE et al., 1965; PESSIER et al., 1992).

$$\tau_{total} = \tau_{translational} + \tau_{rotational} \quad (19)$$

$$\tau_{translational} = F_t . ds = F_t . dv . dt \quad (20)$$

$$\tau_r = \int_0^{N.2\pi} F_r . \frac{OD_{bit}}{2} . d\theta = F_r . \frac{OD_{bit}}{2} . (N.2.\pi - 0) = T_{torque_{sf}} . N.2.\pi \quad (21)$$

N *is the* n^o *of revolution.*

Considering a rotary speed of N revolutions per one minute, a rate of penetration (ROP) or displacement speed (dv) of one inch per one minute, and a volume (dV_{dt}) of excavated rock in one minute equivalent to the drill-bit surface area A_{bit} times the displacement developed with the given ROP (equation (22)) and that the SE would be the work performed by an acting force divided by the volume of rock, rather than by the rock mass itself, the total SE developed to

excavate the rock in one minute can be expressed, after adjusting equations (23) and (24), as per equation (25).

$$dV_{dt} = A_b . ds = A_b . dv . dt \tag{22}$$

$$SE_{axial-rotary} = \frac{\tau_{total}}{dV_{dt}} = \frac{F_t . ds}{A_{bit} . ds} + \frac{2 . \pi . T_{torque_{sf}}}{A_{bit} . ds} \tag{23}$$

$$SE_{axial-rotary} = \frac{F_t}{A_{bit}} + \frac{2 . \pi . T_{torque_{sf}} . N}{A_{bit} . dv . dt} = \frac{F_t}{A_{bit}} + \frac{2 . \pi . T_{torque_{sf}}}{A_{bit} . dv} . \frac{N}{dt} \tag{24}$$

$$SE_{axial-rotary} = \frac{WOB_{sf}}{A_{bit}} + \frac{2 . \pi . T_{torque_{sf}} . RPM_{sf}}{A_{bit} . ROP_{field}} \tag{25}$$

Furthermore, it has been highlighted but not entire proven in terms of different drill-bit types, formation types, and drilling mechanics parameters, that the minimum achievable SE would then be close to the crushing strength of the rock being drilled, said to be equivalent to the compressive strength, given the failure mechanism (Figure 22). The tests were performed under atmospheric pressure conditions for concrete, shale, and sandstone, making use of 12.25 [in] and 1.6875 [in] (slim-hole) roller-cutter bits together with percussion-rotary events. It was observed that the torque could be expressed as a linear relationship to penetration per revolution (P_{ds-rev}) and also that the work performed by the translational axial force portion could be negligible, if compared to the rotary one, and so, disregarded. Thus, the slope of a torque versus penetration per revolution can also directly represent the SE magnitude (Figure 23), exemplified by equations (26) and (27).

$$SE_{rotary} = \frac{2 . \pi . T_{torque_{sf}} . RPM_{sf}}{A_{bit} . ROP_{field}} = \frac{2 . \pi . T_{torque_{sf}}}{A_{bit} . dv} . \frac{N}{dt} = \frac{2 . \pi . T_{torque_{sf}} . N}{A_{bit} . \frac{ds}{dt} . dt} = \frac{2 . \pi}{A_b} . \frac{T_{torque_{sf}} . N}{ds} \tag{26}$$

$$SE_{rotary} = \frac{2 . \pi}{A_{bit}} . \frac{T_{torque_{sf}}}{\frac{ds}{N}} = \frac{2 . \pi}{A_{bit}} . \frac{T_{torque_{sf}}}{P_{ds-rev}} \tag{27}$$

Figure 22 - Graphics showing the convergence of specific energy to rock crushing strength.

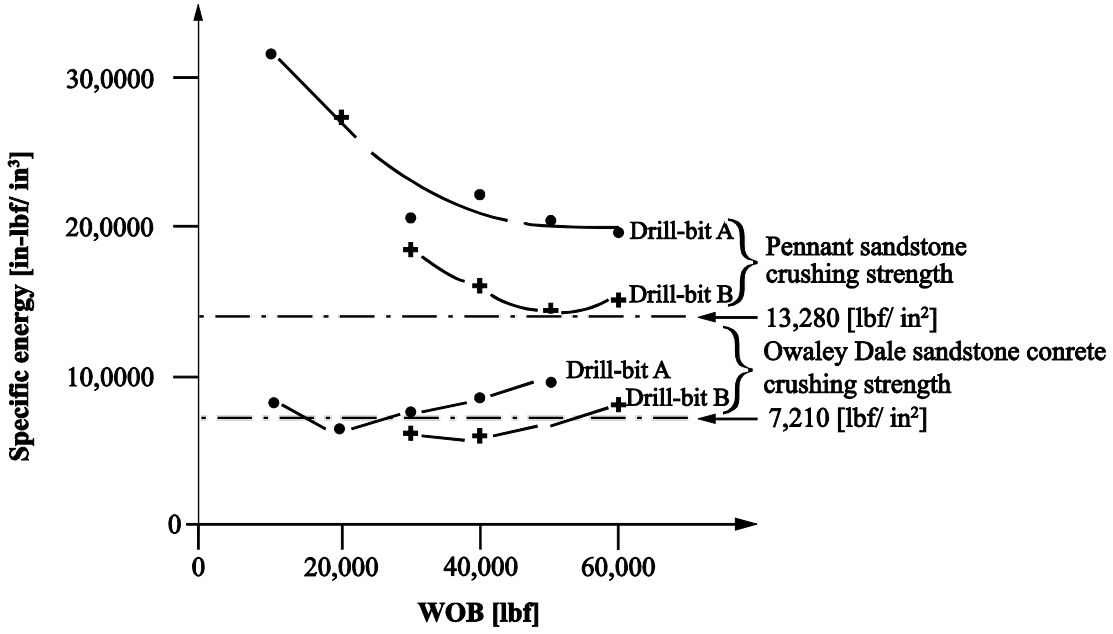

Source: (TEALE et al., 1965).

Figure 23 - Relationship between torque and penetration per revolution.

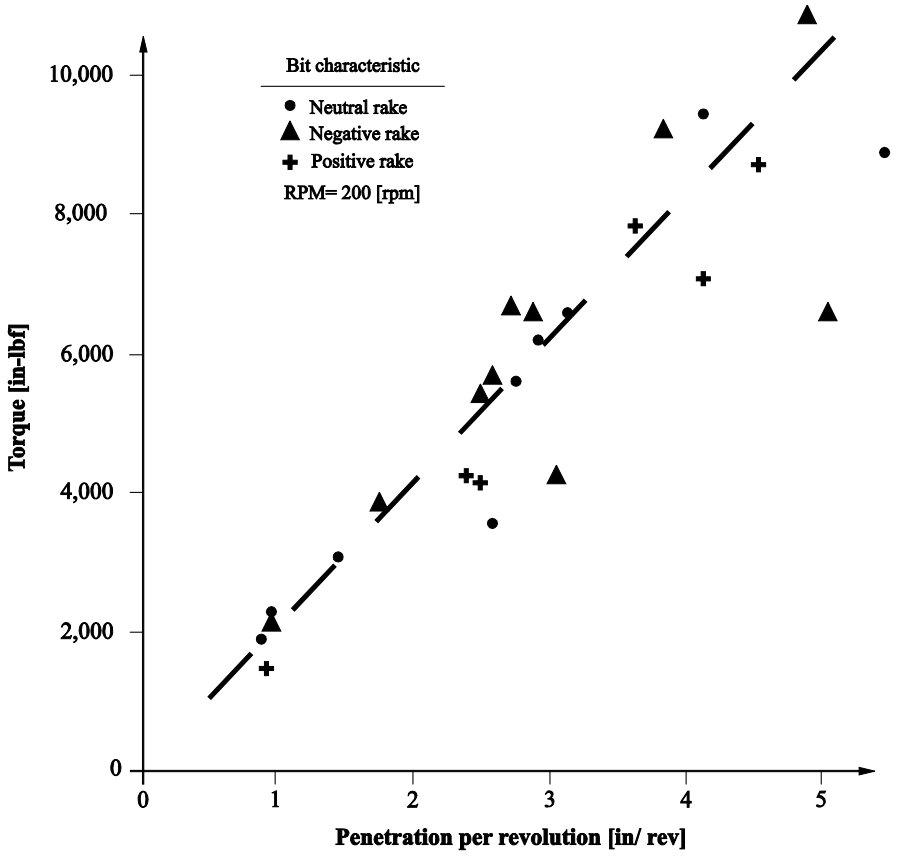

Source: (TEALE et al., 1965).

It was recognized that the SE could not be represented accurately by a single number since it was dependent on many dynamic and fluctuation variables presented in the drilling process, so that approximate and mean values were essentially sufficient to be considered for modeling and prediction of drilling performance. It was also emphasized that all the experiments drive and converge to an understandable and feasible correlation in terms of SE and the crushing strength of the rock, not entirely proving that it may represent just the ultimate compressive strength (UCS). The ratios between SE and crushing strength throughout the various experiments and analysis stayed between 0.8 and 1.6.

After extensive researches over twenty years, Rabia et al. (1985) simplified the equation for SE calculation as per equation (28), stating that the ROP is more sensitive than SE for WOB and rotary speed changes. It was concluded that an increase in the SE (dependent on the drill-bit type and design rather than just rock properties) results in an increase in the cost per foot, and that cumulative cost per foot is directly related to drill-bit performance. The tests were conducted three different 12.25 [in] roller-cutter TCI bits in the Middle East; being the formation type not detailed throughout the paper (RABIA et al., 1985).

$$SE = \frac{20.(WOB_{sf}.RPM_{sf})}{OD_{bit}.ROP_{field}} \tag{28}$$

Some year after, following the achievement of Rabia et al. (1985), Pessier et al. (1992) addressed some interesting studies and summarized, mathematically and theoretically, the importance and possibility of converting the torque shown in the SE equation in terms of WOB and drill-bit sliding friction factors (considering the drill-bit as a flat cylinder and touching the borehole just in the bottom of the hole as per Figure 21). Thus, the SE formulation defined in equation (25), developed by Teale et al. (1965), was also validated for hydrostatic pressure environments and started to be called mechanical specific energy (MSE) instead of just SE. The tests were conducted in grout (construction material - mixture of water cement sand and some gravel) and shale cores using water based muds with TCI and PDC drill-bits of the following sizes: 7.875 [in], 8.5 [in] and 12.25 [in]. For TCI drill-bits, the friction factors ranged between 10 and 20%; for PDC, 30 to 50%. This led to the interpretation that PDC bits need less WOB to provide the same performance of a TCI. Another important interpretation was that hydraulics appear to have a high impact on penetration rate. The deeper the drilling activity, the less effective would be the hydraulic energy reaching the bottom of the hole due to pressure losses across the drill-string and the BHA. In addition, there is heating as a source of energy loss that should not be taken out of consideration on those calculations. The first changes done in the SE

equation accounted for using torque and ROP in field units (units being [ft- lbf] and [ft/ h], respectively), as per equation (29). The second changes applied can be seen in equations (30)-(32), which were based on the schematic shown in Figure 21 and the drawn formulations in it, for expressing the torque as a function of WOB and drill-bit sliding friction factor. In order to convert the applied torque in terms of WOB, one has to consider the Normal Force (F_N) as one specific point on the bit, and the total WOB as being uniformly distributed over the whole cross-section area of the drill-bit (PESSIER et al., 1992).

$$SE_{axial-rotary_{field}} = \frac{WOB_{sf}}{A_{bit}} + \frac{2.\pi.T_{torque_{sf}}.RPM_{sf}.\left(\frac{1}{12}\right)}{A_{bit}.\frac{ROP_{field}}{\left(\frac{1}{60}\right)}.\left(\frac{1}{12}\right)} = \frac{WOB_{sf}}{A_{bit}} + \frac{120.\pi.T_{torque_{sf}}.RPM_{sf}}{A_{bit}.ROP_{field}} \tag{29}$$

$$T_{torque_{sf}} = \int_0^{\frac{OD_{bit}}{2}} \int_0^{2\pi} \delta^2 \frac{4.\mu.WOB_{sf}}{\pi.OD_{bit}^2} d\delta.d\theta = \int_0^{\frac{OD_{bit}}{2}} \frac{8.\mu.WOB_{sf}}{OD_{bit}^2}.\delta^2.d\delta = \frac{8.\mu.WOB_{sf}}{OD_{bit}^2}.\left(\frac{\delta^3}{3}\right)_0^{\frac{OD_{bit}}{2}} = \frac{\mu.WOB_{sf}.OD_{bit}}{3} \tag{30}$$

$$SE_{axial-rotary_{field}} = \frac{WOB_{sf}}{A_{bit}} + \frac{120.\pi.RPM_{sf}.\frac{\mu.WOB_{sf}.OD_{bit}}{36}}{A_{bit}.ROP_{field}} = WOB_{sf}.\left(\frac{1}{A_{bit}} + \frac{120.\pi.\mu.RPM_{sf}.OD_{bit}}{\pi.\frac{OD_{bit}^2}{4}.ROP_{field}.36}\right) = WOB_{sf}.\left(\frac{1}{A_{bit}} + \frac{13.33.\mu.RPM_{sf}}{OD_{bit}.ROP_{field}}\right) \tag{31}$$

$$ROP_{field} = \frac{13.33.\mu.RPM}{OD_{bit}.\left(\frac{SE_{axial-rotary_{field}}}{WOB_{sf}} - \frac{1}{A_{bit}}\right)} \text{ [ft/ h]} \tag{32}$$

Under hydrostatic conditions, it was observed that the drill-bit sliding friction factors had some variance, but not something remarkable, while the SE increased drastically. Explanations for that were drill-bit balling (interference of energy transmission due to accumulated material within the drill-bit teeth-cutters' structures) and bottom-hole balling (known as chip hold-down effect, cuttings accumulate in the bottom-hole by differential pressure interfering in the energy transmitted to rock breakage). Figure 24 exemplifies the relationship between SE and ROP,

where can be seen that by increasing the ROP, the SE is decreased in both scenarios, for atmospheric and overbalanced conditions. These are very important outcomes since for operations where the torque data are not reliable, the WOB measurements would be enough to guarantee surveillance analysis and further, the SE final formulation could be simplified by one variable, allowing faster simulations and real-time operational responses.

Figure 24 - SE and drill-bit sliding friction factor under atmospheric (a) and overbalanced (b) conditions.

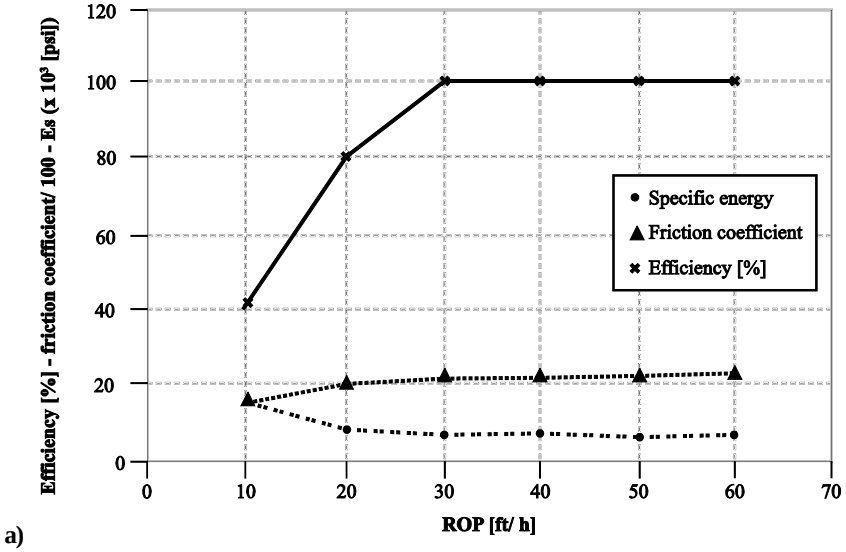

a)

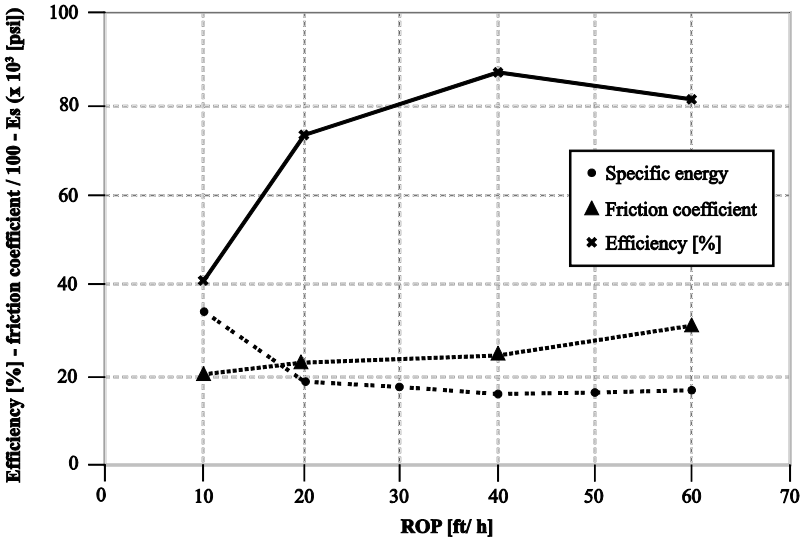

b)

Source: (PESSIER et al., 1992).

But was from the year 2005 with Dupriest et al. (2005 and 2010), that the surveillance of SE started to be effectively used for improving of drilling performance. It was asserted that drill-bit efficiency lays between 30 to 40% as also per Teale et al. (1965), which stated that calculated

SE's were roughly three times the rock crushing strength. It was found that this relates to the drill-bit depth-of-cut (DOC) in a proportional manner, and that the low drilling-related efficiency is a consequence of basically three main factors: drill-bit balling, bottom-hole baling and vibration (evidenced when drilling hard formations with high compressive strength and using inadequate WOB and rotary speed). Further, it was determined that an adequate hydraulics design with decreasing nozzle sizes and a resultant increase in horsepower per square inches [hsi] would have a positive impact on drill-bit balling, helping positively in terms of drillability. The usage of PDC drill-bits does decrease the problematic of bottom-hole balling which is more evidenced in TCI drill-bits type due to its different drill-bit crushing action. In terms of vibration, not much was concluded rather than emphasizing that this parameters alone is not enough to guarantee a correlation with ROP. Figure 25 represents a drill-rate curve (result of a test done just before drilling a specific formation for choosing best set of rotary speed and WOB) modified by Dupriest et al. (2005), which relates to the problematic just disserted. Region I represents a region dependent on the DOC, region II represents the normal tendency of relation between the WOB and ROP in the sense of having the ROP directly proportionally increased by increasing the WOB. Region III represents the foundering region, showing that is not true to have the ROP infinitely increased by increasing the WOB, and that the maximum applicable WOB would be the one representative by the inflection point of the curve. This region III inflection point could be shifted allowing a higher achievable ROP by better designing the problematics presented in the previous sentences, including the hydraulics.

Furthermore, Dupriest et al. (2005) stated that friction losses are the main error in SE determination since the torque measured on the surface is a sort of reactive force or friction encountered and may take into account, not just the down-hole torque of the drill-bit, but also the whole drill-string friction. Never the less, as a trending and qualitative tool and not as quantitative absolute values, it would still be reasonable to be used in drilling operations as a reference chart. In this sense, it was suggested that the SE and MSE ($SE_{axial-rotary_{field}}$) equations, as determined by Teale et al. (1965) and Pessier et al. (1992), should be used after adjusting for the already-known drill-bit efficiency (EFF_M), which lays between 30 and 40%. The final adjusted mechanical specific energy ($MSE_{adjusted}$) would change the specific energy SE curve to fit the rock crushing strength to maximize correlation in its maximum efficiency, and be more feasible for the field personnel (known also as rig crew or field population) to reference, as per equation (33) (DUPRIEST et al., 2005 and 2010).

$$MSE_{adjusted} = SE \,.\, EFF_M \tag{33}$$

Figure 25 - Graph showing a common drill-rate test curve and improvements possibilities.

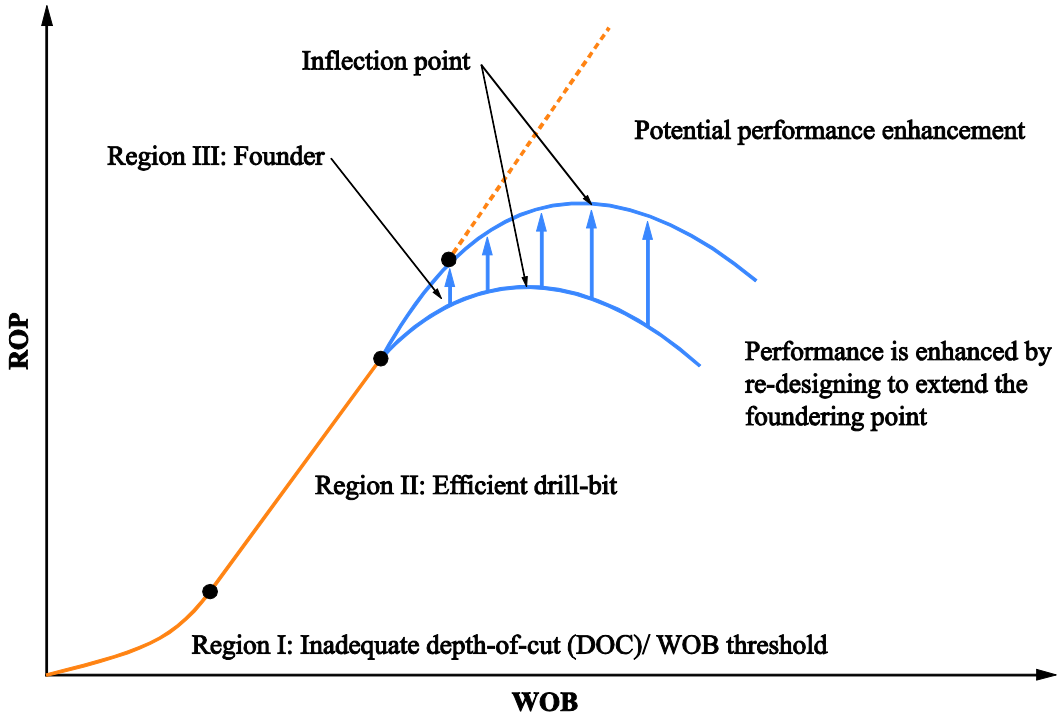

Source: (DUPRIEST et al., 2005).

In the second paper (DUPRIEST, 2010), disserted some interesting thoughts related to field operation conducted with PDC bits of sizes 17.5 [in], 12.25 [in] and 8.5 [in] in hard anhydrites and dolomites (rock strength ranging from 15 to 35 [kpsi]). It was observed that an increase horsepower would increase efficiency, achieved by decreasing nozzle sizes or increasing flow-rate (or hydraulic jet impact force), and that logging-while-drilling (LWD) and measuring-while-drilling (MWD) tools do not show the low vibration level which may also affect the MSE curves, but are designed to accommodate minimum levels that might be harmful for the tools itself.

In terms of vibration, it was stated that lateral vibration, or whirl, could be mitigated by increasing the WOB, changing motors, bent housing configurations versus more straight ones, using near bit stabilizers, using high torque motor, and even increasing the drill-bit gauge length. For torsional vibration or stick-slip, efficiency is enhanced by a decrease in torque (achieved by reducing the WOB) or an increase in rotary speed (which increases the angular momentum). For axial vibration or bit bounce, a reduction in WOB was helpful, considering that it is more frequent when encountering stringers (known as small formation layer of different geology within a formation type) or drilling hard formations.

3 PRE-SALT DATA ANALYSIS

In this chapter, the pre-salt wells are detailed from both technical and economic points of view, starting with the main general characteristics and information, then deepening through the sub-chapters into geological, petrophysical, drilling, and performance characterization.

3.1 GENERAL WELL INFORMATION AND COSTS

Pre-salt wells have gained exposure world-wide, not just because of their possible profitability, but also due to the challenges implicit in their exploration, operations, and well development phases. Considerably remote, hundreds of kilometers from the coast, and in environments known in the industry as deep- and ultradeep-water (Figure 4), these wells have some degree of complexity, one of several factors that make the activities and operations costly.

Table 6 presents a historical summary of information from analogs drilled in the past years in which the wells' locations are shown to vary from 100 to 180 [km] from the coast, in water depths averaging more than 1,500 [m] and with reservoirs (pre-salt section) located approximately 3.5 to 6 [km] deep. All these facts, together with some specific information provided in the subsequent sub-chapters, helps addressing why the activity in such type of wells comes at such considerably expense, with costs estimated to go up to 134,000,000.00 [USD] for the entire operation of a pre-salt well.

It can be considered that the efficiency for effectively drill the pre-salt sections has been, in average, approximately 28.5 [m/ day] with costs ranging from 641,985.00 to 1,374,755.00 [USD/ day] (equivalent to 22,525.00 to 48,237.00 [USD/ m]), dependent on the type of drilling platform in use and unforeseen events followed by unforeseen operational costs that can arise when performing the operation. These costs and average performance for the pre-salt will be used in the next chapters for estimating the potential savings hidden in the pre-salt operations in terms of operational performance.

Furthermore, with the presented information in Table 6 it is possible to better picture the wells´ data set in use for the optimization analysis in the presented thesis, allowing a better visualization of which kind of wells are under study.

Table 6 - Historical pre-salt well costs, sizes, intervals, water depths, and coastal distance.

Well #	Time [days]/ cost [MM USD]		Pre-salt coastal distance [km]/ MD drilled interval [m]/ water depth [m]			Hole size [in]
	Total well/ pre-salt interval	Total well/ pre-salt interval with (NPT [%])	Coast	Depth/ time [days]/ vertical (V) or deviated (D)	Water depth	
A	91.1/ n/a 29.12/ n/a	109.32 (20%)/ n/a 35.34 (21%)/ n/a	110	3,993 - 4,195/ 12.79/ (V)	1,300	8.5
B	102.5/ 133.5 35.55/ 45.25	123 (20%)/ 160 42.66 (20%)/ 54.32	100	3,405 - 3,872/ 21.08/ (V)	900	12.25
C	n/a / n/a n/a / n/a	n/a / n/a n/a / n/a	120	4,487 - 5,313/ 35.29/ (D)	1,800	12.25
D	80.1/ 79.1 12.29/ 7.89	96.1 (20%)/ 93.3 15.14 (23.19%)/ 9.47	130	4,400 - 4,887/ 20.29/ (V)	1,700	8.5
E	100/ 101,4 41.61/ 37.55	120 (20%)/ 120 52.69 (27%)/ 45	130	4,665 - 5,475/ 30.38/ (D)	1,700	10.63
F	n/a / n/a n/a / n/a	n/a / n/a n/a / n/a	100	4,899 - 5,739/ 15.29/ (D)	1,600	12.25
G	120/ 165 15.29/ 21.02	n/a / n/a n/a / n/a	100	5,255 - 5,600/ n/a / (V)	1,700	12.25
H	115/ n/a 25,65/ n/a	134 (20%)/ n/a 30,77 (20%)/ n/a	180	5.050 - 5.840/ 27,09/ (V)	1,800	12.25

Source: (BDEP, 2010; CDC, 2015).

Due also to the fact most of these operations are still linked to exploratory phases rather than to development phases, and considering that a mature experience is still under development, the main focus in such wells has been to avoid unexpected or undesired events while learning any single task, so that the operation itself is not always just speed oriented, but more learning and information gathering oriented, even understanding that the economic factor plays a very important role in the operational context.

3.2 RESERVOIR CHARACTERIZATION

The pre-salt reservoirs are characterized as carbonate reserves with different and specific key features known to present certain challenges. For example, the thickness of the evaporite layers on top of the pre-salt, has to be crossed before reaching the pre-salt accumulations. Historically, these formations are very hard and abrasive, but for various reasons not detailed here since it is considered to be outside of the scope of this research; the hydrocarbon accumulations are of good quality, classified as light and containing some presence of H_2S (expectation ranging up to 250 [ppm]) and CO_2 (ranging up to 40%) that forces cautious by applying specific techniques

when in execution of any exploration and production related phases (BELTRAO ET AL., 2009; MELLO ET AL., 2011; CEZAR et al., 2015; ANDRADE, 2015; BSUQUET, 2015).

These clastic sedimentary rocks, predominantly microbiological and coquinoid limestone along with presences of dolomite, claystone, silica, and shells or molluscs, are known to be a reservoirs with good porosity (reservoir with considerable quality), with a total organic carbon (TOC) index of about 10% or more, what allows classifying it as an excellent potential reservoir, as per petroleum industry references (ROBINSON et al., 2007; MOHRIAK, 2015). Also relevant, their heterogeneity and naturally fractured layers are attached with mineralization, dolomitization, and silicification, giving the layer some indurated characteristics. The confined compressive strengths (CCS) range from 25 to 300 [kpsi] (CHRISTANTE, 2009; HBAIEB et al., 2013). Similar characteristics have been seen along analog wells in the South Atlantic Ocean operations, more specifically in the Brazilian Campos basin, in the Brazilian Santos basin and in the Angolan Kwanza basin (GREENHALGH et al., 2012; MOHRAK, 2015).

The next graphs, Figure 26 and Figure 27, detail historical gamma-ray (GR) readings for the wells under study; most of the readings range between 30 and 75 [ºAPI] and above 15 [ºAPI], which helps to confirm the geological formation previously highlighted: limestones and dolomites with some presence of clay- and shale-stones (NASCIMENTO, 2010).

Figure 26 - Separated histogram of pre-salt historical GR for the wells # A, B, C, D, E and F under analysis.

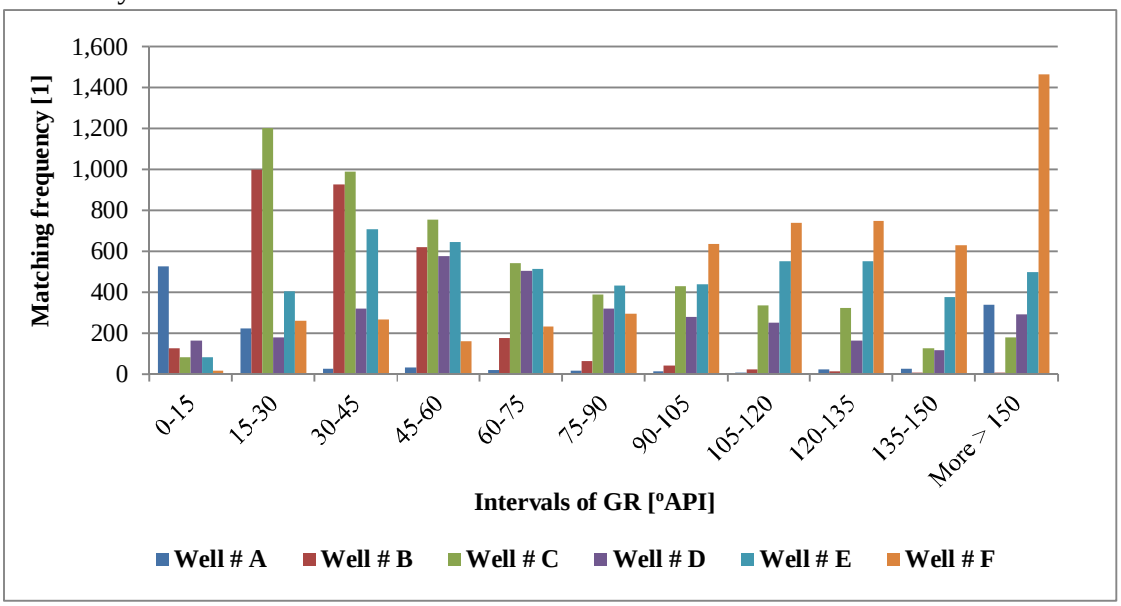

Source: (BDEP, 2010; CDC, 2015).

Figure 27 - Grouped and cumulative histogram of pre-salt historical GR for all wells # A, B, C, D, E and F.

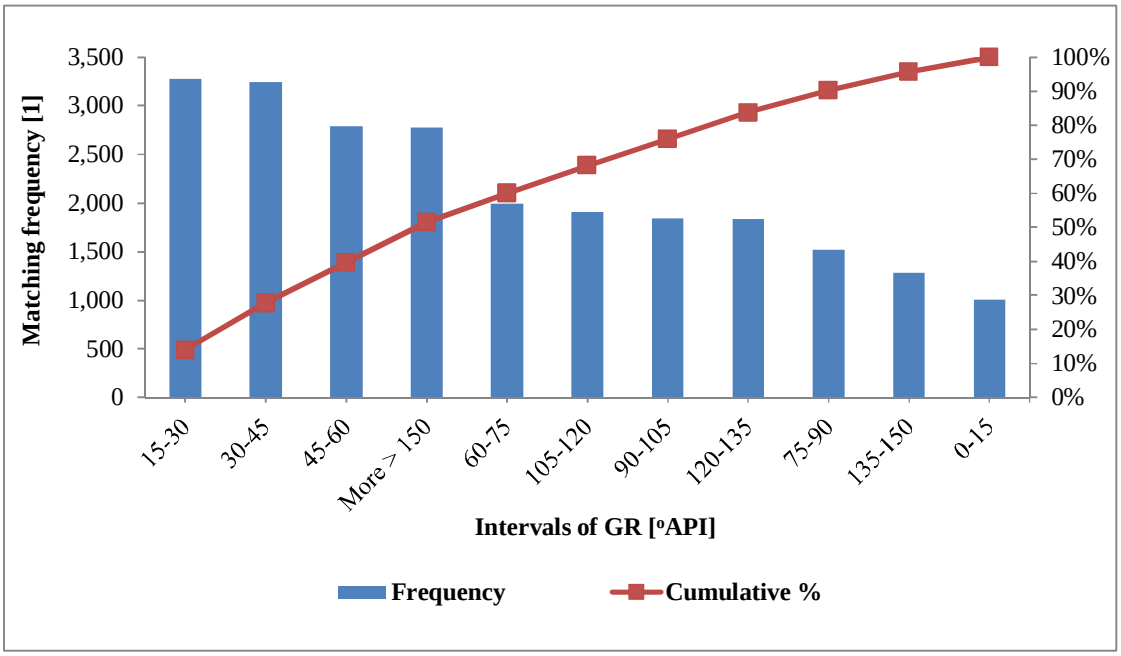

Source: (BDEP, 2010; CDC, 2015).

Figure 27 shows that approximately 60% of the gamma-ray readings are in the range representative for limestone and dolomite, and Figure 26 reveals that, in general, the wells exhibit the same reservoir characteristics when compared to each other. Usually, the pre-salt

reservoir rock porosity ranges from 2 to 16%, while the permeability (usually measured in millidarcy) found is of around 100 [mD] (CARMINATTI, 2008; MELLO et al., 2011; JOHANN et al., 2012).

Following the rock characteristics, Figure 28 shows some pre-salt fluid samples emphasizing traces of limestone (Figure 28-a) and claystone (Figure 28-b), both highlighted by dashed red marks; Figure 29 shows pre-salt rock samples of cavings (Figure 29-a) and cuttings (Figure 29-b) retrieved from the shale-shakers (equipment used in the industry to remove small cuttings from the drilling fluid returned from the bore-hole) after drying. These pictures were obtained together with the data set used for developing the research (BDEP, 2010; CDC, 2015).

Figure 28 - Pre-salt returning fluids samples with traces of limestone (a) and claystone (b).

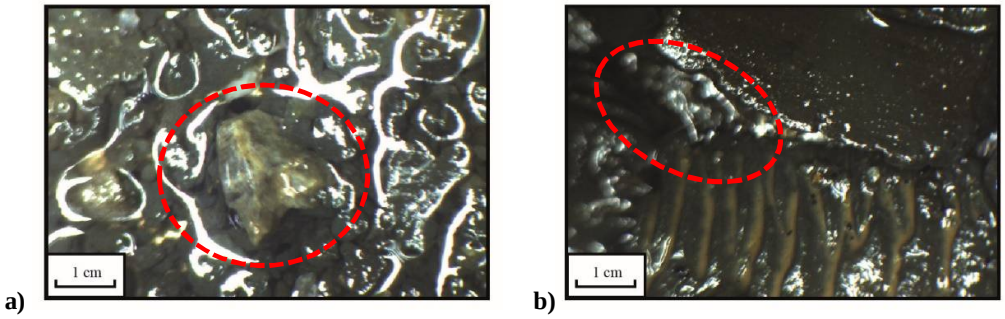

Source: (BDEP 2010; CDC, 2015).

Figure 29 - Pre-salt caving (a) and cuttings (b) examples retrieved from related operations.

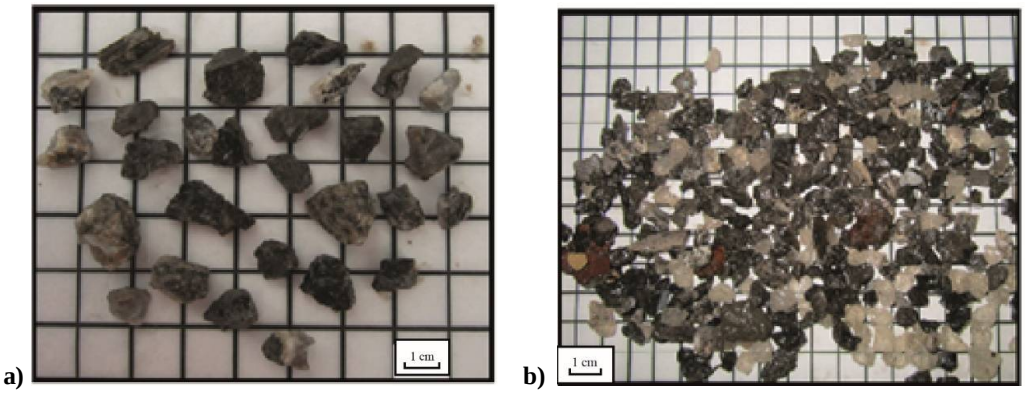

Source: (BDEP 2010; CDC, 2015).

The information and facts addressed in this sub-chapter are important for understanding subsequent discussions in the field of pre-salt activity optimization since it details basic geological characteristics important for the whole context.

3.3 RELATED HYDRAULIC CHARACTERIZATION AND ANALYSIS

Hydraulics, fluid analysis, and drilling fluid designs play a very important role in petroleum activities and have to be treated carefully. Drilling operations use different types of drilling fluids, inhibitors, chemicals, and particles which can be harmful to the environment and the workers (normally a fluid engineer) using these materials. By using the right selection and balance of drilling fluids, well integrity can be secured, allowing operations to be carried on safely. For years, the importance of drilling fluid and hydraulics as influencing variables in drilling rate (DR) optimization have been emphasized. The hydraulics have to be high enough to prevent well break-out events and formation fluids influx (known in the industry as a *kick*) and should not exceed the formation limiting pressure (the boundary of fracturing the formation with the consequence of drilling fluid losses) which can lead to unstable well integrity (NASCIMENTO, 2012). This balance is made by controlling the hydrostatic pressure at the bottom-hole level, driven by the drilling fluid (known in the industry as drilling mud or simply mud) density together with its flow-rate.

Table 7 summarizes the historical information regarding the wells under analysis (wells # A, B, C, D, E, F, G, and H), considering formation pressure (pore pressure - PP), fracturing pressure (FP), temperature (Temp.), formation integrity test (FIT) and leak-off test (LOT). The last two tests are basically a pressure test run until a specific pressure limit is reached, and a pressure test run until reaching the fracturing limit of a specific formation, respectively. These are very important for understanding which type of well is being dealed with and to find the similarity between them in terms of main characteristics and implicit limitations, what will support in driving the mathematical modeling presented in the next chapters.

From Table 7 it can also be seen that the wells' pore pressures range usually from 9.5 to 9.7 [ppg]. Furthermore, in most of the wells, the pressuring test chosen is the FIT and reaches a specific maximum value between 11.8 and 12.5 [ppg]. The LOT seems less useful; with a FIT test positive (no evidence of leakage up to the maximum tested pressure and with a limiting value normally less than the LOT) and that the drilling fluid pressure gradient designed (also known as equivalent mud weight - EMW) would hardly reach up to or be more than the pressuring values measured during the LOT tests, as presented by the well # H where it reaches up to 13.54 [ppg]. The graph shown in Figure 30 presents the historical PP, FP, the FIT/ LOT pressures and the equivalent circulating density/ equivalent static density (ECD/ ESD) in which losses events (e.g. ECD exceeding the fracturing pressure) and kick events (e.g. ESD less than

the formation pore pressure) were experienced in the pre-salt wells under analysis. Important to note is the fact that pressure profiles are dependent on location, so that abnormal pressures spot can be present at any depth. Figure 30 graphs are based in extrapolation curves drawn using some specific pressure samples, what may be responsible for the different tendencies seen for the different pre-salt wells. Also not common, a profile can behave to have the pore pressure decreased in relation to depth, what is the case of well # G.

Table 7 - Wells historical hydraulics and pressure related information.

Well #	Pore pressure [ppg]	Fracture pressure [ppg]	Pressure test [ppg]/ FIT (F) or LOT (L)	Over-burden pressure [ppg]	List of reported mud losses and kick events' depth and pressure	Temp. [ºC]
A	9.5	TVD = 1,505.9 *FP - 14,129	11.8/ (F)	TVD = 698.18 *OP - 6,760	No events reported.	n/a
B	9.5	TVD = 1,867.6 *FP - 19,587	12/ (F)	TVD =723.01 *OP - 8,014.4	Kick event - EMW 9,8 [ppg] Depth [3.436 - 3.447] [m] ECD [10,57 - 10,46] [ppg] ESD [10,22 - 10,26] [ppg]	TVD = 58.48 *T - 763.07
C	9.5	n/a	11.88/ (F)	n/a	No events reported.	n/a
D	9.5	TVD = 1,692.3 *FP - 15,569	11.1/ (F)	TVD = 763.89 *OP - 6,981.9	Loss event - EMW 9,8 [ppg] Depth [4.543 - 4.546] [m] ECD [10,34 - 10,37] [ppg] ESD [10,1 - 10,13] [ppg]	TVD = 39.29 *T + 520.54
E	9.5	TVD = 20 *FP - 19,400	11.9/ (F)	TVD = 3,846.2 *OP - 58,054	No events reported.	TVD = 41.67 *T + 558.33
F	9.5	n/a	11.8/ (F)	n/a	No events reported.	n/a
G	~ 9.7 or TVD = -1,923.8 *PP + 24,327	TVD = 726.85 *FP - 5,082	12.5/ (F)	TVD = 2,974.4 *OP - 34,486	No events reported.	TVD = 35 *T + 1,467.5
H	~ 9.6 or TVD = -7,692.3 *PP + 79,077	TVD = 1,351.4 *FP - 12,068	13.54/ (L)	TVD = 826.45 *OP - 6,834.7	Loss event - EMW 9.6 [ppg] Depth [5,294 - 5,338] [m] ECD [9.84 - 9.93] [ppg] ESD [9.66 - 9.92] [ppg] Kick event - EMW 9.6 [ppg] Depth [5,840] [m] ECD [9.65] [ppg] ESD [9.58] [ppg	TVD = 48.78 *T - 268.29

Source: (BDEP, 2010; CDC, 2015).

Figure 30 - Historical pressures profiles for the pre-salt wells # A, B, C, D, E, F, G and H.

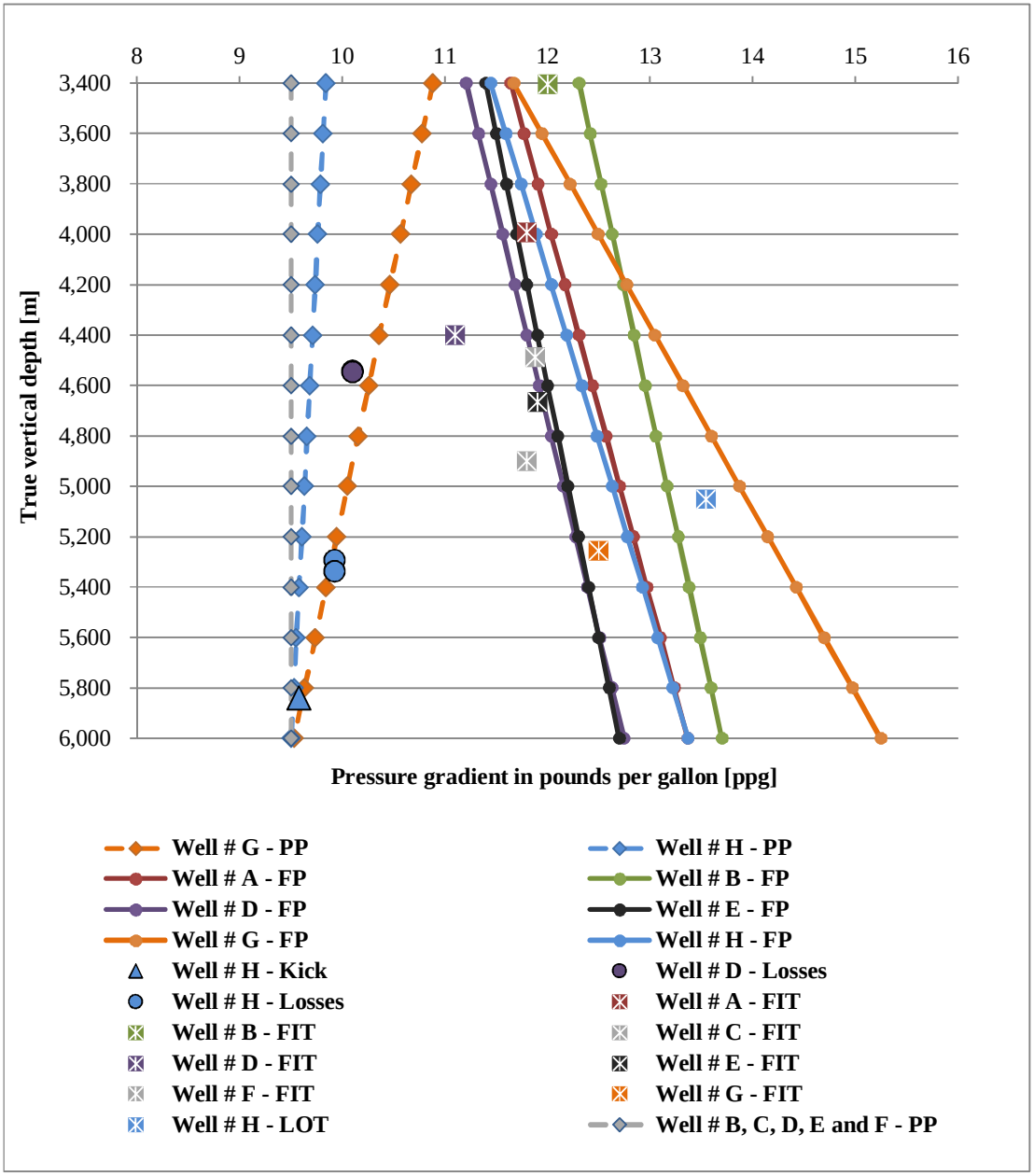

It is understood in the petroleum industry that the tests run before commence drilling a specific section are a very good and reliable references for the subsequent operations, but not a guarantee of values, since abnormal pressuring zones could pop-up while drilling deeper in the section. Considering the historical information presented in Table 7 and Figure 30, it can be interpreted that the EMW should be designed correctly, considering the collection of wells as a single entity, not crossing 10.02 [ppg] in terms of ECD to preventing losses, and not letting the ESD to be less than 9.58 [ppg], to prevent kick occurrences.

This is considered a very narrow window in terms of realistic operations since in tripping activities, the wells are susceptible to swab and surge events (a result of the upward movement of the drill-string in a well, leading to a sudden decrease in bottom-hole pressure, and a result of the downward movement of the drill-string which leads to a sudden increase in bottom-hole pressure, respectively) and since the flowing flow-rate, together with rotary speed, influence the pressure acting against the formation, but at the same time, must be maintained at a minimum magnitude for hole cleaning and drillability purposes, respectively.

Figure 31 and Figure 32 detail other information from these wells with highlights to the overburden pressure trends and the bottom-hole environmental temperatures.

Figure 31 - Historical overburden pressures for the pre-salt wells # A, B, D, E, G and H.

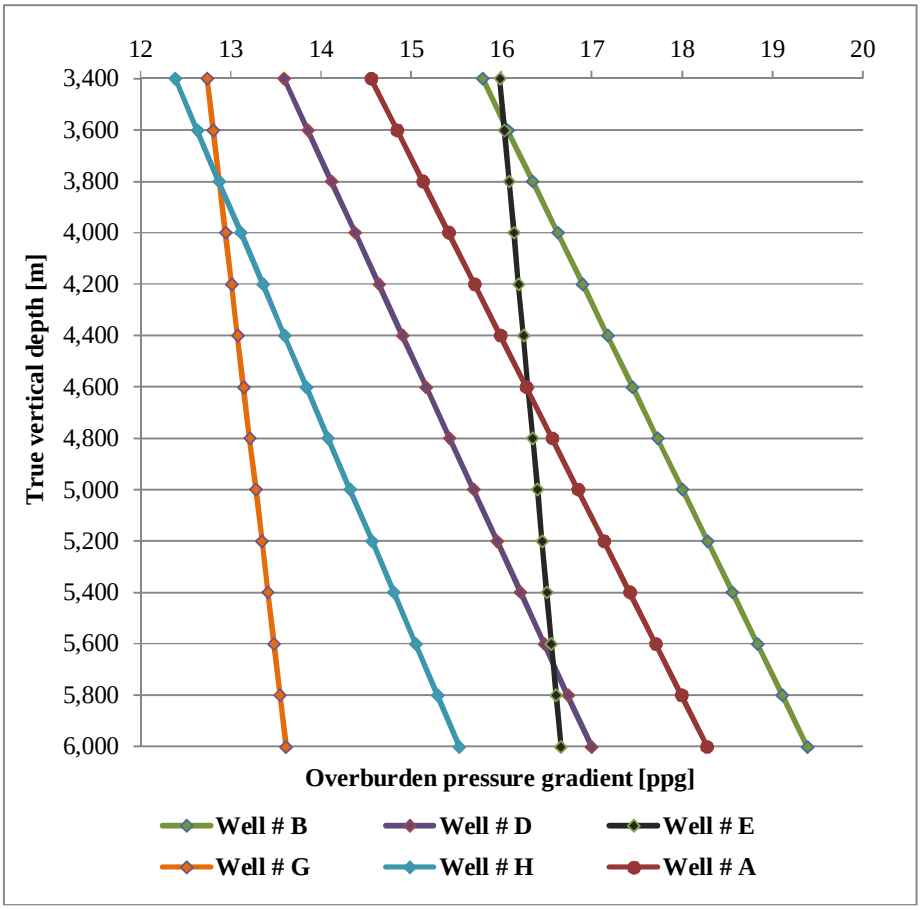

Figure 32 - Historical temperatures for the pre-salt wells # B, D, E, G and H.

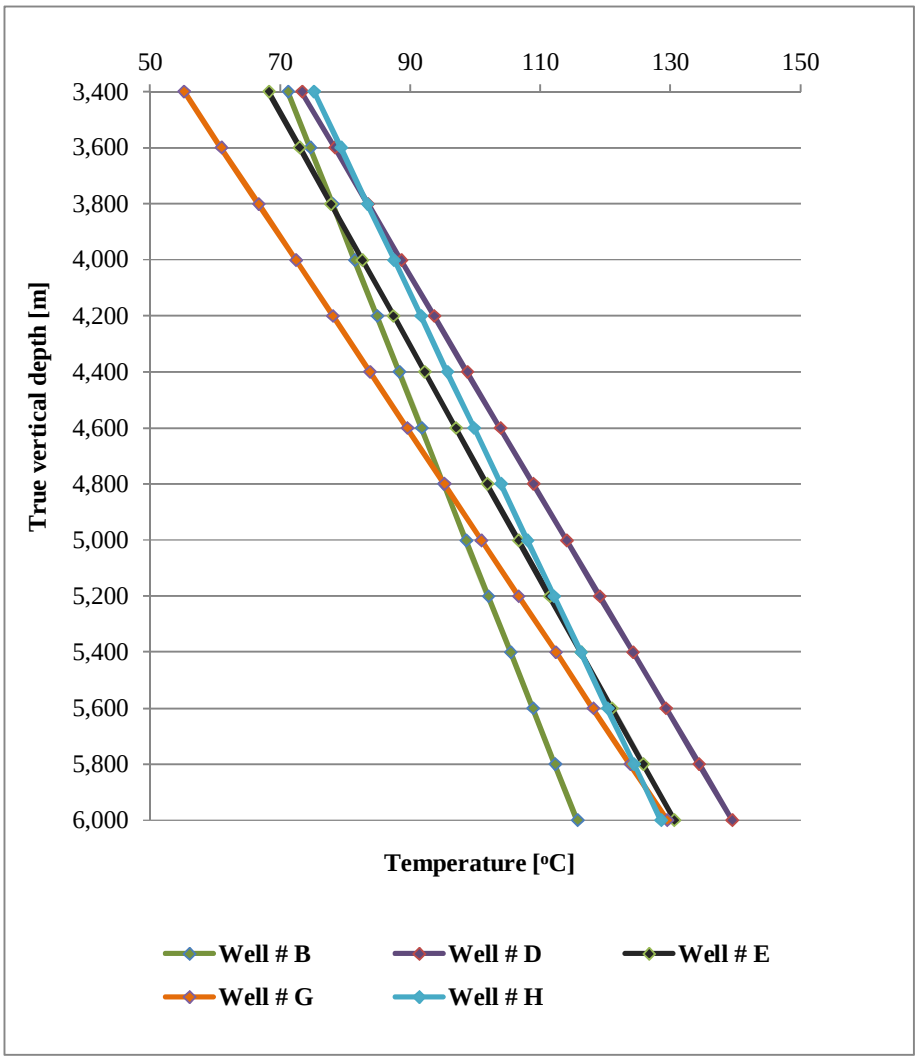

Regarding temperature, the lowest considered level is about 55 [ºC] while the highest is about 140 [ºC]. These temperatures a very close to the industry limit in classifying it as a high temperature (HT) well, which has as a lower boundary limit 149 [ºC] (LEFFLER et al., 2003). Further, once the information about the well is provided, it is important to verify the drilling environments and all have been in use while operating them in order to understand in how far the applicability of the drilling fluids and other factors were in accordance to the integrity needs.

3.4 DRILLING OPERATIONAL PERFORMANCE ANALYSIS

Considering the fact that such pre-salt wells happen in remote locations (Figure 4), these activities demand specific management plans and platforms in order for the operations to be carried out properly. Based on the different types of drilling platforms in the market, the most

suitable for these operations are the drill-ships and the semi-submersibles. The performance of the operation depends on the port, the automation level of a drilling platform, whether single or dual-derrick capable, and the efficiency of the personnel (known in the industry as rig crew). It is important to note that there are, in normal drilling platforms (known in the industry as drilling-rigs), other activities being conducted at the same time and off-line (a term used in the petroleum industry to refer to an activity being performed in parallel to the primary ongoing ones, that does not demand time from the primary one). In most cases, activities are related to each other in a chain of linked tasks, so that improvements gained in one spot could lead to a chain of improvements, thus drastically increasing the performance of the whole operation. All these events, if performed optimally, can lead to a considerable positive impact on drilling activities that are not necessarily linked just to the speed (known in the industry as rate of penetration) that one can effectively penetrate and advance through the pre-salt formation (as presented in the next sub-chapters), but can produce efficiency in operational tasks as well.

Following these facts, it is crucial to distinguish the different tasks and environments in which the activities take place, in order to quantify and to compare their performance by means of a referential benchmark (BMK) or target optimum value, defined as the P50 of a pool of samples; this guarantees a good middle-estimate reference for 50% of the best performances (ANDERSEN et al., 2009; MAIDLA et al., 2010; AFIFI et al., 2015). This methodology allows possible performance improvements in which some of the several comparable scenarios are: activities performed on different drilling-rig types, with different crews working in different working hours, with different sizes of sections (e.g. 8.5, 12.25 and 10.63 [in]), tripping-in/out-of-hole (TH) speed. Also to consider are the time spent in taking surveys, time spent in making-up (M/U) bottom-hole-assemblies (BHAs), in making drill-pipe connections while drilling (known in the industry as connection time weight-to-weight - W2W), in BHA shallow-hole-testing (SHT), among others.

Table 8 summarizes the historically activity trends for drilling operations performed in the wells in reference, in which the representation in the column done by *S.* stands for sampling quantity, meaning the amount of information gathered for allowing calculating the averaged value posted in the table. The table provides: distinguishing between day and night working hours, the pulling-out-of-hole (POOH) or tripping-out speed, the running-in-hole (RIH) or tripping-in speed, the time spent in M/U the BHAs, the time needed for W2W connections, the time spent in taking surveys, and the reported non-productive-time (NPT) of the operations. For the rig crew, night-shift employees are on duty from midnight (24h00min) to noon (12h00min)

and the day-shift on duty from noon (12h00min) to midnight (24h00min). The abbreviation *n/a* stands, in this case, for not available, and substitute the blank field for textual esthetics purposes, since not enough information were available for the well # E.

Table 8 - Historical drilling contractor performance for the wells # A, B, C, D, E, F, G and H.

Well #	Work period	POOH [m/ min]		RIH [m/ min]		W2W connection [min]		Taking survey [min]		M/U BHA + SHT [min]		NPT [min]
		Time	S.	Time	S.	Time	S.	Time	S.	Time	S.	
A	Day	5.73	2	3.51	3	15.17	6	5.5	2	433	3	1,065
	Night	5.6	3	2.24	2	n/a	n/a					
B	Day	4.29	3	4.70	2	n/a	n/a	7	5	480	3	450
	Night	3.97	2	3.53	2	n/a	n/a					
C	Day	4.87	5	4.45	6	12.2	5	5.56	14	375	2	2,745
	Night	4.44	6	5.01	3	12.33	6					
D	Day	6.43	8	4.81	9	12.2	5	6.8	10	344	5	470
	Night	5.55	6	5.33	11	18.5	2					
E	Day	4.34	2	5.39	2	n/a	n/a	n/a	n/a	353	2	No events reported.
	Night	8.14	3	6.05	2	n/a	n/a					
F	Day	4.15	1	5.03	1	11	3	6.88	16	620	1	1,050
	Night	5.69	1	2.08	1	11.67	3					
H	Day	4.45	12	5.34	7	12.5	3	5	2	420	6	4,800
	Night	3.83	9	5.15	8	13.5	4					

Source: (BDEP, 2010; CDC, 2015).

In terms of POOH and RIH speed, presented in the graphs shown in Figures 33 and 34, the existent differences in terms of performance are related to different crews working on different time periods and also working for different hole sizes activities. There are a lot of events that can cause such value differences in terms of rig crew performance, such as: rig crew already onboard for a long period, members in a specific rig crew new to a particular task, experienced rig crew that is too agile or crew members that uses, unfortunately, short-cuts to perform the activities without not considering the mandatory safety precautions, and unforeseen events.

In all these cases, there is no consideration for machinery differences nor drilling conditions, since most of these tripping operations are not strictly related to the penetration of the pre-salt rock itself. The same applies to the W2W connection time, which is from the time-stamp ranging between having the tools in slips to the time of reaching the bottom of the hole again to continue drilling.

The reason for that is linked to the fact that, when drilling pre-salt sections, it is common to ream-up and ream-down (activity known, in this specific case, for smoothing the interval just

drilled) twice at the end of each stand, prior to proceeding with the drill-pipe connection itself. Thus, after finishing drilling the stand, the subsequent task is not necessarily to bring the drill-string into slips. In addition, it is a common practice, given the pre-salt layers depth and the weaknesses of the telemetry signals in these environments, to perform the surveying right after the reaming task and just before bringing the drill-string into slips. This allows a possible second survey to be taken during the connection and provides time for data analysis while performing the connection task takes place. In terms of surveying time, what basically drives it is the action in place for prompting the values and the communications between the surveying personnel and the drillers or directional drillers in order for them to carry on with the operation. In terms the M/U BHA timing, what mainly drives the time spent on it is the rig crew's efficiency combined with the BHA complexity and needs of one or more SHTs (test in which the down-hole tools are tested near the surface or below a specific safety datum for communication and data transmission assurance).

Figures 33 to 35 detail, in histogram graph plots, the information provided in Table 8 in terms of W2W connection time and POOH/ RIH speed for each well under analysis, organized by work shift schedule and hole sizes.

Figure 33 - Historical drilling operational performance indicator for POOH.

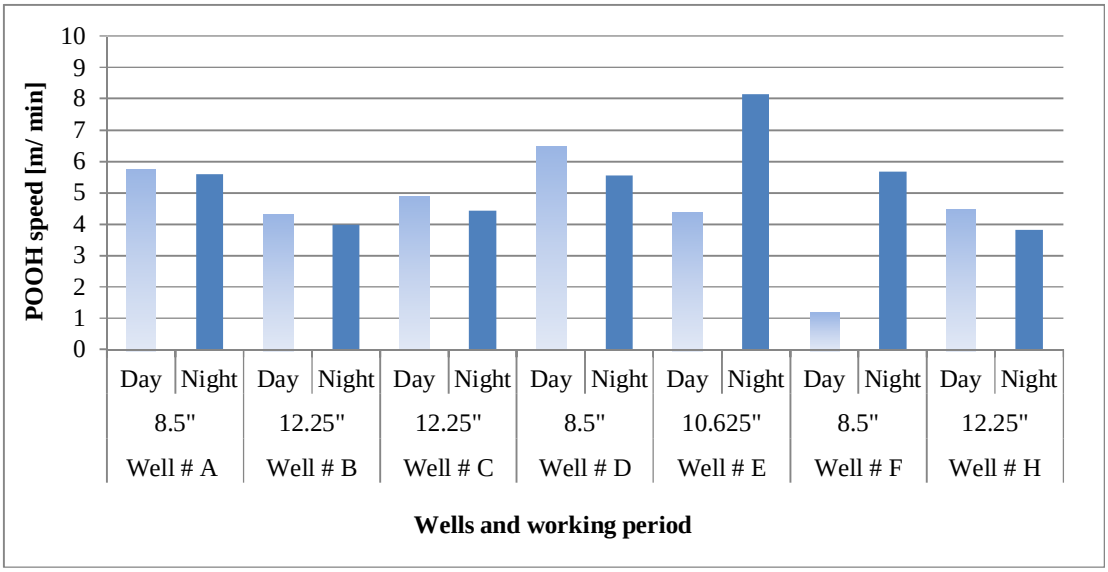

Source: (BDEP, 2010; CDC, 2015).

Figure 34 - Historical drilling operational performance indicator for RIH.

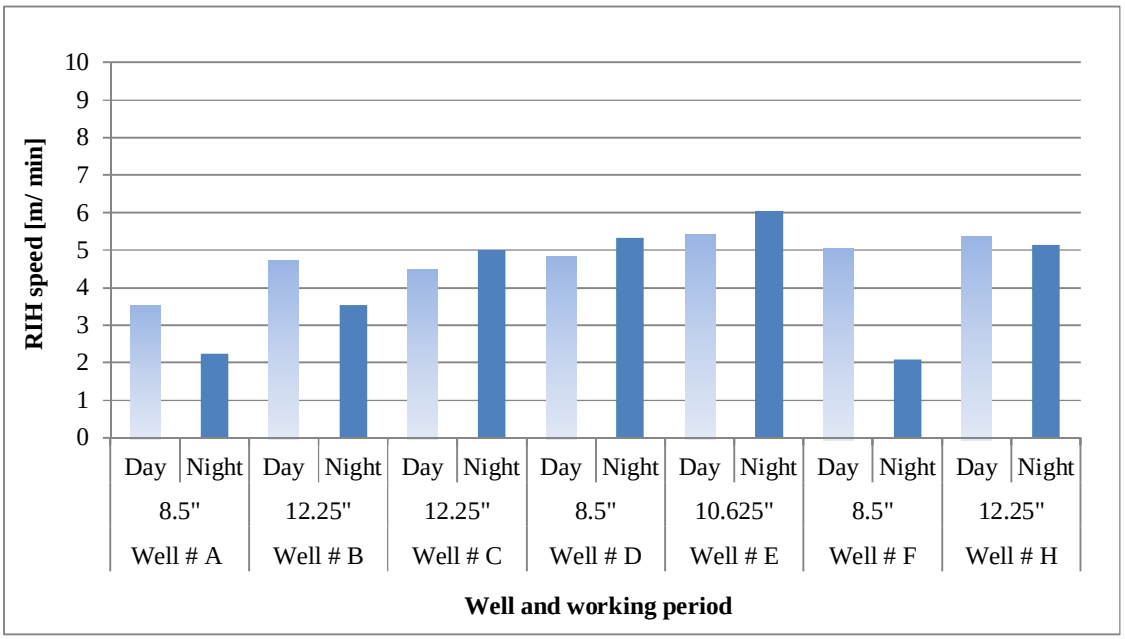

Source: (BDEP, 2010; CDC, 2015).

Figure 35 - Historical drilling crew operational performance indicator for W2W connection.

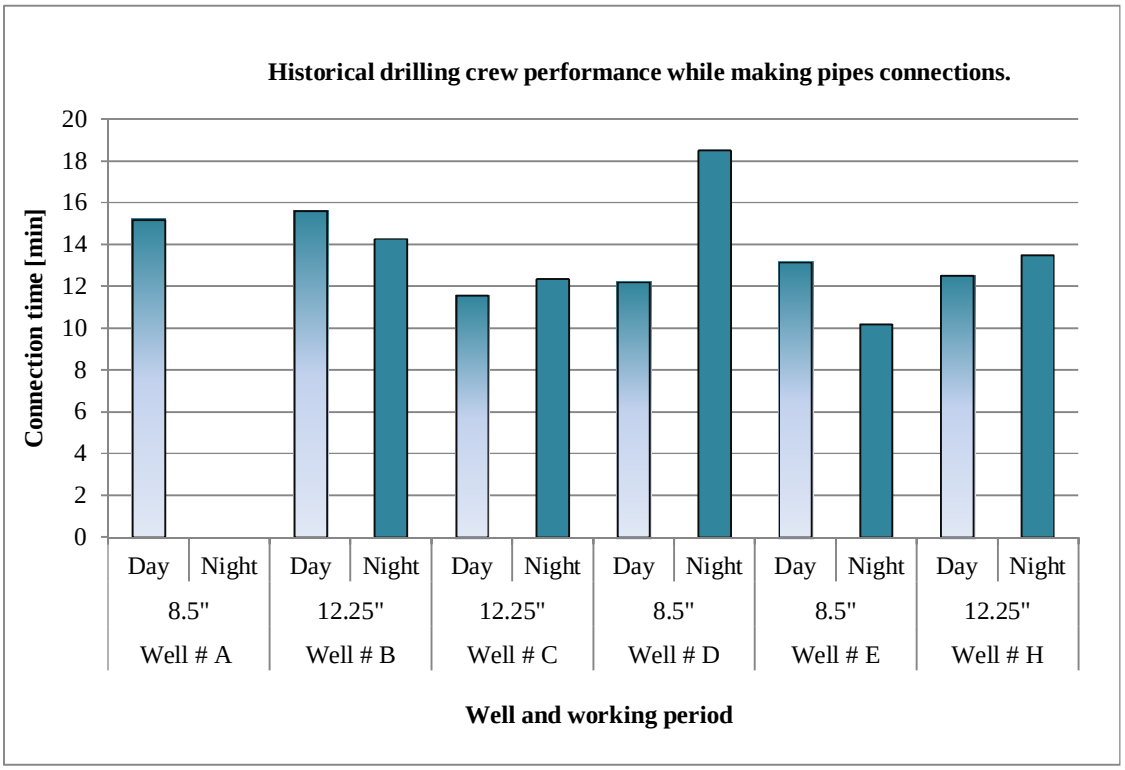

Source: (BDEP, 2010; CDC, 2015).

Considering that the technology available for both drilling-rig types in use for the pre-salt wells and the sections are of the same level (with dual-derrick capability) and considering that, due to the nature of the data provided and the long period attached to a pre-salt section operation which drives to the necessity of combining samples for statistical data analysis, the data set from all the wells were used together to permit trending to a specific benchmark as a reference for the analysis of the activities' performance. This allowed measuring how efficiently the activities were being performed and how much possible invisible lost time (ILT) were implicit in such a way that, considering the benchmarking references, some of the performance could be improved, guaranteeing an operational boost in terms of performance (MAIDLA et al., 2010; AFIFI et al., 2015. Figure 36, Figure 37, Figure 38, Figure 39 and Figure 40 represent historical histograms for POOH speed, RIH speed, W2W connection time, surveying time and BHA make-up time.

From the histograms presented, the red bars represent the P50 and has been set as a benchmarking target value, as a first reference, and before further data were available for benchmarking learning (AFIFI et al., 2015). By setting the target values, the potential savings can be calculated by stating that all events showing performance lower than the targeting value would have potential for improvements, at least, up to the set benchmarking. Important to highlight is the fact that events that were too fast, differing considerably from the histogram distribution mean value, may not represent a real optimum benchmarking choice, but just a possible equipment and/ or machinery technical operational limit. Thus, it may not take into account several specific events and human interaction that has to be accounted on top of just machinery performance, including taking care in the activities, thinking on safety first, double-checking crew understanding for the step-by-step operational tasks, among others.

Figure 36 - Historical performance analysis and benchmark for POOH activity.

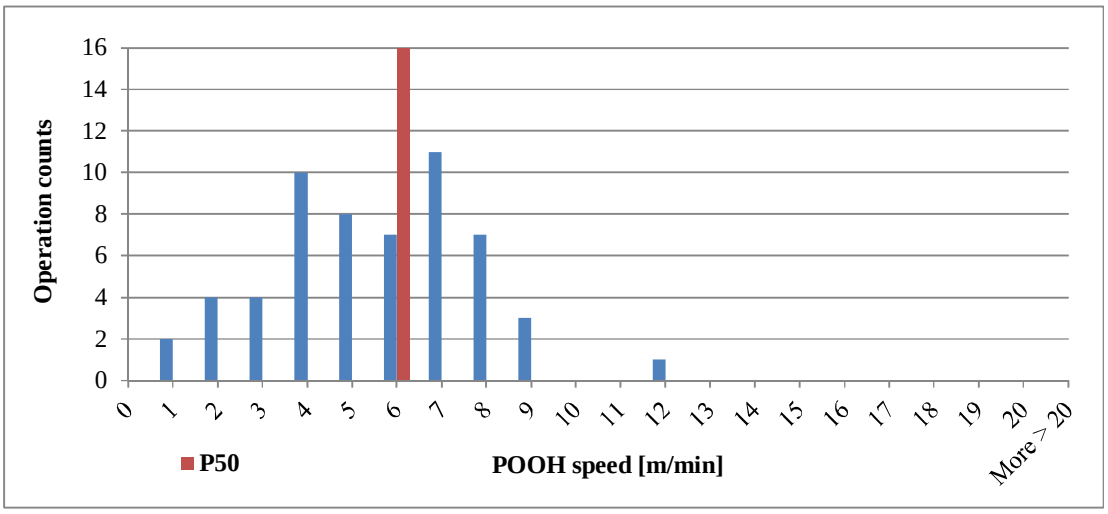

Source: (ANDERSEN et al., 2009; MAIDLA et al., 2010; BDEP, 2010; AFIFI et al., 2015; CDC, 2015).

Figure 37 - Historical performance analysis and benchmark for RIH activity.

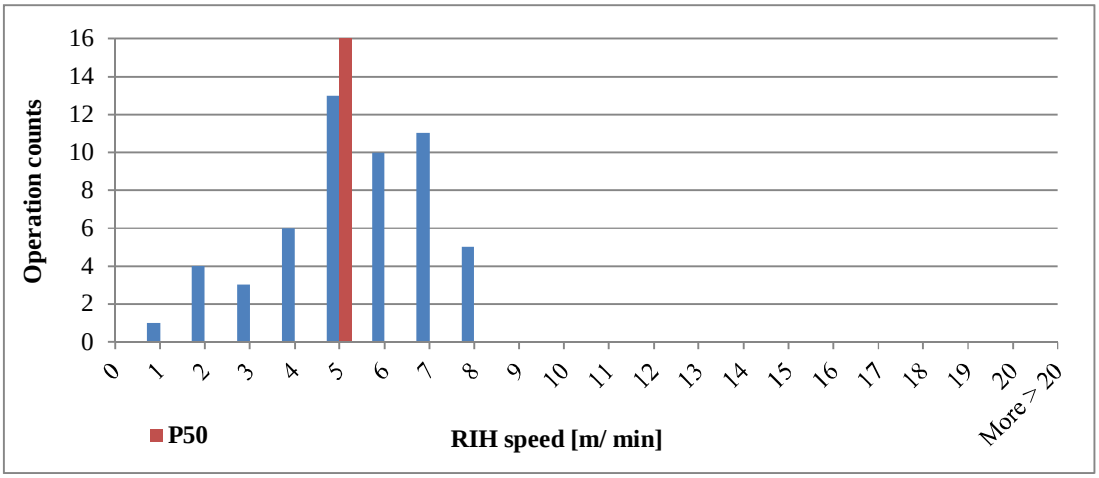

Source: (ANDERSEN et al., 2009; MAIDLA et al., 2010; BDEP, 2010; AFIFI et al., 2015; CDC, 2015).

Figure 38 - Historical performance analysis and benchmark for surveying.

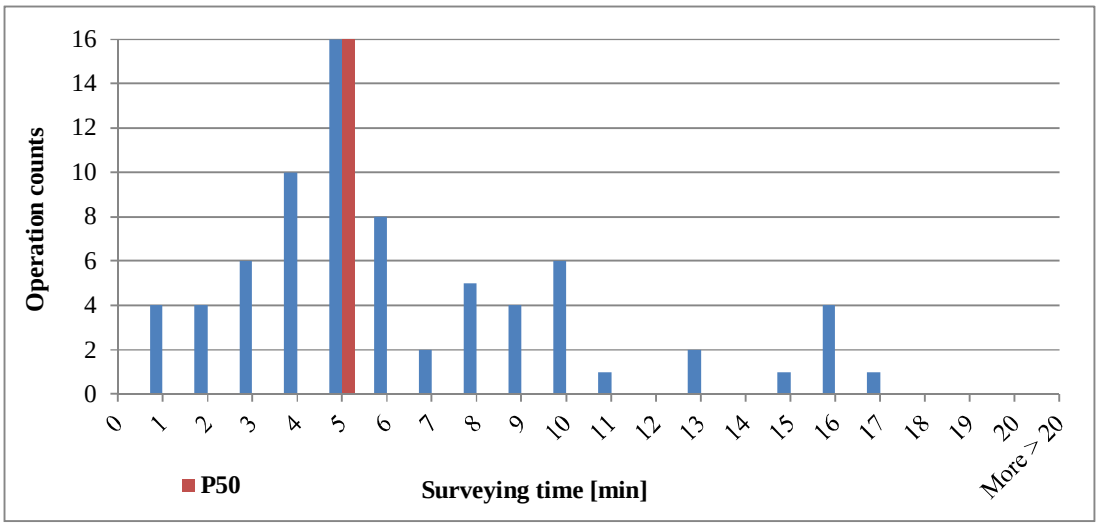

Source: (ANDERSEN et al., 2009; MAIDLA et al., 2010; BDEP, 2010; AFIFI et al., 2015; CDC, 2015).

Figure 39 - Historical performance analysis and benchmark for W2W connection time.

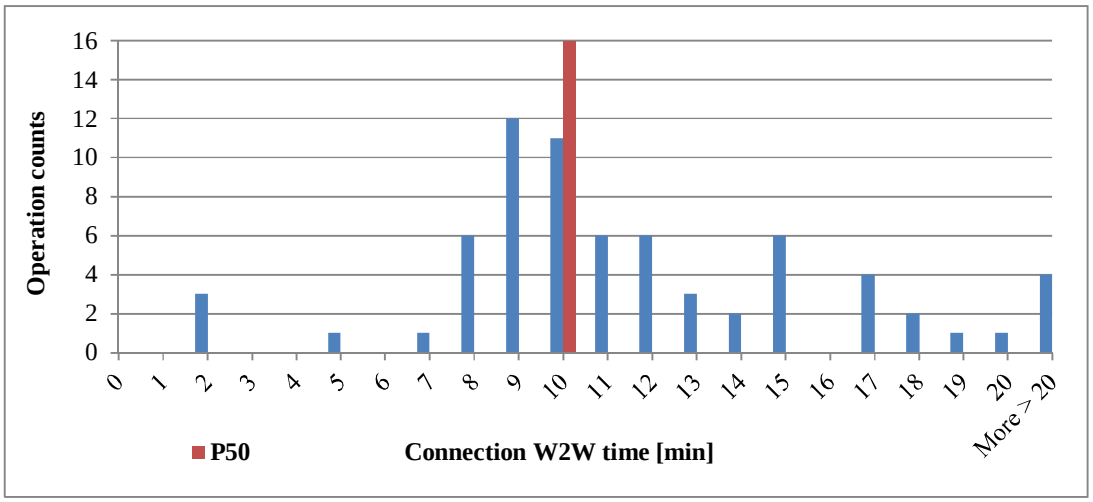

Source: (ANDERSEN et al., 2009; MAIDLA et al., 2010; BDEP, 2010; AFIFI et al., 2015; CDC, 2015).

Figure 40 - Historical performance indicator for M/U of BHAs + SHT.

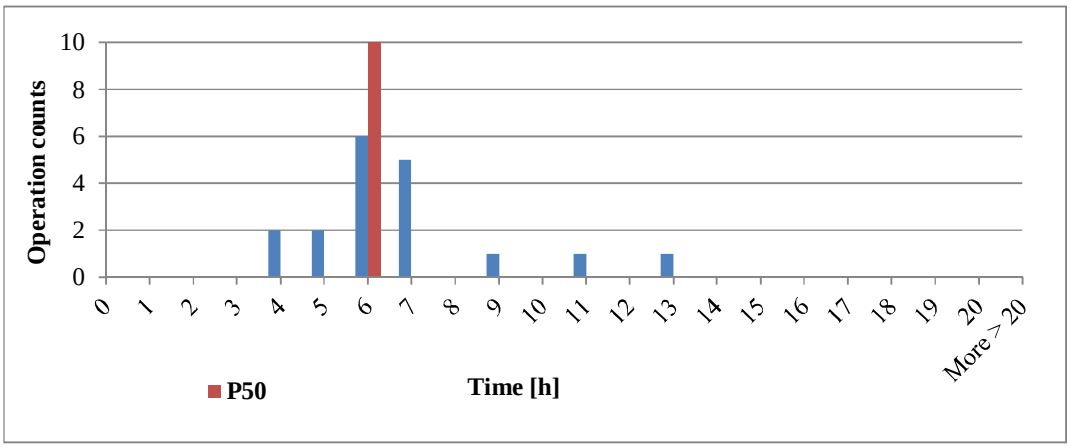

Source: (ANDERSEN et al., 2009; MAIDLA et al., 2010; BDEP, 2010; AFIFI et al., 2015; CDC, 2015).

Following the analysis already performed, Table 9 details possible improvements for the M/U BHA activity, while Table 10 covers the same in terms of RIH and POOH speeds. Table 11 details similar information for surveying and W2W connection time.

Considering that the operation counts for M/U BHAs mean essentially how many times a BHA has to be made-up or further, how many runs, at least, one pre-salt section had for a particular well, the potential time that could be saved for one M/U BHA task was multiplied by the numbers of operation counts that were possible to be gathered, and so, providing the minimum boundary of potential savings. The same idea has been used for the whole wells under analysis demonstrating that savings for this particular task could reach up to six hours for a particular pre-salt well (e.g. well # H).

Table 9 - Data performance analyses from for M/U BHA and SHT as per Figure 40.

Well #	Time-frame [min]			Potential minimum saving [h]
	M/U BHA + SHT	BMK	Operation counts	
A	7.22	6	3	3.66
B	7	6	3	3
C	6.25	6	2	0.5
D	5.73	6	5	0
E	5.88	6	2	0
F	10.33	6	1	4.33
H	7.01	6	6	6.06

Source: (BDEP, 2010; CDC, 2015).

With the same methodology used for calculating the savings for M/U BHA with SHT, Table 10 summarizes the POOH and RIH speeds for the wells under analysis together with the total tripping time for that particular section and respective runs, in which approximately up to 19 [h] of operational tripping activity could have been saved for the well # H. Thus, by comparing these values to the benchmark ones, was possible to verify in how much percentage the speed was under-efficient (again: when compared to the benchmark), enabling translating it in tripping time improvements, yielding possible minimum operational saving hours. For this analysis in particular, all tripping activities were considered similar (with no distinguishment between POOH and RIH activities) so that from the total tripping time gathered, half has been counted as RIH and half as POOH activity. And, in Table 11, the analysis are considering counting for surveying and W2W connection time together, in which up to 30 [min] of potential time saving could be drawn for the well # F (for this calculation, each W2W connection and surveying time were subtracted from the benchmark and then multiplied by the amount of evidenced operation counts, being summed up together to yield the final potential saving).

In terms of POOH and RIH, the difference between the actual speed and the benchmarking speed was computed in such a way that the faster is tripped, the less would the tripping time be, and so, allowing to save time for the operation. The tripping time, per specific run, was divided into two, and one half of the tripping time was then compared to the possible benchmarking speed difference allowing then more reliable potential savings estimation. In terms of W2W connection and surveying time, the possible operational savings, in time, would be the subtraction of the actual time spent and the benchmark.

Important to note for verifying Table 10 and Table 11 is that under-efficiency means, basically, the difference between the real experienced values and the set benchmarks. The column *op. c.* is an abbreviation for operational counts and *connec.* an abbreviation for connection. These abbreviation were necessary since it was not feasible to write the full text name text in space given by the tables' field.

Table 10 - Operational efficiency analysis for POOH and RIH speed for the wells # A, B, C, D, E, F and H.

Well #	Speed [m/ min]						Tripping time [h]										Potential minimum saving [h]
							Run #										
	POOH	BMK	Under-efficiency %	RIH	BMK	Under-efficiency %	1	2	3	4	5	6	7	8	9	10	
A	5.73	5	0	3.51	5	29.8	56	19.98	27.12	n/a	n/a	n/a	n/a	n/a	n/a	n/a	15.36
B	4.29	5	14.2	4.7	5	6	32.08	34.07	24.34	n/a	n/a	n/a	n/a	n/a	n/a	n/a	9.13
C	4.87	5	2.6	5.01	5	0	33.1	29.5	40.58	32.91	35.16	n/a	n/a	n/a	n/a	n/a	2.23
D	6.43	5	0	5.33	5	0	24.5	25.33	25.61	25.17	23.75	25.75	24.12	n/a	n/a	n/a	0
E	8.14	5	0	6.05	5	0	26.5	26.45	n/a	n/a	n/a	n/a	n/a	n/a	n/a	n/a	0
F	5.69	5	0	5.03	5	0	40.05	43.43	n/a	n/a	n/a	n/a	n/a	n/a	n/a	n/a	0
H	4.45	5	11	5.34	5	0	35.33	36.78	48.02	38.14	44.1	35	51.32	41.6	30.05	x	19.82

Source: (BDEP, 2010; CDC, 2015).

Table 11 - Wells drilling contractor efficiency analysis for W2W connection and surveying for the wells # A, B, C, D, E, F and H.

Well #	Time-frame [min]						Drilled footage [m]										Potential minimum saving [min/ h]
							Run #										
	W2W Connec.	BMK	Op. c.	Sur-veying	BMK	Op. c.	1	2	3	4	5	6	7	8	9	10	
A	15.17	12	6	5.5	5	2	135	37,7	29,3	n/a	n/a	n/a	n/a	n/a	n/a	n/a	20.02/ 0.33
B	n/a	12	n/a	7	5	5	102	153	163	n/a	n/a	n/a	n/a	n/a	n/a	n/a	10/ 0.16
C	12.2	12	11	5.56	5	14	78	194	193	92	266	n/a	n/a	n/a	n/a	n/a	10.04/ 0.16
D	12.2	12	7	6,8	5	10	146	46	64	40	54	60	77	n/a	n/a	n/a	19.4/ 0.32
E	n/a	12	n/a	n/a	5	n/a	35	54	n/a	60	23	75	63	95	44	208	n/a
F	11	12	2	6.88	5	16	248	95	x	x	x	x	X	x	x	x	30.08/ 0.5
H	12.5	12	7	5	5	2	n/a	74	89	39	n/a	39	56	167	138	x	3.5/ 0.05

Source: (BDEP, 2010; CDC, 2015).

It is important to note that these findings by themselves may not look much expressive, but, considering the endorsements from the beginning where it was highlighted how much expensive such pre-salt operations are (raging between 641,985.00 to 1,374,755.00 [USD/ day]), just the potential saving of 48.8 [h] for the well # C (Table 12) can represent, minimally, an operational cost reduction of about 522,147.80 [USD].

Table 12 - Historical total potential savings for the pre-salt wells under analysis.

Well #	ILT [h]			NPT [h]	Total potential minimum saving [h]
	M/U BHA + SHT	Connection + survey	TIH		
A	3.66	0.33	15.36	17.75	37.1
B	3	0.16	9.13	7.5	19.79
C	0.5	0.16	2.23	45.75	48.8
D	0	0.32	0	7.83	8.15
E	0	n/a	0	0	0
F	4.33	0.51	0	17.5	22.34
H	6.06	0.06	19.82	80	105.94

Source: (BDEP, 2010; CDC, 2015).

All these information and analysis are crucial for understanding and quantifying where exactly exist possibilities of improvements, and also to serve as key data for feeding the subsequent analysis presented in the next sub-chapters.

3.5 DRILLING MECHANICS PERFORMANCE AND ANALYSIS

Considering that, essentially, there are different variables influencing the drilling processes, and that some of these variables are more flexible for adjustments and that some are not adjustable at all, it is important to highlight which of the drilling mechanics parameters allows certain degree of changeability and their subsequent window of variation or constrains. The constrains and limitations to be considered may not be always related just to the choosiness of best parameters for a better performance, but are also related to the limitation of the down-hole tools (e.g. tools for logging-while-drilling - LWD and measuring-while-drilling - MWD, rotary steerable systems - RSS, positive displacement motors - PDM, turbines, among others) in use for a particular operation. From the different parameters in place and governing the drilling activity, there are some that have to be chosen considering in a first step and for economic reasons the life of the down-hole tools, and then, the optimum ones in order to guarantee better efficiency. The main parameters to be considered are: fluid flow-rate, WOB, torque, rotary speed, ECD/ ESD (dependent mainly on EMW, secondarily on flow-rate and tertiary on rotary

speed), among others. But, historical data gathered from the pre-salt wells under analysis show that in some particular cases (Table 13), the boundaries limitations specified from the drilling programs (Drill. prog.) have been allowing rooms for self-decision while the drilling operations were on going in which the final chosen drilling mechanics parameters values could exceed the down-hole tools limitations, as is the case evidenced for the WOB (e.g. wells # D, E and H) and flow-rate (e.g. wells # E and H).

Table 13 - Historical parameters boundaries from equipment and drilling programs.

Well #	**EMW [ppg]**	**Flow-rate [gpm]**	**Torque [ft-klbf]**	**WOB [klbf]**	**Rotary speed [rpm]**	**Bit size [in]**	**MD [m]**
	Lower boundary - Upper boundary						
A Tools/ Drill. prog.	n/a/ 9.5 - 9.8	400 - 800/ n/a	n/a - 12/ n/a	n/a - 20/ n/a	n/a - 250/ n/a	8.5	3,993 - 4,195
B Tools/ Drill. prog.	n/a/ 9.3 - 10	400 - 800/ 600 – 800	n/a - 35/ n/a - 12	n/a - 80/ 20 – 60	n/a - 250/ 80 - 150	12.25	3,405 - 3,872
C Tools/ Drill. prog.	n/a/ n/a	600 - 1,200/ n/a	n/a - 23/ n/a	n/a - 55/ n/a	n/a - 220/ n/a	12.25	4,487 - 5,313
D Tools/ Drill. prog.	n/a/ 9.8 - 10	342 - 600/ x - 550	n/a - 12/ 5 - 8	n/a - 24/ 15 - 35	n/a - 220/ n/a - 150	8.5	4,400 - 4,887
E Tools/ Drill. prog.	n/a/ n/a	400 - 1,200/ n/a - 750	n/a - 23/ 10 - 20	n/a - 54/ x - 60	n/a - 220/ n/a - 150	10.63	4,665 - 5,475
F Tools/ Drill. prog.	n/a/ 9.2 - 9.8	600 - 1,200/ n/a	n/a - 35/ n/a	n/a - 56/ n/a	n/a -220/ n/a	12.25	4,899 - 5,879
G Tools/ Drill. prog.	n/a/ 9.93 - n/a	n/a/ 660 - 740	n/a/ n/a	n/a/ 2 - n/a	20 - 150/ 60 - 120	12.25	5,255 - 5,600
H Tools/ Drill. prog.	n/a/ 9.6 - 10.2	600 - 1,200/ 600 - 800	n/a - 23/ n/a	n/a - 33/ 10 - 70	20 - 150/ 80 - 140	12.25	5,050 - 5,840

Source: (BDEP, 2010; CDC, 2015).

The flow-rate limitations from the tool's side represent a minimum magnitude needed for them to turn-on, while the maximum represents how much flow could be withstand by them. The rotary speed, WOB and torque limitations show basically the maximum value that could be withstood by the down-hole tools and that should be used when drilling considering optimization designs, while the minimum represents basically minimum needs for measuring purposes and a starting point from which the formation starts feeling the parameters imposed, understood in general as a threshold. In terms of the EMW it is noticeable that the window

allowed for its design in the drilling programs have differed from the possible limits shown in terms of the narrow window between the pore pressure and fracturing pressure presented in previous sub-chapter.

The drilling mechanics parameters used in the pre-salt wells under analysis and the respective ROPs are detailed one by one in extensive tables in Appendix A.

3.6 DRILL-BIT PERFORMANCE AND ANALYSIS

In terms of drill-bit performance analysis it is crucial to verify the drillability achieved in terms of footage and operating time effectively on bottom while making new hole; this, in order to allow a reliable analysis of the possibilities of optimization for the pre-salt, given the gathered information from the sections under analysis. All the thirty eight pre-salt recorded runs are presented in the Tables 14, 15, 16 and 17, being organized per type of drill-bit used: PDC, TCI, hybrid and diamond impregnated, respectively (the definition of each type of drill-bit can be seen in chapter two). Note that the letter “x” is being used in these tables to denote and mark the problems encountered when grading the drill-bits. More drill-bit performance detailed information, organized per pre-salt well, are presented in Appendix B.

From all these information, was possible to drive statistical analysis in terms of which drill-bits have had better performance on top of the other types, considering that all drill-bits used were new and that the main reason given for POOH was the low ROPs experienced. For the analysis performed, almost 50% of the runs comprehended usage of PDC drill-bits, 33% usage of TCI drill-bits and the remaining, usage of hybrid and diamond impregnated drill-bit (abbreviated as *diamond impreg.* in the graphs and tables for better visualization purposes) (Figure 41).

Figure 41 - Historical distribution of drill-bits usage for the pre-salt wells # A, B, C, D, E, F, G and H.

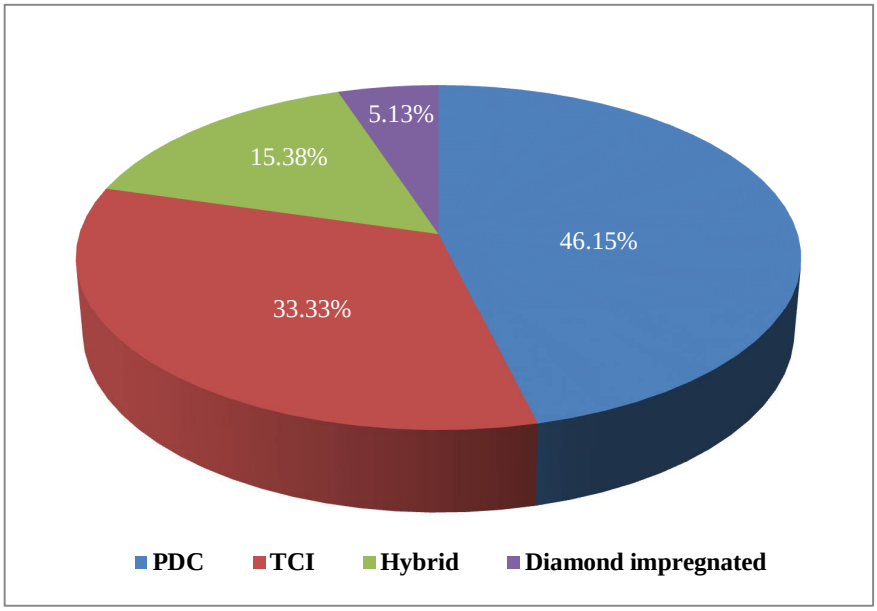

Source: (BDEP, 2010; CDC, 2015).

Table 14 - Historical pre-salt PDC drill-bit performance and record.

PDC #	Gauge		Teeth-cutters characteristics				Teeth-cutters wear/loss level		Bit performance		
	In	Out	Broken	Worn	Chipped	Others	Inner	Outer	Footage [m]	Hours [h]	ROP [m/ h]
1	x		x			x	4	2	135	54.5	2.48
2	x		x		x		0	1	102	42.9	2.38
3	x			x	x		1	1	163	61	2.67
4	x			x	x		1	2	78	18	4.33
5	n/a	n/a	n/a	n/a	n/a	n/a	n/a	n/a	92	73.53	1.25
6	x				x		1	1	266	54.98	4.84
7	x		x			x	7	2	146	46.9	3.11
8	x				x	x	7	4	46	19.15	2.4
9	x		x			x	4	2	32	26.9	1.19
10	x		x	x			2	1	208	51.91	4.01
11	n/a	n/a	n/a	n/a	n/a	n/a	n/a	n/a	248	68.62	3.61
12	x			x			1	2	592	82	7.22
13	x		x				0	2	75	14.7	5.1
14		x				x	8	8	89	42.25	2.11
15		x	x	x			7	5	39	17.48	2.23
16		x		x	x		5	4	56	39.34	1.42
17		x	x	x			4	4	167	110.85	1.51
18	x			x	x		1	3	138	48.61	2.84

Source: (BDEP, 2010; CDC, 2015).

Table 15 - Historical pre-salt TCI drill-bit performance and record.

TCI #	Gauge		Teeth-cutters characteristics				Teeth-cutters wear/loss level		Bit performance		
	In	Out	Broken	Worn	Chipped	Others	Inner	Outer	Footage [m]	Hours [h]	ROP [m/ h]
1	x			x			2	1	40	17.3	2.31
2		x				x	4	8	60	29.61	2.03
3	x		x		x		1	1	77	37.41	2.06
4	x			x			1	1	54	50.03	1.08
5	x			x			1	1	61	29.5	2.07
6		x	x			x	4	2	23	23.23	0.99
7	x					x	8	1	75	68.9	1.09
8	x		x				2	1	63	52.07	1.21
9	x				x		1	1	96	83.48	1.15
10	x		x		x		8	8	44	48.89	0.9
11		x	x	x			2	7	32	19.38	1.65
12		x	x	x			3	8	114	49.57	2.3
13		x	x		x		2	7	39	42.01	0.93

Source: (BDEP, 2010; CDC, 2015).

Table 16 - Historical pre-salt hybrid drill-bit performance and record.

Hy-brid #	Gauge		Teeth-cutters characteristics				Teeth-cutters wear/loss level		Bit performance		
	In	Out	Broken	Worn	Chipped	Others	Inner	Outer	Footage [m]	Hours [h]	ROP [m/ h]
1	x				x		2	1	37.7	31.02	1.22
2	x		x		x		2	1	29.3	34.92	0.84
3	x		x			x	6	6	153	48.5	3.15
4	x		x	x	x		5	6	194	81.33	2.39
5	n/a	n/a	n/a	n/a	n/a	n/a	n/a	n/a	193	92.44	2.09

Source: (BDEP, 2010; CDC, 2015).

Table 17 - Historical pre-salt diamond impregnated drill-bit performance and record.

Dia-mond impreg. #	Gauge		Teeth-cutters characteristics				Teeth-cutters worn/loss level		Bit performance		
	In	Out	Broken	Worn	Chipped	Others	Inner	Outer	Foota-ge [m]	Hou-rs [h]	ROP [m/ h]
1	x			x		x	2	6	64	25.2	2.54
2	x					x	4	8	54	23.58	2.29

Source: (BDEP, 2010; CDC, 2015).

Further, it is possible to visualize in Figure 42 the distribution characteristics per drill-bit after having drilled the pre-salt sections. For the whole runs under analysis, the most presented issues were to have the teeth-cutters broken, and secondly, to have the teeth-cutters worn. These

characteristics are important to be verified into details in order to allow an exactly visualization of which problems may be arising most when penetrating these carbonate formations. Being beyond the main focus of this thesis, the drill-bits manufacturing specifications are not detailed.

Figure 42 - Historical teeth-cutters characteristics after having drillined pre-salt sections.

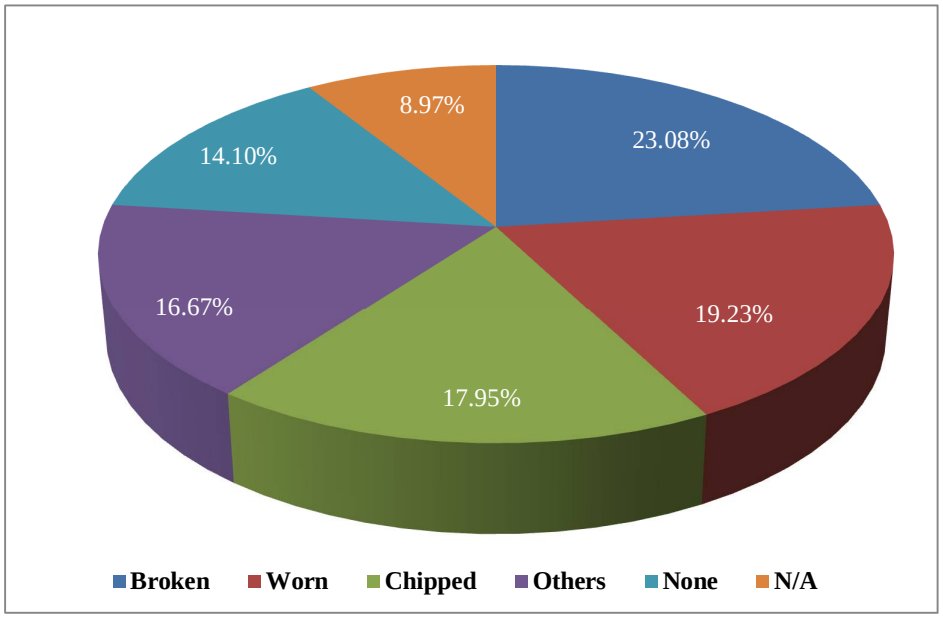

Source: (BDEP, 2010; CDC, 2015).

Considering the footage and ROP achieved with each drill-bit type, the histogram presented in Figure 43 and Figure 44 detail the distribution of events recorded per specific intervals in terms of ROP and footage, respectively. Since these events are interconnected to each other, an isolated analysis may not drive to accurate conclusions; thus, by verifying both distributions together, it is possible to understand that the PDC drill-bit shows a much better performance in terms of footage achieved and ROP on top of the TCI ones. Further, even if there were not much samplings of the other two drill-bit types for allowing a reliable interpretation, from the gathered information presented it is possible to derive, roughly, the idea that the best choices of drill-bits would be, from the best to the worst order of choice: PDC, hybrid, TCI and diamond impregnated. Important variables not taken into account in this step are the cost of a specific drill-bit, the extra work-force, and the extra down-hole tools needed for running it, what would be the case of the diamond impregnated drill-bit. For instance, since for a diamond impregnated drill-bit a high rotary speed may be necessary, an extra down-hole tool (turbine) has to be attached to the BHA in order to provide the extra rotary speed necessary to bring the drill-bit to perform as necessary, what my increase the cost of the operation. Thus, if a much better

performance with the diamond impregnated drill-bit is not clear, it ought not to have it as the best of choice given the expressed point of view.

Figure 43 - Histogram distribution of ROPs per pre-salt used drill-bit.

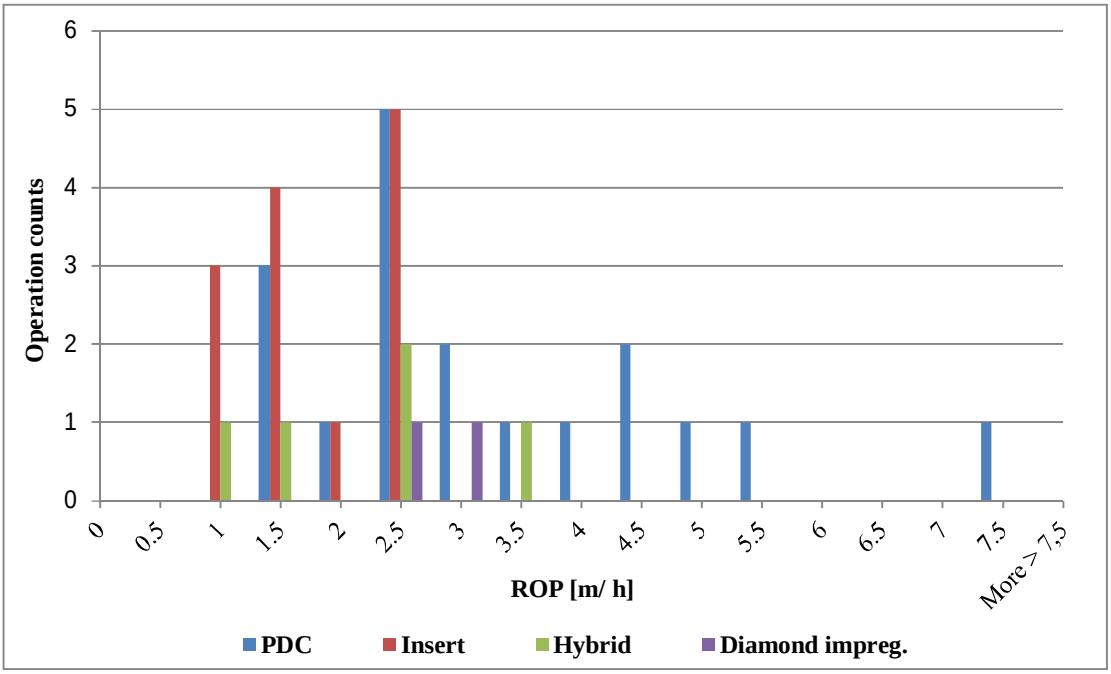

Source: (BDEP, 2010; CDC, 2015).

A methodology to be used in order to quantitatively compare the drill-bits is to bring them to the bases of percentage of teeth-cutters' wear per meter of hole drilled and per effectively hours spent with it drilling on bottom. Thus, Figure 45 presents the available values of teeth-cutters wear evolution in percentage per drill-bit type, accounting, separately, for its inner and outer part. It is conclusive that the PDC presents the lowest level of wear in footage and operating time.

Figure 44 - Histogram distribution of footage per drill-bit type used in the pre-salt wells.

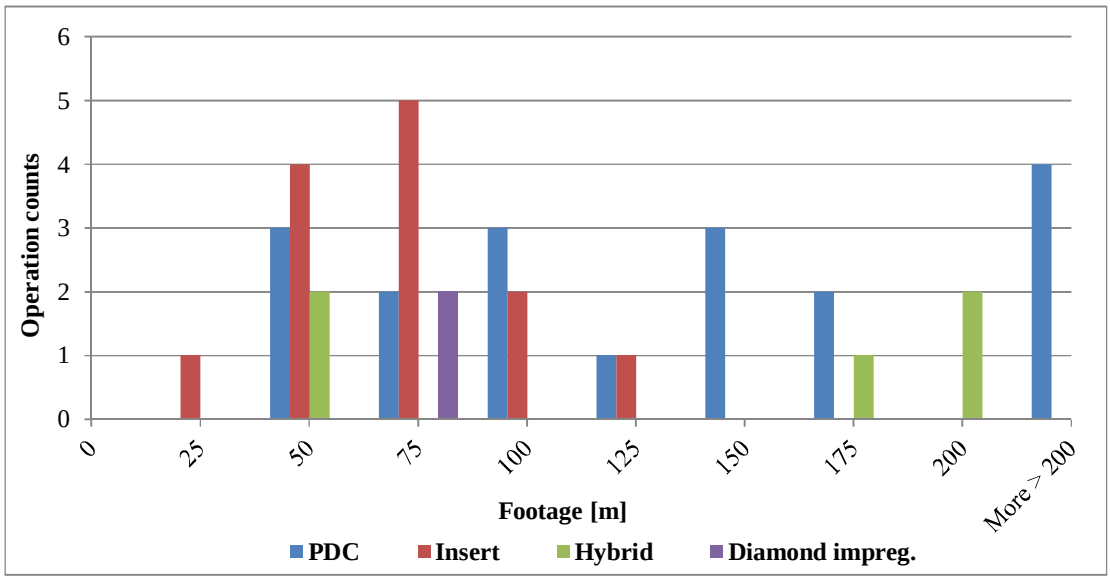

Source: (BDEP, 2010; CDC, 2015).

Figure 45 - Histogram distribution of ROPs per pre-salt used drill-bit type and its dullness.

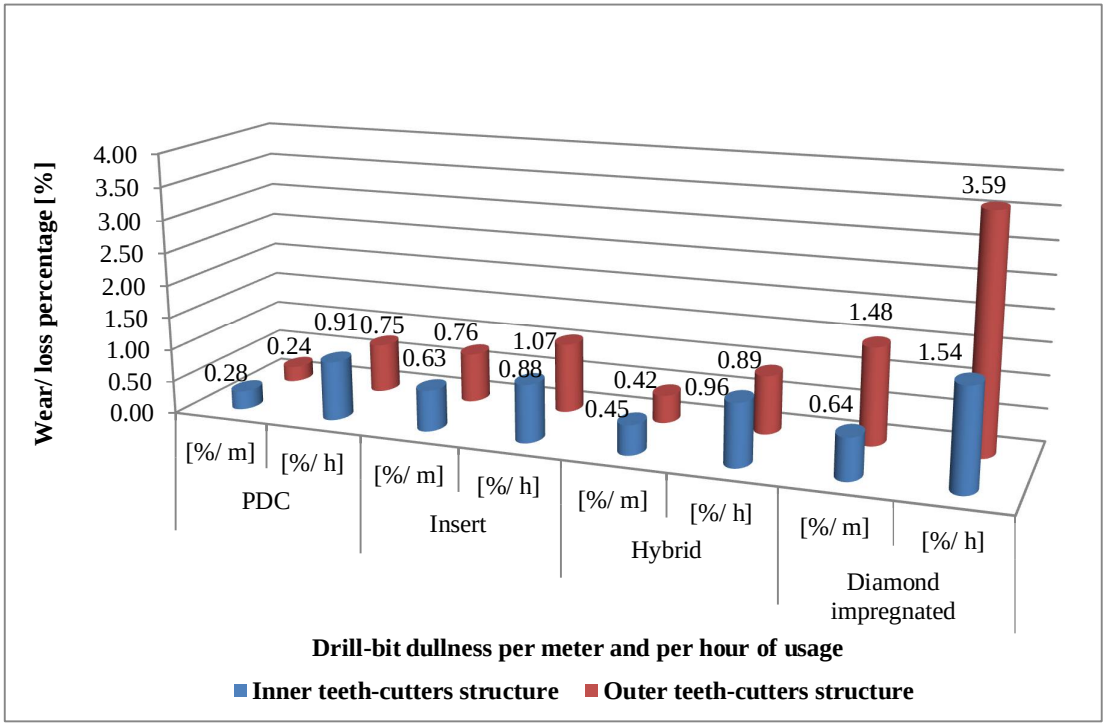

Source: (BDEP, 2010; CDC, 2015).

All these drill-bit information are crucial for feeding the mathematical model presented in the next chapter, since the wear rate has considerable influence in the rate of penetration and specific energy, and so, plays an important role in the optimization processes.

4 OPTIMIZATION MODELING AND RESULTS

From the literature review, there are mainly just a few models in the industry for ROP modeling and some studies in terms of the SE concept. Something new and not raised up to the moment is the SE modeling concept, in which by modeling the ROP itself and placing it in the SE equation followed by specific adjustments, one would be able to model the SE directly. This could then be used on top of the ROP modeling in order to decide upon the operations best set of drilling mechanics parameters to be applied, since SE is less susceptible to small drilling mechanics parameters changes if compared to the ROP (RABIA, 1985), what may allow a better modeling.

4.1 ROP MODEL CHOOSINESS

Following the raised methodology, in a first step, three different ROP models, Cunningham (1960), Maurer (1962) and Bourgoyne Jr. and Young Jr. (1974), were used together with data from the pre-salt well # B - run # 1 to evaluate the best applicable model to these carbonate formation. By making use of the software Oracle Crystal Ball version 11.1.2.3.500 (ORACLE, 2014), a Microsoft Excel add-on, simulations were run (Figure 46), from which the yielded coefficients and residual errors for the modeling are presented in the Table 18.

Figures 47, 48 and 49 detail, graphically, a comparison between the field and the modeled ROP, while Figure 50 shows the software's final simulated results tab for the three mentioned models.

Figure 46 - Example of a simulation run with the software Oracle Crystal Ball.

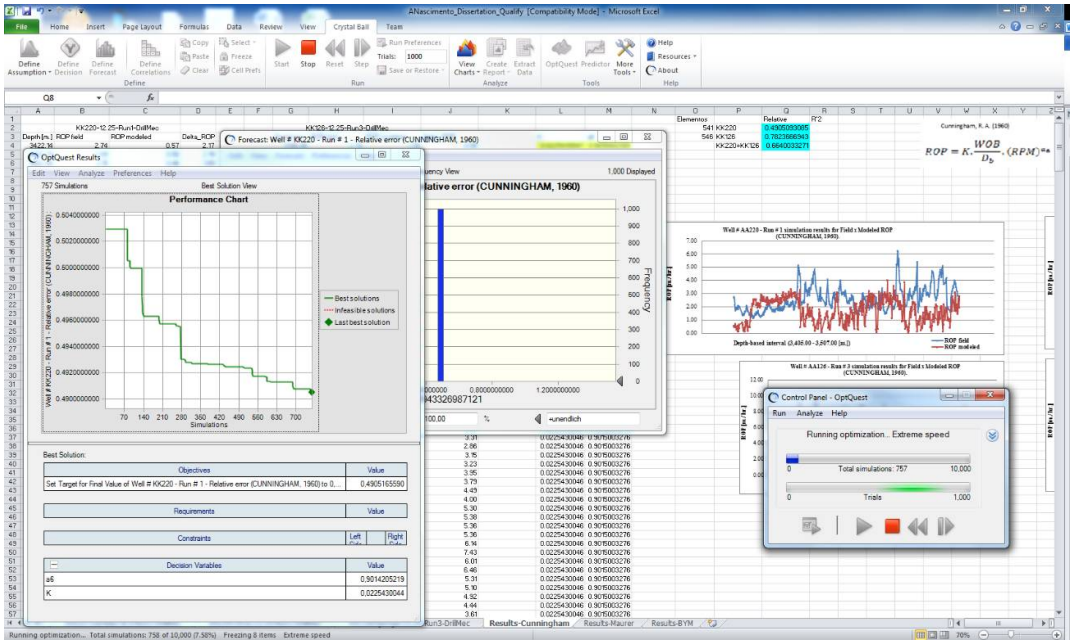

Table 18 - Simulation results for the different ROP models in reference.

Model	Coefficients	Simulation results	Coefficients boundary	
			Lower	Upper
Cunningham (1960)	a_6	0.2481	0	1
	K	0.4745	0	10
	Relative error	0.5826	n/a	
Maurer (1962)	a_5	0.001	0	2
	a_6	0.5	0	0.5
	K	2.7164	0	10
	Relative error	0.423	n/a	
Bourgoyne Jr. and Young Jr. (1974)	a_1	1.9	0.5	1.9
	a_2	0.0001	0.0001	0.05
	a_3	0.0409	0.0001	0.09
	a_4	0.0001	0.0001	0.01
	a_5	0.5	0.5	2
	a_6	1	0.4	1
	a_7	0.3	0.3	1.5
	a_8	0.5388	0.3	0.6
	Relative error	0.3652	n/a	

Figure 47 - Field ROP versus modeled ROP using Cunningham (1960) model.

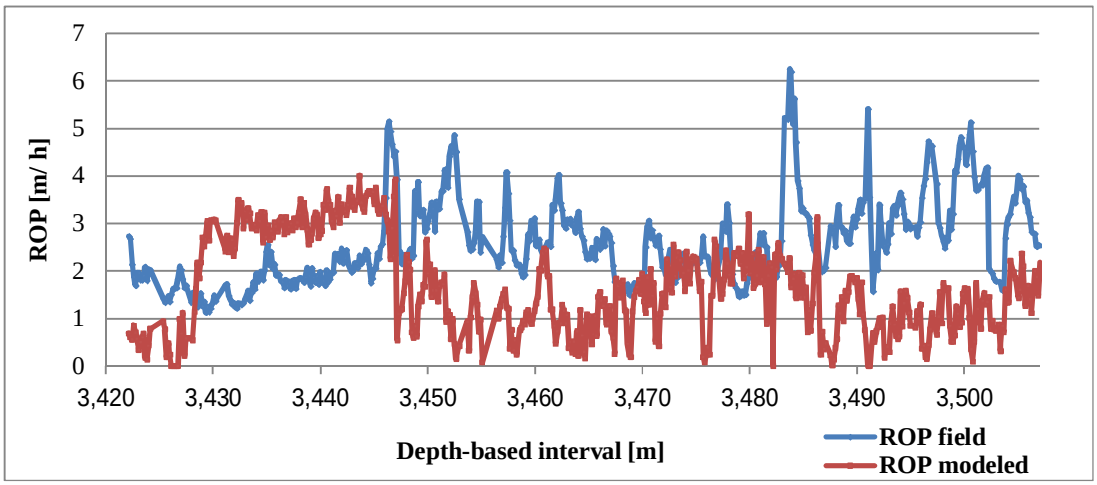

Figure 48 - Field ROP versus modeled ROP using Maurer (1962) model.

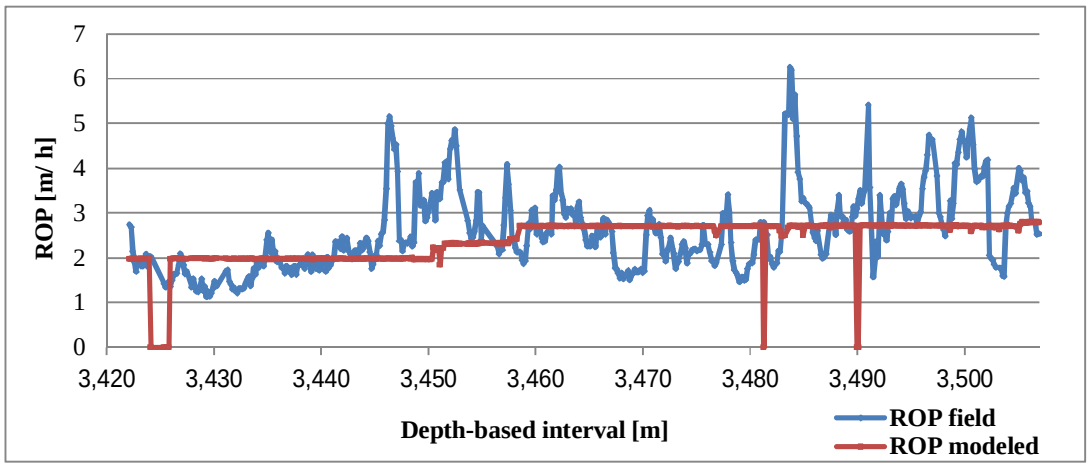

Figure 49 - Field ROP versus modeled ROP using Bourgoyne Jr. and Young Jr. (1974) model.

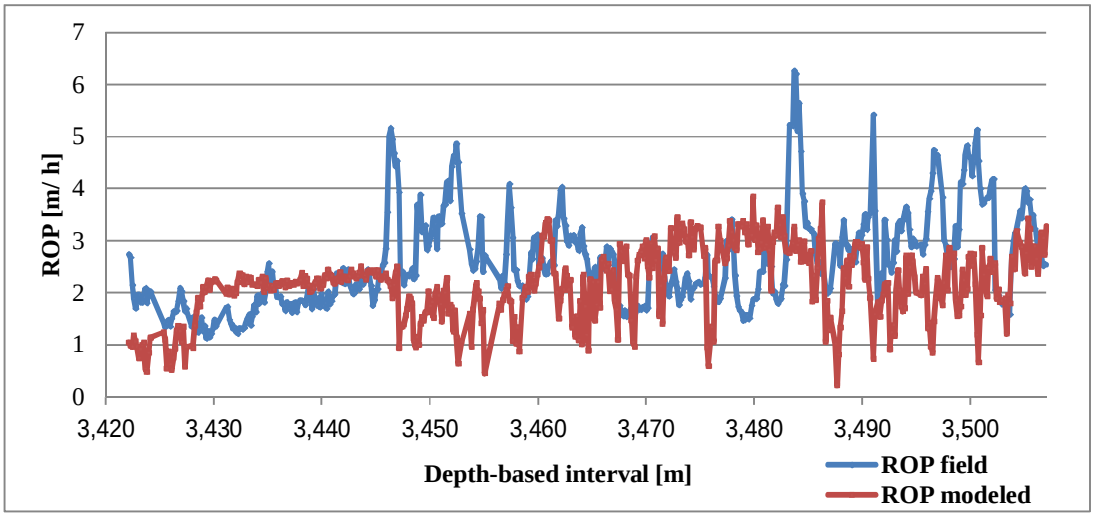

Figure 50 - Simulation result for the (a) Cunningham (1960), (b) Maurer (1962) and (c) Bourgoyne Jr. and Young Jr. (1974) models.

a)

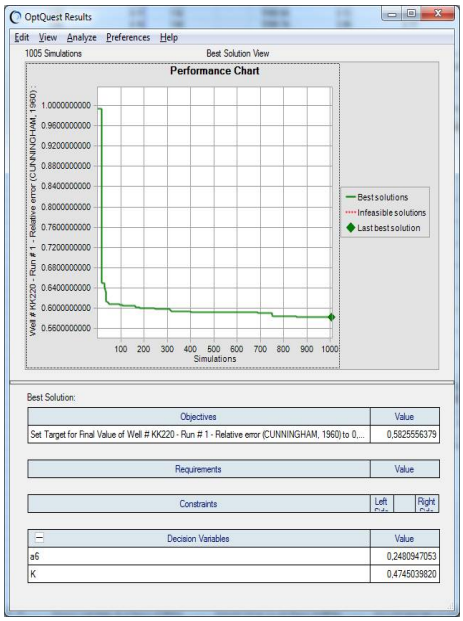

b)

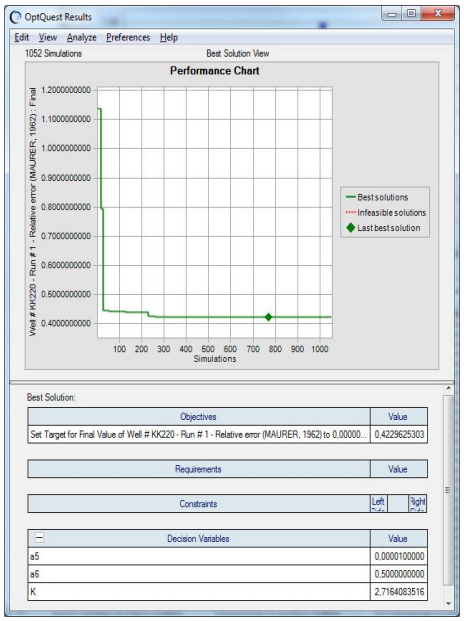

c)

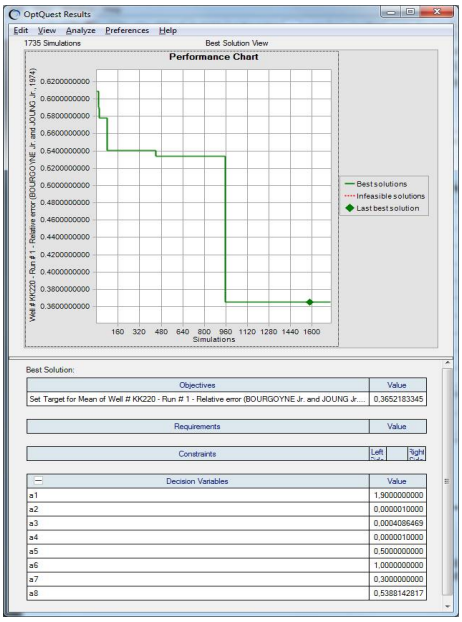

Considering the past researches, the relative error presented through the simulations show consistency if compared to the results presented in Table 18. Also, it is noticeable that the Bourgoyne Jr. and Young Jr. Model (BYM) provides better results and fitting between the field and the modeled ROP (Figure 49), with 36.52% of relative error, and thus, is the model chosen for further development.

The next step is to feed and change the chosen model with specific pre-salt parameters in order converge it to a better correlation, and just after that, to move forward to the specific energy analysis step. Thus, all the analysis performed in the previous chapter three are used in this particular step for feeding and adjust the ROP model for better fitting. Basically the adjustments performed in the BYM were the following values replacements and definition: 100 [rpm] to 80 [rpm], 4 [lbf/ in] to 2 [lbf/ in], linear drill-bit dullness to 0.26 [%/ m], 9 [ppg] to 9.5 [ppg] and 10,000 [ft] to 11,228 [ft]. Also, the coefficients ranges have been increased in order to allow the script routine simply to pick the best choices from all the positive possibilities, being the lower and upper boundary 1 x 10^{-9} and 20, respectively.

Considering the fitting results shown in the graph of Figure 51 with correlations converging just from approximately 3,450 [m], it is possible to understand from the raw drilling mechanic parameters shown by Figure 52, that it basically lays into two different main groups of rotary speed, of low and high rotary speed, 80 [rpm] and 150 [rpm]. This may be the responsible agent interfering in the fitting convergence for the entire data analyzed. As a matter of comparison and try and error as well, this plot was split in two data sets for better development with the presented methodology, so that just the portion concerning the 150 [rpm] group was further analyzed. The highlighted portion of Figure 51 with dashed red marks represents the portion of the data set further detailed.

Figure 51 - Field versus modeled ROP after BYM model adjustments.

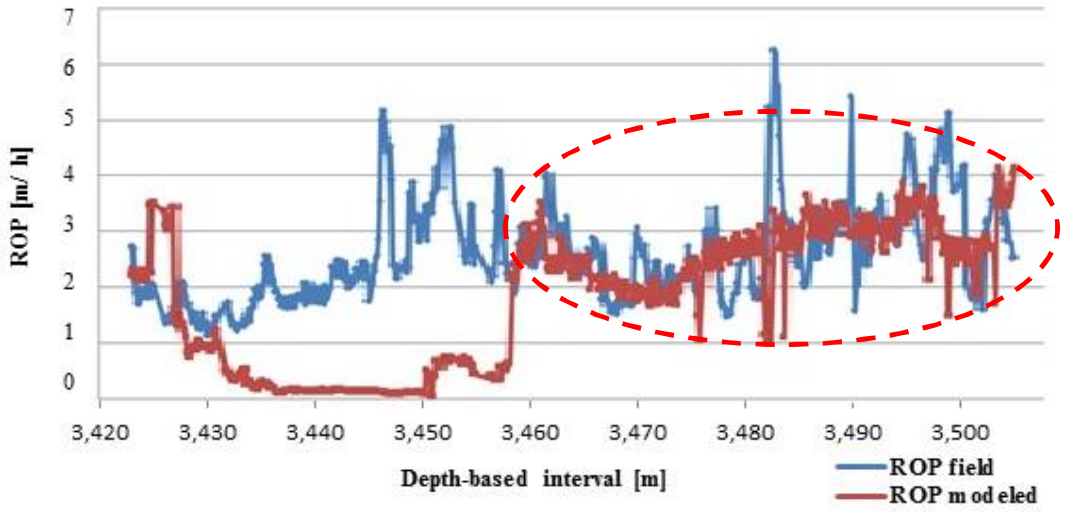

Figure 52 - Raw drilling mechanics parameters with highlights to the rotary speed.

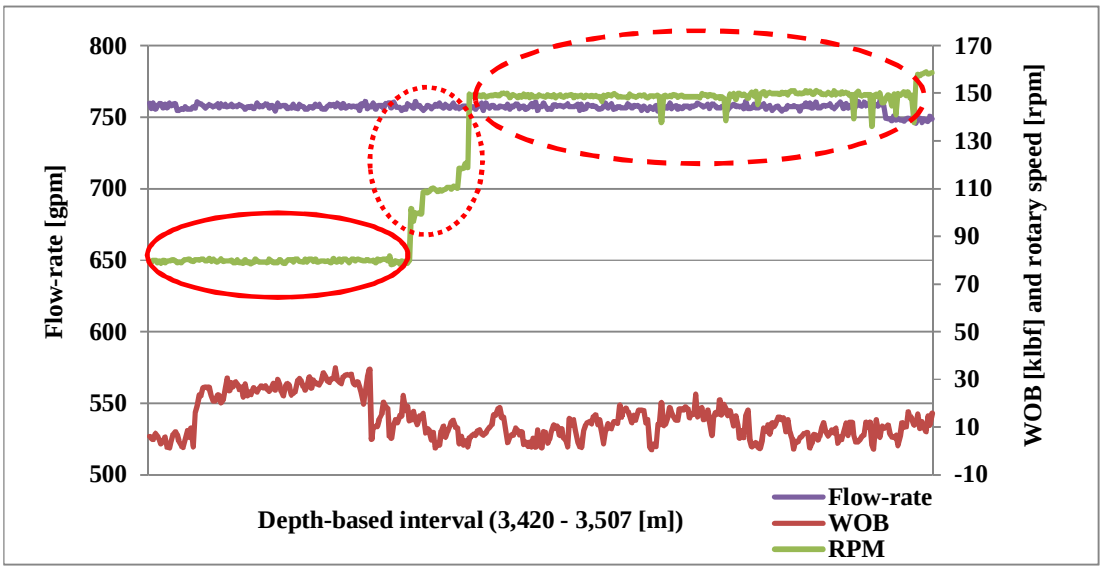

After the split, the results are shown in Table 19 and Figure 53, in which the fitting has a relative error of approximately 13% lower than before, having as a final value 23.12%.

Table 19 - Simulation results for the modeled ROP BYM model adjustments.

Model	Coefficients	Simulation results	Coefficients boundary	
			Lower	Upper
Final coefficients modeled and found by using Bourgoyne Jr. and Young Jr. (1984) model.	a_1	7.7963	1 x 10^{-9}	20
	a_2	0.4784	1 x 10^{-9}	20
	a_3	1.0589	1 x 10^{-9}	20
	a_4	0.0641	1 x 10^{-9}	20
	a_5	0.0441	1 x 10^{-9}	20
	a_6	6.1828	1 x 10^{-9}	20
	a_7	0.0014	1 x 10^{-9}	20
	a_8	0.1367	1 x 10^{-9}	20
	Relative error	0.2312	n/a	

Figure 53 - Field versus modeled ROP after BYM model adjustments for the group with rotary speed of 150 [rpm].

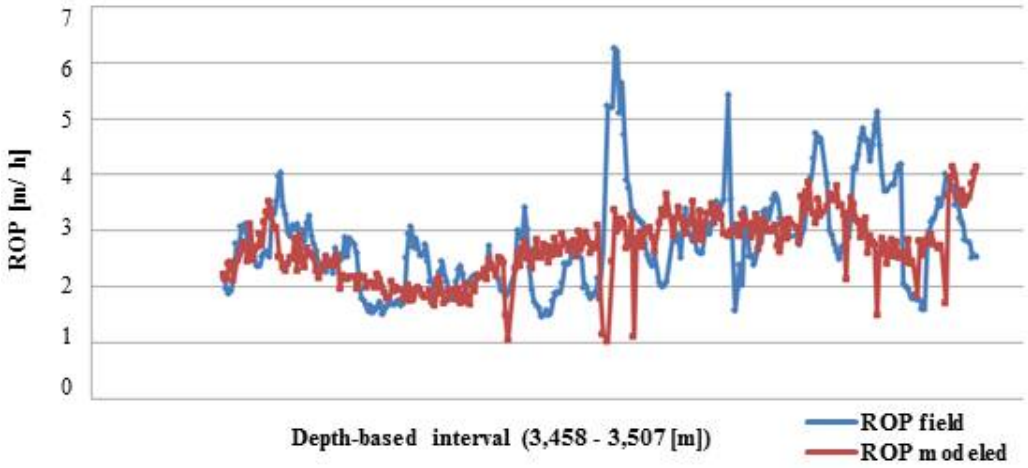

4.2 SPECIFIC ENERGY CROSS-ANALYSIS WITH ROP MODEL

As a next step in the methodology, the idea is to look for a fitting between the specific energy curves instead of the ROP ones, moving forward with the concept of SE modeling rather than just the ROP. Figure 54 details the MSE together with the ROP, for which a 50% of drill-bit sliding friction factor (for PDC) was used (PESSIER et. al., 1992) to calculate the final MSE values. It is visible that the behavior of the MSE shows itself to opposite the ROP as e.g. inefficiency (high MSE) for low ROP, and vice-versa. From the equation (24) is visible that the higher the rate of penetration is the, the less would be the specific energy involved. Considering the pre-salt UCS to range between 25 to 30 [kpsi] (CHRISTANTE, 2009; HBAIEB, 2013), parameter highlighted in the Figure 54 by dashed black lines, it does drive to the understanding that the lowest achievable level of specific energy lay, in fact, between 0.6 to 3 times the UCS of the rock being drilled, as raised by Teale et al. (1965) and evidenced by Dupriest et al. (2005). Thus, Figure 54 shows that as a reference, if throughout the whole run the MSE would have staid as low as the UCS, the ROP would be at its highest, ranging between 3 and 5 [m/ h]. This figure is presented trying to show the relationship and behavior of MSE in terms of ROP changes and vice-versa, also highlighting that the minimum MSE achieved over the specific run presented lays close to the UCS of the pre-salt rock.

Figure 54 - Field ROP and field MSE with highlights in black dashed lines for the UCS presented for the 150 [rpm] rotary speed group.

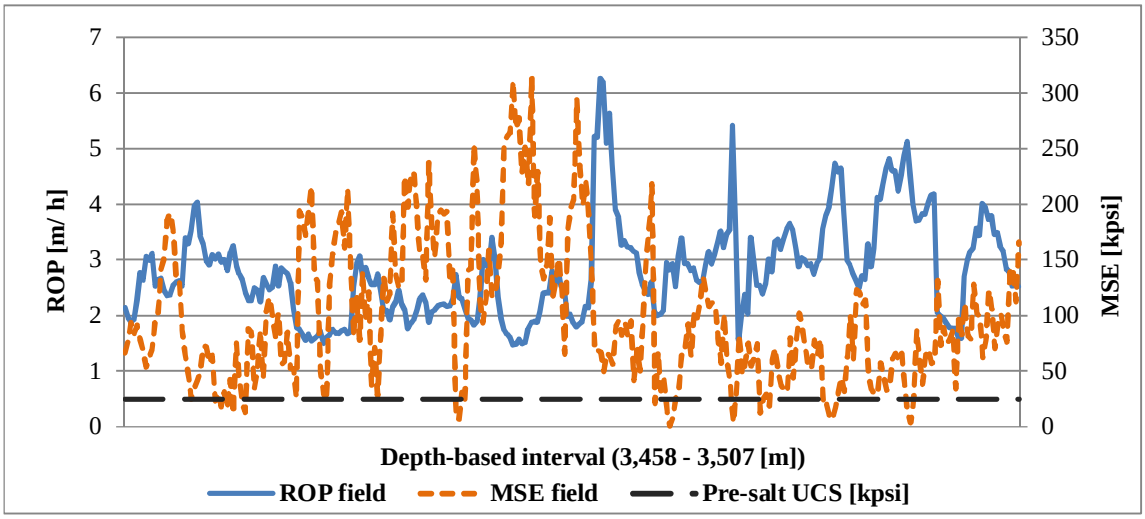

In order to analyze the MSE in terms of its modeling, the modeled ROP has been fitted into the MSE formulation in reference resulting in the modeled MSE drawn in Figure 55, which interestingly has a relative error of just 21.2%, less than the modeled ROP, which showed an error of 23.12% (Figure 53 and Table 19). The fitting is also visually much better than the one shown for the ROP in Figure 53.

Figure 55 - Field versus modeled MSE for group with rotary speed of 150 [rpm].

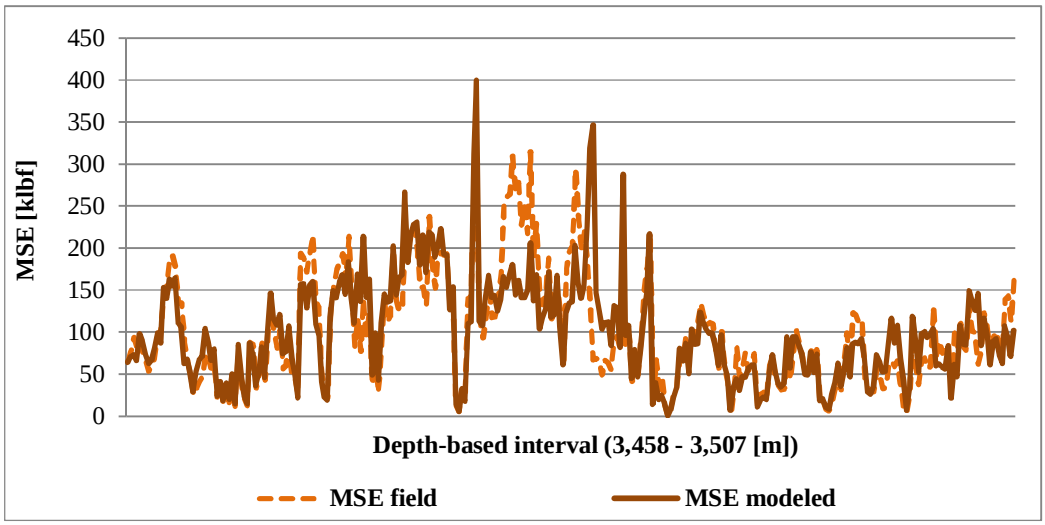

4.3 OPTIMIZATION DETERMINATION METHODOLOGY

For the optimization determination it is crucial to understand what the drilling mechanics parameters limitations are as detailed in chapter three. Particularly for determining the

maximum applicable WOB for this specific case, it is possible to use a methodology of applying a reverse engineering into the raw drilling mechanics data in order to re-build the drill-rate test curve, as per Figure 25 (DUPRIEST et al., 2005). By grouping the WOBs in steps of 5 [klbf] and averaging them together with the respective ROPs for a specific group of parameters set (e.g. flow-rate constant around 750 [gpm] and rotary speed equal to 150 [rpm] in average, Figure 52), the graph can be re-built, allowing the tendency of the ROP versus the WOB to be seen in a quadratic mathematical distribution, in which the derivative or its maximum represents the foundering point and, approximately, the maximum applicable WOB in order to guarantee maximum efficiency of the drilling process. By exceeding this value, the ROP would start dropping again, as can be seen in the Figure 56 by the green lines, which represents the data group of rotary speed of 150 [rpm] (the portion of the simulation split resulted from the modeling run in the previous sub-chapter). Thus, the maximum viable WOB in this case would be 10.85 [klbf] (fitting and representative equation embedded in the graph Figure 56).

Figure 56 - Re-built of drill-rate curve.

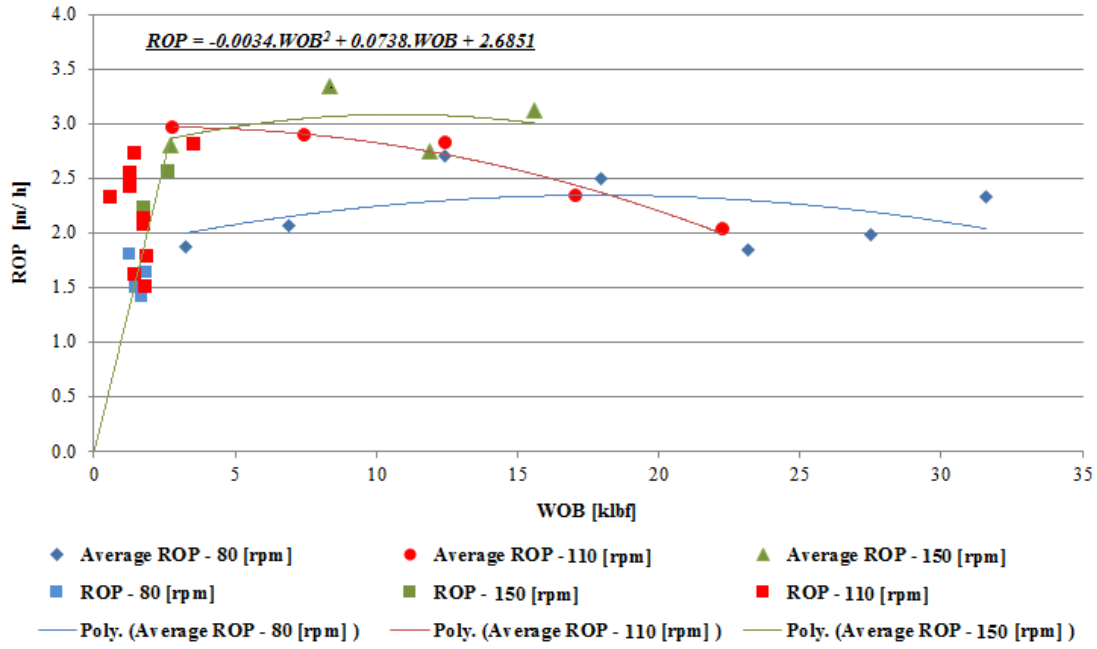

Moving forward, considering that the ESD and the ECD have a narrow window to be played with due to well integrity issues linked to kick and losses events in such pre-salt formation (Figure 30), the choice of changing much the flow-rate is limited for wider values, but could be increase up to 800 [gpm] if there would be a way to keep the ECD not that much high, which could be controlled lowering the EMW from the actual 10 [ppg] to a value less and between 9.79 [ppg] and 10 [ppg]. Considering that the pore pressure weights 9.5 [ppg], the minimum

applicable one would be 9.79 [ppg], since a precaution of a 3% of safety margin has to be applied when designing the drilling fluids. Table 20 details the drilling mechanics parameters limitation for the case under analysis.

Table 20 - Details of the drilling mechanics parameters limitation after simulation.

Drilling parameter	Lower limit	Upper limit
Flow-rate [gpm]	400	800
Rotary speed [rpm]	80	150
WOB [klbf]	n/a	10.85
ECD/ ESD [ppg]	9.79	n/a
EMW [ppg]	9.79	10

By running the simulation again, considering the model's coefficients already calculated and the drilling mechanics parameters highlighted in Table 20, it is then possible to re-draw the ROPs for the whole interval looking for its highest performance, hence, looking for the lowest MSE. Seeking for an average MSE of 50 [kpsi] for the entire run (given the lowest MSE threshold visible in Figure 54), the simulation results yielded the following parameters: flow-rate of 750 [gpm], WOB of 8.6 [klbf], rotary speed of 120 [rpm] and ECD of 10.25 [ppg].

The green line in the graph of Figure 57 displays the MSE forecasts considering the optimized parameters for the specific run, being nominated as "MSE optimized drilling parameters" in the legend of the referred figure.

Figure 57 - Simulation for optimum drilling mechanics choosiness.

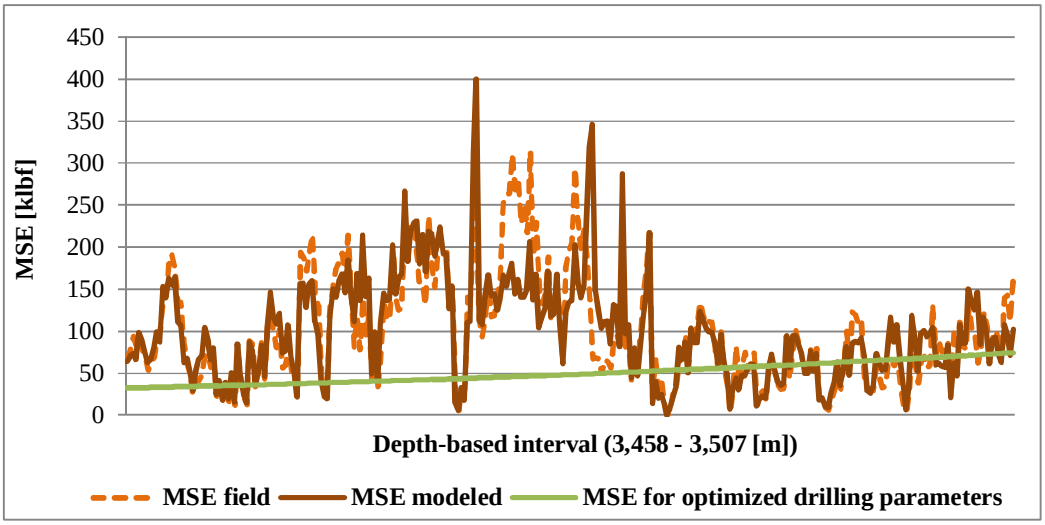

5 CONCLUSION

Pre-salt basins and its exploration have become more and more frequently mentioned over the years. Considered a very important petroleum-related source given the world energetic demand forecast scenario, seeking ways to support in making these fields effectively commercially viable has its value.

Supporting filling this gap, the exploration of the pre-salt reserves from related areas of the South Atlantic Ocean (in special the Brazilian and Angolan coast) has a very important role in this context, since they can be considered twin pre-salt analog clusters. Seen as a considerably high operational cost to develop these fields, due to several facts disserted, this wells can cost up to 134,000,000.00 [USD]. Hence, to address performance and possible ways for improving the efficiency of the pre-salt operation has been a route aiming support the refereed problematics.

With the support of eight pre-salt wells and thirty eight run information, statistical analyses were drawn from the gathered and filtered data, allowing the following conclusion in terms of operational performance:

- From the total of thirty eight runs, almost half of them were drilled using a PDC drill-bit. From the other types, the hybrid showed to be appropriated as well, while the TCI and diamond impregnated did not show to have good performance. The most frequent encountered problem in the drill-bits relates to broken and worn teeth-cutters.
- For some runs, the allowed drilling mechanics parameters choosiness window were going beyond the down-hole tools limitations, what certainly influenced related BHA related failure, consequently leading to operational down-time.
- The operational performance showed to still allow improvements considering the non-productive time and invisible-lost time analyzed. The following total minimum potential operational time savings was found: 37.1 [h] for well # A, 19.79 [h] for well # B, 48.8 [h] for well # C, 8.15 [h] for well #D, 22.34 [h] for well # F and 105.94 [h] for well # H, totalizing approximately 242 [h] (or 10 [days]), equivalent to 13,747,550.00 [USD].

Considering the drillability improvements, much has been understood from the used models, allowing driving the following conclusions:

- The Bourgoyne Jr. and Young Jr. ROP model is suitable for pre-salt formations, but some parameters adjustments were necessary to make it realistic for these carbonate formations. With a starting point of model fitting with 36.52% as a relative error, this model showed to correlate most. The relative error dropped to 23.12% after the pre-salt adjustments.
- The SE modeling shows to be more reliable than the ROP modeling in terms of simulation fitting. By comparing the field with the modeled data, the SE showed to have a relative error lower the one calculated for the ROP, of 21.12%.
- The reverse engineering methodology seems to be a very good way of re-building the drill-rate test curve for better visualization and drilling parameters boundaries determination.
- Considering the pre-salt well # B used for the simulation as a case study, it was possible to verify that for sake of better analysis and clarification, filtering and data split may also apply in research with similar purposes.

This thesis details a lot of step-by-step from data analysis up to final drilling mechanics parameters choosiness, allowing understanding where the room for a better performance in the pre-salt operations are.

For future work it may be interesting to address self- ROP/ SE models based on the pre-salt drilling mechanics information presented, in special on the drilling fluid details and flowing patterns, considering that the whole data set used for developing the thesis had reliable fluid mechanics information making a practicable research. Also, given the delicate narrow pressure window available for managing the equivalent circulating density and the equivalent static density, it may be very interesting to implement the usage of the manage pressure drilling concept for the pre-salt wells, what could have its applicability and well control assurance studied, in a first step, in extensive research, and subsequently, its implementation tested in real pre-salt related job. Another interesting thematic to be studied in a future work is the combination of big data concept together with the needs of reliable and in real-time decision making tools in drilling activities. By having a robust data collection of these pre-salt wells being stored as one, from activities developed and under development in the African and Brazilian coast, a very robust data set for statistical analysis would be present, helping in on-line decision making. Still in this research line, the improvement of the real-time drill-rate tests is something very promising as a new well monitoring and analysis methodology, allowing the

operational crew to have in its accustomed way a view of a new tool supporting drilling optimization and drilling efficiency enhancement. Considering these new ideas and their novelty in the industry, attached to these future works, it would be possible to foresee the deposit of new petroleum-related patents.

REFERENCES

AFIFI, S. E. et al. **Enhance the Drilling & Tripping Performance on Automated Rigs with fully automated performance measurement**. Abu Dhabi: Society of Petroleum Engineers, 2015. 12 pp.

ANDRADE, A. M T. et al. **Offshore Production Units for Pre-salt Projects**. Houston: Society of Petroleum Engineers, 2015. 14 pp.

ANDERSEN, P. A. et al. **Case History: Automated Drilling Performance Measurement of Crews and Drilling Equipment Ketil**. Amsterdam: Society of Petroleum Engineers, 2009. 14 pp.

BAKER. Baker Hughes. **Drill Bits Catalog for Advanced Reservoir Performance**. Houston: Baker Hughes, 2013. 83 pp.

BDEP. Bando de Dados de Exploração e Produção da Agência Nacional do Petróleo, Gás Natural e Biocombustíveis. Rio de Janeiro: ANP, 2010.

BELTRAO; R. et al. **Pre-salt Santos Basin - Challenges and New Technologies for the Development of the Pre-salt Cluster**, **Santos Basin, Brazil**. Houston: Society of Petroleum Engineers, 2009. 11 pp.

BONITRON. Bonitron Inc. **Oil and Gas Extraction.** Accessible at: <http://www.bonitron.com/industry-oil-drawworks.html>. Acessed on: 11. May. 2015.

BOURGOYNE Jr., A. T.; YOUNG Jr., F. S. **A Multiple Regression Approach to Optimal Drilling and Abnormal Pressure Detection**. Houston: Society of Petroleum Engineers, 1974. 14 pp.

_____. **Applied Drilling Engineering Handbook**. 1st ed. Houston: Society of Petroleum Engineers, 1986. 502 pp.

BSUQUET, F. **Update 1 - Test confirms continuity of the accumulation of Guara in the Brazilian Pre-salt**. São Paulo: BRAZIL Pre-salt category press, 2011. Accessible at: <http://www.presalt.com/en/brazil-Pre-salt-oil-gas/2095-update-1-test-confirms-continuity-of-the -accumulation-of-guara-in-the-brazilian-Pre-salt.html>. Accessed on: 26. Sep. 2014.

CARMINATTI, G., L. **New exploratory frontiers in Brazil**. Madrid: World Petroleum Congress, 2008. 11 pp.

CDC, Chair of Drilling and Completion Engineering. **Not published data information**. Leoben: Department of Petroleum Engineering, Montanuniversität Leoben, 2015.

CEZAR, et al. **Subsea Solutions in the Pre-salt Development Projects**. Houston: Society of Petroleum Engineers, 2015. 20 pp.

COOPER, I. et al. **Advanced Drilling and Well Technology**. Houston: Society of Petroleum Engineers, 2009. 888 pp.

CHEN, G. et al. **Thermoporoelastic Effect on Wellbore Stability**. Houston: Society of Petroleum Engineers, 2005. 9 pp.

CHRISTANTE, L. Geologia. **Pré-sal: desafios científicos e ambientais**. São Paulo: Unesp Ciência, 2009. 3 pp.

COMBS, G. D. **Prediction Of Pore Pressure From Penetration Rate**. Houston: Society of Petroleum Engineers, 1968. 16 pp.

CUNNINGHAM, R. A. et al. **Laboratory Study of Effect of Overburden, Formation and Mud Column Pressures on Drilling Rate of Permeable Formations**. Houston: Society of Petroleum Engineers, 1959. 9 pp.

CUNNINGHAM, R. A. **Laboratory Studies of the Effect of Rotary Speed on Rock-bit Performance and Drilling Cost**. New York: American Petroleum Institute, 1960. 8 pp.

DUPRIEST, F. E. et al. **Maximizing ROP With Real-Time Analysis of Digital Data and MSE**. Qatar: Society of Petroleum Engineers, 2005. 8 pp.

DUPRIEST, F. E. et al. **Borehole Quality Design and Practices To Maximize Drill Rate Performance**. Florence: Society of Petroleum Engineers, 2005. 18 pp.

DUPRIEST, F. E. et al. **Maximizing Drill Rates with Real-Time Surveillance of Mechanical Specific Energy**. Houston: Society of Petroleum Engineers, 2005. 10 pp.

ECKEL, J. R. **Microbit Studies of the Effect of Fluid Properties and Hydraulics on Drilling Rate**. Houston: Society of Petroleum Engineers, 1968. 4 pp.

EDWARDS, J. H. **Engineering Design of Drilling Operations**. New York: American Petroleum Institute, 1964. 17 pp.

EIA. Energy Information Administration. **Annual Energy Outlook**. Washington: Department of Energy from the United States of America, 2015. DOE/EIA-0383(2015). Washington, 2015. 154 pp.

EREN, T. **Real-Time-Optimization of Drilling Parameters During Drilling Operations**. Ankara: Middle East Technical University, 2010. 165 pp.

FORMIGLI, J. M F. **Santos basin Pre-salt Cluster: how to make production development technical and economically feasible**. Oral Press Seminar not officially published. Rio de Janeiro: Rio Oil & Gas Expo and Conference, 2008.

FRAGA, C. T. C. et al. **Brazilian Pre-salt: An Impressive Journey from Plans and Challenges to Concrete Results**. Houston: Society of Petroleum Engineers, 2015. 15pp.

GAFFNEY. G Gaffney, Cline & Associates. **West Africa Pre-salt Opportunities and Challenges**. London: The Royal Institution, 2014. 19 pp.

GALLE, E. M et al. **Best Constant Weight and Rotary Speed for rotary Rock Bits**. New York: American Petroleum Institute, 1963. 26 pp.

GREENHALGH, J. **Petroleum Plays and Prospectivity in the Kwanza and Benguela Basins of Offshore Angola**. Singapore: AAPG, 2012. 7 pp.

HBAIEB, S. et al. **Innovative Hybrid Bit Mitigates Geological Uncertainties, Improves Drilling Performance in Brazilian Pre-salt Formations**. Amsterdam: Society of Petroleum Engineers, 2013. 11 pp.

IRAWAN, S et al. **Optimization of Weight on Bit During Drilling Operation Based on Rate of Penetration Model**. Tehran: Research Journal of Applied Sciences, Engineering and Technology, 2012. 6 pp.

JOHANN, P. R. et al. **Reservoir Geophysics in Brazilian Pre-salt Oilfields**. Houston: Society of Petroleum Engineerrs, 2012. 10 pp.

KOEDERITZ, W. **A Real-Time Implementation of MSE**. Houston: National Technical Conference and Exhibition, 2005. 8 pp.

KONING, T. **Continental drift theory supports hopes that this African nation also holds working petroleum system beneath the salt layer**. Houston: Industry eager for repeat of Brazil pre-salt boom offshore Angola category press, 2014. Accessible at: <http://www.drillingcontractor.org/industry-eager-for-repeat-of-brazil-pre-salt-boom-offshore-angola-30574>. Accessed on: 10. Jun. 2015.

LEFFLER, L. W. et al. **Deepwater Petroleum Exploration & Production: A Nontechnical Guide**. 2nd ed. Tulsa: Penwell, 2003. 372 pp.

MAIDLA, E. E. et al. **Rigorous Drilling Nonproductive-Time Determination and Elimination of Invisible Lost Time: Theory and Case Histories**. Lima: Society of Petroleum Engineers, 2010. 9 pp.

MAURER, W. C. **The "Perfect - Cleaning" Theory of Rotary Drilling**. Houston: Journal of Petroleum and Technology, 1962. 5 pp.

MELLO, M et al. **Giant Sub-Salt Hydrocarbon Province of the Greater Campos Basin, Brazil**. Rio de Janeiro: Society of Petroleum Engineers, 2011. 9 pp.

MCLEAN, R. H. **Crossflow and Impact Under Jet Bits**. Houston: Journal of Petroleum Technology, 1964. 8pp.

MITCHELL, R. F.; MISKA, S. Z. **Fundamentals of Petroleum Engineering**. Houston: Society of Petroleum Engineering, 2011. 696 pp.

MOHRIAK, W. **Pre-salt Carbonate Reservoirs in the South Atlantic and World-wide Analogs**. New Orleans: AAPG, 2015. 39 pp.

MUNIZ, C. **Deepwater Brazilian Presalt: The Way Ahead for Research and Development**. Rio de Janeiro: Baker Hughes Academia, 2013. 3 pp.

MURRAY, A. S.; CUNNINGHAM, R. A. **Effect of Mud Column Pressure on Drilling Rates. *Society* of Petroleum Engineers**. Houston: Society of Petroleum Engineers, 1955. 9 pp.

NASCIMENTO, A. **Analysis of Block BMS09 Petroleum Exploration, Santos Basin** Leoben: Petroleum Engineering Department, Montanuniversität Leoben, 2010. 75 pp.

_____. **Drilling Fluid: a Stochastic Rop Optimization Approach for the Brazilian Pre-salt Carbonates**. Leoben: Petroleum Engineering Department, Montanuniversität Leoben, 2012. 99 pp.

ORACLE. **Oracle Crystal Ball Classroom Faculty Edition**. Redwood shore: version 11.1.2.3.500. Accessible at: <http://www.oracle.com/us/products/applications/crystalball/overview/index.html>. Accessed on: 15. Nov. 2014.

PEIXOTO, F. T. et al. **Brazilian Pre-salt: The Challenges of Coring at a New Frontier**. Lima: Society of Petroleum Engineers: 2010. 7 pp.

PESSIER, R. C. et al. **Quantifying Common Drilling Problems with Mechanical Specific Energy and a Bit-Specific Coefficient of Sliding Friction**. Washington: Society of Petroleum Engineers, 1992. 16 pp.

PETROBRAS. Petróleo Brasileiro S.A. **Pré-Sal e Marco Regulatório de Exploração e Produção de Petróleo e Gás**. Rio de Janeiro, 2009.

PINHEIRO, R. S. et al. **Well Construction Challenges in the Pre-salt Development Projects**. Houston: Society of Petroleum Engineers, 2015. 13 pp.

PUTOT, C. J. et al. **Quantifying Drilling Efficiency and Disruption: Field Data vs. Theoretical Model**. Houston: Society of Petroleum Engineers, 2000. 12 pp.

RABIA, H. et al. **Specific Energy as a Criterion for Bit Selection**. Houston: Journal of Petroleum Technology, 1985. 5 pp.

ROBINSON, P.; HSU, C. S. **Practical Advances in Petroleum Processing**. 1st ed. New York: Springer, 2007. 419 pp.

TEALE, E. et al. **The Concept of Specific Energy in Rock Drilling**. Amsterdam: Journal of Rock Mechanics and Mining Sciences & Geomechanics, 1965. 17 pp.

THOMAS, J. E et al. **Fundamentos de engenharia de petróleo**. 2nd ed. Rio de Janeiro: Interciência, 2002. 271 pp.

THONHAUSER, G. **Handbook of Drilling Process Evaluating and Planning**. Material not formally published. Leoben: Department of Petroleum Engineering, Montanuniversität Leoben, 2009. 20 pp.

WARREN, T. M. **Drilling Model for Soft-Formation Bits**. Houston: Journal of Petroleum Technology, 1981. 8 pp.

WARREN, T. M. et al. **The Effect of Nozzle Diameter on Jet Impact for a Tricone Bit**. Houston: Society of Petroleum Engineers, 1984. 10 pp.

WARREN, T. M. **Penetration Rate Performance of Roller Cone Bits**. Houston: Society of Petroleum Engineers, 1987. 10 pp.

WWF. World Wildlife Fund. **The Energy Report: 100% Renewable Energy by 2050**. Gland: WWF The Energy Report, 2011. 253 pp.

APPENDIX A - HISTORICAL PRE-SALT ROP AND DRILLING PARAMETERS

All Tables presented in this Appendix A (Table 21, Table 22, Table 23, Table 24, Table 25, Table 26, Table 27, Table 28, Table 29, Table 30, Table 31 and Table 32) are related to the historical gathered ROP and drilling parameters referred to the pre-salt wells under analysis. The drilling mechanics parameters were detailed as following: slack-off weight (SO) in [klbf] , pick-up weight (PU) in [klbf], rotary free weight (RAB) in [klbf], rotary speed in [rpm], flow-rate (FLOW) in [gpm], rate of penetration (ROP) in [m/ h], weight-on-bit (WOB) in [klbf], torque on bottom (TOR_on) in [ft-klbf], torque off bottom (TOR_off) in [ft-klbf], stand pipe pressure on bottom (SPP_on) in [psi], stand pipe pressure off bottom (SPP_off) in [psi], equivalent circulating density (ECD) in [ppg], temperature (TEMP) in [^{o}C] and bottom-hole pressure (BHP) in [psi]. The abbreviation *n/a* presented in the tables represents information that were not available.

Table 21 - Historical ROP and drilling parameters for the well # A - runs # 1, 2 and 3.

Run #	Depth_i [m]	Depth_f [m]	ROP [m/ h]	Drilling parameters
1	3,993	4,040	3.62	SO=566, PU=573, RAB=560, ROTARY SPEED=80, FLOW=500, ROP=2.46, WOB=25, TOR_on=16, TOR_off=9, SPP_on=1,500, SPP_off=1,400, ECD=9.92- 9.94, TEMP=44, BHP=6,763 - 7,021.
	4,040	4,090	2.08	
	4,090	4,128	2.17	
2	4,128	4,138	1.74	SO=569, PU=593, RAB=577, ROTARY SPEED=110, FLOW=600, ROP=1.41, WOB=25, TOR_on=7, TOR_off=5, SPP_on=2,800, SPP_off=2,780, ECD=9.92 - 9.93, TEMP=44 - 45, BHP=7,049.
	4,138	4,166	1.15	
	4,166	4,166	0.05	
3	4,166	4,172	2.58	SO=569, PU=593, RAB=577, ROTARY SPEED=100 - 120, FLOW=600, ROP=0.85, WOB=25 - 28, TOR_on=5 - 6, TOR_off=3, SPP_on=2,550, SPP_off=2,523 - 2,530, ECD=9.92 - 10.02, TEMP=48, BHP 7,114 - 7,168.
	4,172	4,187	1.02	
	4,187	4,195	0.57	

Source: (BDEP, 2010; CDC, 2015).

Table 22 - Historical ROP and drilling parameters for the well # B - runs # 1, 2 and 3.

Run #	Depth_i [m]	Depth_f [m]	ROP [m/ h]	Drilling parameters
1	3,405	3,407	2.4	SO=641 - 715, PU=660, RAB=661, ROTARY SPEED=80, FLOW=410 - 750, ROP=4.61, WOB=15 - 25, TOR_on=7 - 12, TOR_off=4, SPP_on=2,150 - 2,280, SPP_off=730 - 2,280, ECD=9.77 - 9.89, TEMP=45 - 48, BHP=5,784 - 6,167.
	3,407	3,427	2.22	
	3,427	3,436	1.5	
	3,436	3,447	1.89	
	3,447	3,480	2.08	
	3,480	3,502	3.14	
	3,502	3,507	2	
Coring	3,507	3,536	Coring	n/a
2	3,536	3,617	3.6	SO=692 - 715, PU=712 - 754, RAB=703 - 721, ROTARY SPEED=60 - 100, FLOW=500 - 750, WOB=30 - 55, TOR_on=17 - 18, TOR_off=5, SPP_on=1,225 - 2,387, SPP_off=1,225 - 2,387, ECD=10.3 - 10.43,TEMP=44 - 48, BHP=6,127 - 6,529.
	3,617	3,640	3.28	
	3,640	3,679	2.39	
	3,679	3,688	1.88	
	3,688	3,689	2.67	
Coring	3,689	3,709	Coring	n/a
3	3,709	3,717	2.58	SO=720 - 745, PU=648 - 780, RAB=710, ROTARY SPEED=110 - 150, FLOW=750, WOB=50 - 54, TOR_on=14 - 25, TOR_off=7, SPP_on=2,310 - 2,836, SPP_off=2,310 - 2,836, ECD=10.4 - 10.5, TEMP=45 - 52, BHP=6,608 - 6,813.
	3,717	3,784	3.26	
	3,784	3,795	2.93	
	3,795	3,832	2.9	
	3,832	3,853	2.38	
	3,853	3,872	1.75	

Source: (BDEP, 2010; CDC, 2015).

Table 23 - Historical ROP and drilling parameters for the well # C - runs # 1, 2 and 3.

Run #	Depth_i [m]	Depth_f [m]	ROP [m/ h]	Drilling parameters
1	4,487	4,499	2.77	SO=n/a, PU=n/a, RAB=n/a, ROTARY SPEED=120 - 160, FLOW=790 - 800, ROP=4.5, WOB=10 -35, TOR_on=15 - 24, TOR_off=9, SPP_on=2.370 - 2,490, SPP_off=2,345, ECD=10.18 - 10.23, TEMP=45, BHP=7,600.
	4,499	4,533	4.29	
	4,533	4,539	7.22	
	4,539	4,551	5.14	
	4,551	4,565	2.8	
Coring	4,565	4,568	Coring	n/a
2	4,568	4,588	3.28	SO=660 - 680, PU=725 - 735, RAB=700 - 730, ROTARY SPEED=50 - 100, FLOW=790 - 800, ROP=2.34, WOB=45 - 60, TOR_on=15 - 20, TOR_off=14 - 16, SPP_on=2,460 - 2,620, SPP_off=2,547 - 2,570, ECD=10.18 - 10.29, TEMP=47 - 48, BHP=7,727 - 7,995.
	4,618	4,627	3.48	
	4,627	4,655	4.02	
	4,655	4,664	3.95	
	4,664	4,684	3.18	
	4,684	4,692	2.18	
	4,692	4,713	1.6	
	4,713	4,728	2.18	
	4,728	4,730	0.77	
	4,730	4,742	2.03	
	4,742	4,746	2.33	
	4,746	4,753	1.68	
	4,758	4,762	1.68	
3	4,762	4,765	1.33	SO=665 - 690, PU=740, RAB=697 - 705, ROTARY SPEED=80, FLOW=800 - 810, ROP=1.7, WOB=55 - 60, TOR_on=18 - 19, TOR_off=15 - 16, SPP_on=2,643 - 2,700, SPP_off=2,625 - 2,695, ECD=10.18 - 10.29, TEMP=48, BHP=8,046 - 8,216.
	4,765	4,768	2.04	
	4,768	4,796	2.46	
	4,796	4,825	3.54	
	4,825	4,827	1.41	
	4,827	4,854	2.33	
	4,854	4,870	1.5	
	4,870	4,880	1.7	
	4,880	4,883	1.58	
	4,883	4,898	2.69	
	4,898	4,907	2.04	
	4,907	4,912	2.4	
	4,912	4,915	2.3	
	4,915	4,927	1.48	
	4,927	4,928	2.73	
	4,928	4,929	1.1	
	4,929	4,936	1.35	
	4,936	4,941	1.36	
	4,941	4,949	1.59	
	4,949	4,955	1.64	

Source: (BDEP, 2010; CDC, 2015).

Table 24 - Historical ROP and drilling parameters for the well # C - runs # 4 and 5.

Run #	Depth_i [m]	Depth_f [m]	ROP [m/ h]	Drilling parameters
4	4,955	4,961	1.6	SO=675 - 685, PU=750, RAB=710 - 715, ROTARY SPEED=120 - 140, FLOW=875 - 950, ROP=1.21, WOB=30 - 42.5, TOR_on=19.5 - 20, TOR_off=7 - 15, SPP_on=2,860 - 3,310, SPP_off=2,847 - 3,310, ECD=10.25 - 10.33, TEMP=54 - 55, BHP=8,302 - 8,350.
	4,961	4,963	1.14	
	4,963	4,970	1.06	
	4,970	4,974	1.6	
	4,974	4,990	1.23	
	4,990	4,997	0.88	
	4,997	5,003	1.57	
	5,003	5,012	1.46	
	5,012	5,018	0.38	
	5,018	5,028	1.22	
	5,028	5,031	0.95	
	5,031	5,047	1.48	
5	5,047	5,048	1.82	SO=675 - 705, PU=760 - 775, RAB=728 - 745, ROTARY SPEED=110 - 140, FLOW=845 - 860, ROP=2.77, WOB=40 - 45, TOR_on=18 - 24, TOR_off=14 - 16, SPP_on=2,800 - 2,820, SPP_off= 2,800 - 2,820, ECD 10.17 - 10.29, TEMP=55 - 58, BHP=8,452 - 8,732.
	5,048	5,072	9	
	5,072	5,076	4.29	
	5,076	5,085	4.82	
	5,085	5,087	4.62	
	5,087	5,114	5.31	
	5,114	5,127	4.02	
	5,127	5,128	8.57	
	5,128	5,143	4	
	5,143	5,149	4.34	
	5,149	5,152	7.2	
	5,152	5,153	3.75	
	5,153	5,156	4.5	
	5,156	5,162	4.19	
	5,162	5,166	5	
	5,166	5,172	3.71	
	5,172	5,184	4.40	
	5,184	5,201	4.74	
	5,201	5,230	4.58	
	5,230	5,247	4.3	
	5,247	5,259	3.6	
	5,259	5,268	4.78	
	5,268	5,288	6.86	
	5,288	5,313	5.28	

Source: (BDEP, 2010; CDC, 2015).

Table 25 - Historical ROP and drilling parameters for the well # D - runs # 1, 2, 3, 4 and 5.

Run #	Depth_i [m]	Depth_f [m]	ROP [m/ h]	Drilling parameters
1	4,400	4,421	3.04	SO=512.5 - 515, PU=520, RAB=n/a, ROTARY SPEED=115 - 140, FLOW=550, ROP=2.5, WOB=15 - 30, TOR_on=4.53, TOR_off=n/a, SPP_on=2,426 - 2,486, SPP_off=2,400 - 2,490, ECD=9.75 -10.29, TEMP=47 - 62, BHP=7,857 - 7,958.
	4,421	4,521	3.4	
	4,451	4,464	3.32	
	4,479	4,480	2	
	4,480	4,500	2.2	
	4,500	4,509	2.26	
	4,509	4,511	1.54	
	4,511	4,514	5	
	4,514	4,525	5.84	
	4,525	4,530	7.5	
	4,530	4,541	1.91	
	4,541	4,546	2.16	
2	4,546	4,565	2.28	SO=514, PU=522 - 532, RAB=n/a, ROTARY SPEED=60 - 62, FLOW=525 - 547, ROP=1, WOB=5 - 15, TOR_on=4.5, TOR_off=2.4, SPP_on=4,376 - 4,460, SPP_off=4,340 - 4,415, ECD=10.12 - 10.2, TEMP=47 - 55, BHP=7,937 - 7,950.
	4,565	4,571	0.86	
	4,571	4,583	1.64	
	4,583	4,585	1.03	
	4,585	4,591	1.09	
	4,591	4,592	0.59	
3	4,592	4,599	1.83	SO=520 - 525, PU=530 - 535, RAB=n/a, ROTARY SPEED=40 - 60, FLOW=542 - 547, ROP=1.58, WOB=10 - 15, TOR_on=3.5, TOR_off=3.4, SPP_on=4,093 - 4,190, SPP_off=4,047 - 4,150, ECD=10.13 - 10.25, TEMP=48 - 52, BHP=7,966 - 8,026.
	4,599	4,611	2.57	
	4,611	4,612	5	
	4,612	4,618	2.57	
	4,618	4,626	2.89	
	4,626	4,629	1.2	
	4,629	4,641	2.82	
	4,641	4,642	2.73	
	4,642	4,656	2.24	
4	4,656	4,677	2.58	SO=526 - 533, PU=535 - 537, RAB=n/a, ROTARY SPEED=50 - 74, FLOW=535 - 547, ROP=2, WOB=10 - 25, TOR_on=8, TOR_off=5.3, SPP_on=2,450 - 2,490, SPP_off=2,440 - 2,450, ECD=10.26 - 10.34, TEMP=45 - 56, BHP=8,089 - 8,193.
	4,678	4,679	4.29	
	4,679	4,684	2.27	
	4,684	4,693	2.6	
	4,693	4,694	1.2	
	4,694	4,695	3.53	
	4,695	4,696	2.61	
5	4,696	4,697	0.33	SO=520, PU=535, RAB=n/a, ROTARY SPEED=60, FLOW=547, ROP=1.16, WOB=7.5 - 15, TOR_on=4 - 5, TOR_off=2 - 3, SPP_on=4,092, SPP_off=4,055, ECD=10.16 - 10.28, TEMP=55 - 63, BHP=8,185 - 8,255.
	4,697	4,726	2.45	
	4,726	4,728	1.76	
	4,728	4,733	1.19	
	4,733	4,743	2.37	
	4,743	4,750	1.98	

Source: (BDEP, 2010; CDC, 2015).

Table 26 - Historical ROP and drilling parameters for the well # D - runs # 6 and 7.

Run #	Depth_i [m]	Depth_f [m]	ROP [m/ h]	Drilling parameters
6	4,750	4,770	3.53	SO=535 - 538, PU=547, RAB=n/a, ROTARY SPEED=63 - 82, FLOW=550, ROP=1.54, WOB=10 - 32, TOR_on=3.5 - 5, TOR_off=1.5 - 3, SPP_on=3,238 - 3,350, SPP_off=3,230 - 3,300, ECD=10.27 - 10.31, TEMP=53 - 54, BHP=8,304 - 8,376.
	4,770	4,771	4	
	4,771	4,774	1.16	
	4,774	4,792	1.85	
	4,792	4,802	1.28	
	4,802	4,808	1.85	
	4,808	4,810	1.14	
7	4,810	4,815	1.79	SO=538 - 539, PU=542 - 550, RAB=552 - 556, ROTARY SPEED=69 - 88, FLOW=300 - 547, ROP=1.47, WOB=40 - 45, TOR_on=2.7 - 5, TOR_off=2 - 3, SPP_on=4,030 - 4,139, SPP_off=3,990 - 4,120, ECD=10.27 - 10.3, TEMP=52 - 55, BHP=8,416 - 8,534.
	4,815	4,832	1.89	
	4,832	4,836	2.18	
	4,836	4,846	2.97	
	4,846	4,848	1.74	
	4,848	4,856	3	
	4,856	4,860	3.33	
	4,860	4,869	2.11	
	4,869	4,877	1.29	
	4,877	4,883	2.06	
	4,883	4,885	0.86	
	4,885	4,887	1.33	

Source: (BDEP, 2010; CDC, 2015).

Table 27 - Historical ROP and drilling parameters for the well # E - runs # 1, 2, 3, 4, 5 and 6.

Run #	Depth_i [m]	Depth_f [m]	ROP [m/ h]	Drilling parameters
1	4,665	4,697	1.84	SO=n/a, PU=n/a, RAB=n/a, ROTARY SPEED=60, FLOW=500 - 700, ROP=1.84, WOB=10 - 30, TOR_on=12 - 17, TOR_off=n/a, SPP_on=2,144, SPP_off=2,093, ECD=10.04 - 10.13, TEMP=44 - 49, BHP=7,300 - 7,800.
Coring	4,697	4,701	Coring	n/a
2	4,701	4,719	1.3	SO=n/a, PU=n/a, RAB=n/a, ROTARY SPEED=600 - 150, FLOW=745 - 807, ROP=1.3, WOB=50 - 70, TOR_on=14 - 17, TOR_off=n/a, SPP_on=2,550, SPP_off=2,583, ECD=10.08 - 10.29, TEMP=46 - 52, BHP=7,850 - 7,887.
	4,719	4,728	0.78	
	4,728	4,736	1	
	4,736	4,755	1.8	
Coring	4,755	4,766	Coring	n/a
3	4,766	4,769	2.93	SO=310, PU=350, RAB=320, ROTARY SPEED=110 - 150, FLOW=740, ROP=2.93, WOB=45 - 60, TOR_on=15 - 26, TOR_off=n/a, SPP_on=2,389, SPP_off=2,383, ECD=10.21 - 10.38, TEMP=47 - 59, BHP=8,100 - 8,221.
	4,769	4,781	2.67	
	4,781	4,818	3.08	
	4,818	4,843	2.08	
	4,843	4,867	2.05	
	4,867	4,856	2.17	
Coring	4,856	4,906	Coring	n/a
4	4,906	4,914	1.45	SO=295, PU=336, RAB=306, ROTARY SPEED=150, FLOW=740 - 750, ROP=2.93, WOB=30, TOR_on=17 - 36, TOR_off=2 - 3, SPP_on=2,340 - 2,400, SPP_off=2,343 - 2,345, ECD=10.28, TEMP=53 - 56, BHP=8,250 - 8,360.
	4,914	4,943	1.21	
	4,943	4,967	1.29	
5	4,967	4,989	0.99	SO=650, PU=740, RAB=675, ROTARY SPEED=150, FLOW=740, ROP=0.99, WOB=55 - 60, TOR_on=15 - 17, TOR_off=n/a, SPP_on=2,450, SPP_off=2,430, ECD=10.3 - 10.34, TEMP=58, BHP=8,300 - 8,385.
6	4,989	5,064	1.1	SO=n/a, PU=n/a, RAB=n/a, ROTARY SPEED=100 - 135, FLOW=740, ROP=1.1, WOB=55 - 60, TOR_on=15 - 36, TOR_off=n/a, SPP_on=2,400, SPP_off=2,388, ECD=10.25 - 10.32, TEMP=53 - 62, BHP=8,390 - 8,490.

Source: (BDEP, 2010; CDC, 2015).

Table 28 - Historical ROP and drilling parameters for the well # E - runs # 8, 9 and 10.

Run #	Depth_i [m]	Depth_f [m]	ROP [m/ h]	Drilling parameters
7	5,064	5,127	1.21	SO=n/a, PU=n/a, RAB=n/a, ROTARY SPEED=115 - 130, FLOW=740, ROP=1.21, WOB=55 - 65, TOR_on=15 - 17, TOR_off=n/a, SPP_on=2,450, SPP_off=2,432, ECD=10.23 - 10.36, TEMP=54 - 58, BHP=8,480 - 8,600.
8	5,127	5,223	1.15	SO=n/a, PU=n/a, RAB=n/a, ROTARY SPEED=100-120, FLOW=740, ROP=1.15, WOB=60, TOR_on=15-17, TOR_off=n/a, SPP_on=2,370, SPP_off=2,366, ECD=10.3, TEMP=52-54, BHP=8,610 - 8,750.
9	5,223	5,267	0.9	SO=n/a, PU=n/a, RAB=n/a, ROTARY SPEED=100 - 150, FLOW=730, ROP=0.9, WOB=60, TOR_on=15 - 18, TOR_offn/a, SPP_on=2,360, SPP_off=2,357, ECD=10.25 - 10.33, TEMP=55 - 56, BHP=8,780 - 8,815.
10	5,267 5,397 5,422 5,451 5,464	5,397 5,422 5,451 5,464 5,475	5 8.33 7.25 1.3 2.4	SO=320, PU=370, RAB=n/a, ROTARY SPEED=80 - 150, FLOW=730 - 821, ROP=4.3, WOB=20 - 35, TOR_on=16 - 30, TOR_off=n/a, SPP_on=3,296, SPP_off=3,285, ECD=10.21 - 10.3, TEMP=56 - 59, BHP=9,210.

Source: (BDEP, 2010; CDC, 2015).

Table 29 - Historical ROP and drilling parameters for the well # F - run # 1.

Run #	Depth_i [m]	Depth_f [m]	ROP [m/ h]	Drilling parameters
	4,899	4,902	2.4	
	4,902	4,905	1.56	
	4,905	4,908	1.17	
	4,968	4,975	4.42	
	4,975	4,994	3.02	
	4,994	4,996	1.6	
	4,996	5,001	3.38	
	5,001	5,011	3	
	5,011	5,026	2.94	
	5,026	5,043	4.95	
	5,043	5,045	3.08	
	5,045	5,054	4.74	
	5,054	5,056	3	SO=680 - 685, PU=775 - 795, RAB=715 - 735,
	5,056	5,061	5.88	ROTARY SPEED=80 - 140, FLOW=850 - 900, ROP=1.7,
1	5,061	5,074	5.65	WOB=15 - 50, TOR_on=22 - 29, TOR_off=15 - 19,
	5,074	5,084	8.11	SPP_on=2,620 - 3,090, SPP_off=2,605 - 3,075,
	5,084	5,093	4.15	ECD=9.74 - 10.59, TEMP=53 - 86, BHP=8,087 - 8,825.
	5,093	5,097	3.43	
	5,097	5,099	3.64	
	5,099	5,101	4.8	
	5,101	5,104	2.86	
	5,104	5,112	3.72	
	5,112	5,123	4.68	
	5,123	5,125	4.17	
	5,125	5,128	6	
	5,128	5,142	5.09	
	5,142	5,144	3.33	
	5,144	5,146	1.2	
	5,146	5,147	0.61	

Source: (BDEP, 2010; CDC, 2015).

Table 30 - Historical ROP and drilling parameters for the well # F - run # 2.

Run #	Depth_i [m]	Depth_f [m]	ROP [m/ h]	Drilling parameters
2	5,140	5,150	1	SO=680 - 735, PU=800 - 850, RAB=730 -790, ROTARY SPEED=90 - 140, FLOW=850, ROP=3.7, WOB=35 - 45, TOR_on=22 - 29, TOR_off=17 - 19, SPP_on=2,820 - 2,980, SPP_off=2,805 - 2,965, ECD=10.42 - 10.65, TEMP=61 - 70, BHP=8,879 - 9,727.
	5,150	5,170	12.25	
	5,170	5,176	3.43	
	5,176	5,206	9.5	
	5,206	5,221	5.29	
	5,221	5,234	5.78	
	5,234	5,264	7.79	
	5,264	5,283	8.5	
	5,283	5,293	6.45	
	5,293	5,319	6	
	5,319	5,327	9.2	
	5,327	5,333	15	
	5,333	5,344	7.86	
	5,344	5,350	10.29	
	5,350	5,361	8.8	
	5,361	5,380	9.5	
	5,380	5,396	8.89	
	5,396	5,408	7.83	
	5,408	5,437	8.92	
	5,437	5,450	10.54	
	5,450	5,464	8.16	
	5,464	5,471	10.5	
	5,471	5,495	8.14	
	5,495	5,514	8.51	
	5,514	5,525	6.17	
	5,525	5,553	8.75	
	5,553	5,582	9.5	
	5,582	5,583	7.52	
	5,583	5,593	8	
	5,593	5,611	8.57	
	5,611	5,616	13.64	
	5,616	5,636	7.41	
	5,636	5,640	2.89	
	5,640	5,644	4.62	
	5,644	5,650	6.2	
	5,650	5,652	9.8	
	5,652	5,669	5.33	
	5,669	5,675	10.59	
	5,675	5,699	5.5	
	5,699	5,706	2.73	
	5,706	5,727	2.99	
	5,727	5,731	3.12	
	5,731	5,738	3.44	
	5,738	5,739	3.14	

Source: (BDEP, 2010; CDC, 2015).

Table 31 - Historical ROP and drilling parameters for the well # H - runs # 1, 2, 3, 4, 5 and 6.

Run #	Depth_i [m]	Depth_f [m]	ROP [m/ h]	Drilling parameters
1	5,050	5,054	1.16	SO=566, PU=573, RAB=560, ROTARY SPEED=60 - 100, FLOW=750 - 800, ROP=1.5, WOB=25 - 50, TOR_on=16, TOR_off=9, SPP_on=1,500, SPP_off=1,400, ECD=9.92 - 9.94, TEMP=44, BHP=6,763 - 7,021.
	5,054	5,082	1.65	
Coring	5,082	5,123	Coring	n/a
Coring			Coring	n/a
2	5,123	5,198	5.29	SO=653 - 665, PU=660 - 680, RAB=656 - 665, ROTARY SPEED=120 - 130, FLOW=800, ROP=3.22, WOB=5 - 25, TOR_on=6 - 14,25, TOR_off=3, SPP_on=2,804, SPP_off=2,800, ECD=10.5, TEMP=59, BHP=9,271.
3	5,198	5,198	2.4	SO=665 - 670, PU=660 - 700, RAB=668 - 672, ROTARY SPEED=80 - 120, FLOW=800, ROP=2, WOB=10 - 20, TOR_on=8 - 12, TOR_off=3.6 - 4.5, SPP_on=2,720, SPP_off=2,700, ECD=10.12, TEMP=60, BHP=8,991.
	5,198	5,257	3.9	
	5,257	5,260	2	
	5,272	5,286	0.77	
	5,286	5,287	0.26	
4	5,287	5,302	2.24	SO=667 - 680, PU=677 - 700, RAB=665 - 685, ROTARY SPEED=120 - 140, FLOW=600 - 612, ROP=2.58, WOB=10 - 25, TOR_on=9 - 20, TOR_off=3 - 7, SPP_on=1,780, SPP_off=1,760, ECD=9.84, TEMP=55, BHP=8,907.
	5,302	5,317	6.6	
	5,317	5,320	1.31	
	5,320	5,326	0.81	
5	5,326	5,333	3.26	SO=700, PU=708.5, RAB=n/a, ROTARY SPEED=80 - 100, FLOW=600 - 610, ROP=2.3, WOB=24.5 - 45, TOR_on=5 - 10, TOR_off=3.34, SPP_on=1,802, SPP_off=892, ECD=9.93, TEMP=53.5, BHP=9,042.
	5,333	5,343	1.67	
	5,343	5,365	1.83	
	5,365	5,378	2.17	
	5,378	5,440	3	
6	5,440	5,456	1.38	SO=705, PU=715, RAB=n/a, ROTARY SPEED=80 - 100, FLOW=600 - 610, ROP=2.11, WOB=25 - 55, TOR_on=6, TOR_off=4.25, SPP_on=1,820, SPP_off=1,810, ECD=n/a, TEMP=54.5, BHP=9,189.
	5,456	5,464	0.99	
	5,464	5,473	0.69	
	5,473	5,479	0.66	

Source: (BDEP, 2010; CDC, 2015).

Table 32 - Historical ROP and drilling parameters for the well # H - runs # 7, 8 and 9.

Run #	Depth_i [m]	Depth_f [m]	ROP [m/ h]	Drilling parameters
	5,479	5,491	2.43	
	5,491	5,505	1.59	SO=698 - 712,5, PU=720, RAB=n/a,
	5,505	5,510	2.46	ROTARY SPEED=110 - 150, FLOW=615, ROP=0,8,
7	5,510	5,524	1.1	WOB=25 - 42, TOR_on=7 - 18, TOR_off=4,5 - 6,
	5,524	5,525	0.81	SPP_on=1.923 - 1.915, SPP_off=1.915 - 1.923,
	5,525	5,527	1.02	ECD=9,86, TEMP=58 - 59,5, BHP=9.258 - 9.318.
	5,527	5,535	0.77	
	5,535	5,570	2.89	
	5,570	5,575	1.44	
	5,576	5,583	0.99	
	5,583	5,594	0.96	
	5,594	5,598	0.82	
	5,598	5,607	0.94	
	5,607	5,620	0.88	SO=780 - 715, PU=790 - 720, RAB=n/a,
	5,620	5,627	1.17	ROTARY SPEED=137 - 160, FLOW=600 - 705, ROP=1,
8	5,627	5,665	5.33	WOB=24 - 46, TOR_on=7 - 16, TOR_off=6,6 - 10,
	5,665	5,650	3.08	SPP_on=1.880 - 2.489, SPP_off=1.880 - 2.482,
	5,650	5,656	0.95	ECD=n/a, TEMP=59,5 - 61, BHP=9.359 - 9.621.
	5,656	5,665	1.53	
	5,665	5,677	1.97	
	5,677	5,681	0.85	
	5,681	5,693	1.8	
	5,694	5,698	1.09	
	5,698	5,702	1.07	
	5,702	5,706	1.37	
	5,706	5,766	4.14	SO=780 - 715, PU=790 - 720, RAB=n/a,
	5,766	5,794	4.67	ROTARY SPEED=137 - 160, FLOW=600 - 705, ROP=1,
9	5,794	5,804	1.15	WOB=24 - 46, TOR_on=7 - 16, TOR_off=6.6 - 10,
	5,804	5,825	2.33	SPP_on=1,880 - 2,489, SPP_off=1,880 - 2,482,
	5,825	5,831	1	ECD=n/a, TEMP=59.5 - 61, BHP=9,359 - 9,621.
	5,831	5,840	1.31	

Source: (BDEP, 2010; CDC, 2015).

APPENDIX B - HISTORICAL PRE-SALT DRILL-BIT RECORD

All tables presented in this Appendix B (Table 33, Table 34, Table 35, Table 36, Table 37, Table 38, Table 39, Table 40, Table 41, Table 42, Table 43, Table 44, Table 45 and Table 46) are related to the historical bit-records and performance gathered from the pre-salt wells under analysis. These data support the summarized tables presented throughout the thesis aiming a statistical understanding about the different drill-bits usage within the pre-salt operations. The abbreviation *n/a* presented in the tables represents information that were not available.

Table 33 - Drill-bit performance and record for the well # A - runs # 1, 2 and 3.

Run #	Drill-bit					BHA		Interval
	Size [in]/ length [m]	**TFA [in²]/ nozzles [in]**	**Type/ IADC code/ Vendor nomeclature**	**Dull grading/ observation/ POOH motive**	**Footage [m]/ rev [k-rev]/ TBRT [h]/ tripping/ [h]/ pumping [h]/ rotary [h]**	**Tools**	**Boundary [lower-upper]**	**MD [m]/ TVD [m]/ INC [º]/ AZIM [º]**
1	8.5/ 0.32	1.208/ 7 * 15	PDC/ M232/ MDSi716	4-2-CD-N-E-I-BT-PR/ cutter delimitation in the nose and broken teeth-cutters, in gauge/ POOH x ROP	135/ 262/ 117.5/ 56/ 54.5/ 54.5	MWD LWD STAB	400 - 800 [gpm] n/a n/a	3,993 - 4,128/ 3,991 - 4,125/ 0.34 - 0.34/ 308 - 308
2	8.5/ 0.31	0.798/ 2 * 14, 2 * 18	Hybrid (PDC-TCI)/ n/a/ HP524	2-1-CT-A-E-I-NO-PR/ chipped teeth-cutters in all area, in gauge/ POOH x ROP	37.7/ 205/ 100.25/ 19.98/ 37.95/ 31.02	MWD LWD STAB	400 - 800 [gpm] n/a n/a	4,128 - 4,166/ 4,125 - 4,165/ 0.34 - 0.09/ 308 - 121
3	8.5/ 0.25	1.043/ 4 * 14, 4 * 12	Hybrid (PDC-TCI)/ M432/ KH813M	2-1-CT-A-X-I-BT-TD/ chipped and broken teeth-cutters in all area, in gauge/ POOH x Well TD	29.3/ 230/ 64.37/ 27.12/ 35.68/ 34.92	MWD LWD STAB	400 - 800 [gpm] n/a n/a	4,166 - 4,195/ 4,165 - 4,193/ 0.09 - 1.02/ 120.99 - 101.44

Source: (BDEP, 2010; CDC, 2015).

Table 34 - Drill-bit performance and record for the well # B - runs # 1, 2 and 3.

Run #	Drill-bit					BHA		Interval
	Size [in]/ length [m]	**TFA [in²]/ nozzles [in]**	**Type/ IADC code/ Vendor nomeclature**	**Dull grading/ observation/ POOH motive**	**Footage [m]/ rev [k-rev]/ TBRT [h]/ tripping/ [h]/ pumping [h]/ rotary [h]**	**Tools**	**Boundary [lower-upper]**	**MD [m]/ TVD [m]/ INC [º]/ AZIM [º]**
1	12.25/ 0.37	0.9027/ 7 * 12, 1 * 13	PDC/ M321/ MDSiZ816-LPBX	0-1-CT-N-X-I-BT-CP/ chipped and broken teeth-cutters in the nose, in gauge/ POOH x coring	102/ 266/ 117.75/ 32.08/ 69.3/ 42.9	MWD LWD STAB	400 - 800 [gpm] n/a n/a	3,405 - 3,507/ 3,403 - 3,505/ 3.35 - 2.94/ 114.96 - 116.6
Coring								3,507 - 3,536
2	12.25/ 0.41	0.969/ 3 * 14, 3 * 15	Hydbrid (PDC-TCI)/ M132/ KM533X	6-6-BT-A-X-I-ER-CP/ broken teeth-cutters and erosion, in gauge/ POOH x coring	153/ 223/ 94.5/ 34.07/ 60.35/ 48.5	MWD LWD STAB	400 - 800 [gpm] n/a n/a	3,536 - 3,689/ 3,534 - 3,687/ 2.68 - 2.27/ 121.99 - 121.14
Coring								3,689 - 3,709
3	12.25/ 0.28	0.9027/ 7 * 12, 1 * 13	PDC/ M243/ MDSi816	1-1-WT-S-X-I-CT-TD/ worn and chipped teeth-cutters, in gauge/ POOH x Well TD	163/ 512/ 93.75/ 24.34/ 67.21/ 61	MWD LWD STAB	400 - 800 [gpm] n/a n/a	3,709 - 3,872/ 3,707 - 3,870/ 2.2 - 1.93/ 121.9 - 110.28

Source: (BDEP, 2010; CDC, 2015).

Table 35 - Drill-bit performance and record for the well # C - runs # 1, 2 and 3.

Run #	Drill-bit					BHA		Interval
	Size [in]/ length [m]	**TFA [in²]/ nozzles [in]**	**Type/ IADC code/ Vendor nomeclature**	**Dull grading/ observation/ POOH motive**	**Footage [m]/ rev [k-rev]/ TBRT [h]/ tripping/ [h]/ pumping [h]/ rotary [h]**	**Tools**	**Boundary [lower-upper]**	**MD [m]/ TVD [m]/ INC [º]/ AZIM [º]**
1	12.25/ 0.28	1.052/ 7 * 14	PDC/ M323/ MDSi716-LBPX	1-2-CT-S-XI-WT-CP/ chipped and worn teeth-cutters, in gauge/ POOH x coring	78/ 227/ 113.5/ 33.1/ 57.27/ 18	MWD LWD RSS	600 - 1,200 [gpm] n/a 450 - 1,550 [gpm]	4,487 - 4,565/ 4,350 - 4,416/ 34.66 - 34.73/ 148.36 - 150.09
Coring								4,565 - 4,568
2	12.25/ 0.41	0.969/ 3 * 15, 3 * 14	Hybrid/ n/a/ KM533X	5-6-BT-A-X-I-WT-PR (PDC), 1-5-WT-G-E-I-CT-PR (TCI)/ broken and two worn teeth-cutters, worn and chipped teeth-cutters, in gauge/ POOH x ROP	194/ 447/ 128/ 29.5/ 97.89/ 81.33	MWD LWD RSS	600 - 1,200 [gpm] n/a 450 - 1,550 [gpm]	4,568 - 4,762/ 4,442 - 4,578/ 34.74 - 34.9/ 149.47 - 150.8
3	12.25/ 0.41	0.969/ 3 * 15, 3 * 14	Hybrid/ n/a/ KM533X	n/a/ n/a/ POOH x ROP	193/ 444/ 144.25/ 40.58/ 103.6/ 92.44	MWD LWD RSS	600 - 1,200 [gpm] n/a 450 - 1,550 [gpm]	4,762 - 4,955/ 4,578 - 4,736/ 34.9 - 34.74/ 150.8 - 149.54

Source: (BDEP, 2010; CDC, 2015).

Table 36 - Drill-bit performance and record for the well # C - runs # 4 and 5.

Run #	Drill-bit					BHA		Interval
	Size [in]/ length [m]	**TFA [in²]/ nozzles [in]**	**Type/ IADC code/ Vendor nomeclature**	**Dull grading/ observation/ POOH motive**	**Footage [m]/ rev [k-rev]/ TBRT [h]/ tripping/ [h]/ pumping [h]/ rotary [h]**	**Tools**	**Boundary [lower-upper]**	**MD [m]/ TVD [m]/ INC [º]/ AZIM [º]**
4	12.25/ 0.28	0.8836/ 8 * 12	PDC/ n/a/ MDSi816-LBPX	n/a/ n/a/ POOH x change BHA	92/ 580/ 115/ 32.91/ 81.96/ 73.53	MWD LWD STAB	600 - 1,200 [gpm] n/a n/a	4,955 - 5,047/ 4,736 - 4,809/ 34.74 - 38.16/ 149.54 - 150.54
5	12.25/ 0.41	1.034/ 4 * 11, 6 * 12	PDC/ M423/ QD507-FHX	1-1-CT-S-X-I-NO-TD/ chipped teeth-cutters, in gauge/ POOH x Well TD	266/ 462/ 114.25/ 35.16/ 78.21/ 54.98	MWD LWD RSS	600 - 1,200 [gpm] n/a 450 - 1,550 [gpm]	5,047 - 5,313/ 4,809 - 5,055/ 38.16 - 34.10/ 150.54 - 148.27

Source: (BDEP, 2010; CDC, 2015).

Table 37 - Drill-bit performance and record for the well # D - runs # 1, 2 and 3.

Run #	Drill-bit					BHA		Interval
	Size [in]/ length [m]	**TFA [in²]/ nozzles [in]**	**Type/ IADC code/ Vendor nomeclature**	**Dull grading/ observation/ POOH motive**	**Footage [m]/ rev [k-rev]/ TBRT [h]/ tripping/ [h]/ pumping [h]/ rotary [h]**	**Tools**	**Boundary [lower-upper]**	**MD [m]/ TVD [m]/ INC [º]/ AZIM [º]**
1	8.5/ 0.29	0.8836/ 8 * 12	PDC/ M433/ n/a	7-2-RO-N-X-I-BT-PR/ ring-out in the nose, broken teeth-cutters, in gauge/ POOH x ROP	146/ 352/ 115.3/ 24.5/ 64.31/ 46.9	MWD LWD STAB	300 - 600 [gpm] n/a n/a	4,400 - 4,546/ 4,400 - 4,546/ 1.48 - 2.16/ 237.87 - 210.43
2	8.5/ 0.39	0.7777/ 6 * 13	PDC/ M433/ n/a	7-4-CT-C-X-1-LT-PR/ chipped and lost teeth-cutters, 0.0625 [in] under gauge/ POOH x ROP	46/ 70/ 62/ 25.33/ 33.99/ 19.15	MWD LWD TURB	300 - 600 [gpm] n/a 342 - 610 [gpm]	4,546 - 4,592/ 4,546 - 4,592/ 2.16 - 1.75/ 210.43 - 213.58
3	8.5/ 0.42	n/a/ n/a	Diamond impregnated/ M842/ TBPXC	2-6-WT-A-X-I-LT-PR/ worn and lost teeth-cutters, in gauge/ POOH x ROP	64/ 80/ 65.5/ 25.61/ 35.82/ 25.2	MWD LWD TURB	300 - 600 [gpm] n/a 342 - 610 [gpm]	4,592 - 4,656/ 4,592 - 4,666/ 1.75 - 1.73/ 213.58 - 197.20

Source: (BDEP, 2010; CDC, 2015).

Table 38 - Drill-bit performance and record for the well # D - runs # 4, 5, 6 and 7.

Run #	Drill-bit					BHA		Interval
	Size [in]/ length [m]	**TFA [in^2]/ nozzles [in]**	**Type/ IADC code/ Vendor nomeclature**	**Dull grading/ observation/ POOH motive**	**Footage [m]/ rev [k-rev]/ TBRT [h]/ tripping/ [h]/ pumping [h]/ rotary [h]**	**Tools**	**Boundary [lower-upper]**	**MD [m]/ TVD [m]/ INC [º]/ AZIM [º]**
4	8,5/ 0,24	0,8222/ 3 * 18, 1 * 10	TCI/ 882/ MXL-C20DX	2-1-WT-A-X-I-NO-PR worn teeth-cutters, in gauge/ POOH x ROP	40/ 67/ 50,5/ 25,17/ 24,22/ 17,3	MWD LWD STAB	300 - 600 [gpm] n/a n/a	4,656 - 4,696/ 4,666 - 4,696/ 1.73 - 2.04/ 197.2 - 192.75
5	8,5/ 0,42	0,5185/ 4 * 13	Diamond impregnated/ M842/ TBPXC	4-8-RO-S-X-I-HC-PR/ ring-out and heated, in gauge/ POOH x ROP	54/ 56/ 59,58/ 23,75/ 33,58/ 23,58	MWD LWD TURB	400 - 800 [gpm] n/a 342 - 610 [gpm]	4,696 - 4,750/ 4,696 - 4,722/ 2.04 - 2.04/ 192.75 - 192.45
6	8,5/ 0,24	0,4479/ 1 * 10, 1 * 14, 2 * 12	TCI/ 537/ MX-C30DX	4-8-BT-G-E-3-CT-PR/ broken and chipped teeth-cutters, 0,1875 [in] under guage, sealed bearing/ POOH x ROP	60/ 130/ 63,17/ 25,75/ 35,21/ 29,61	MWD LWD STAB	400 - 800 [gpm] n/a n/a	4,750 - 4,810/ 4,722 - 4,800/ 2.04 - 2.41/ 192.45 - 192.57
7	8,5/ 0,24	0,3313/ 3 * 12	TCI/ 517/ MX-C20DX	1-1-BT-A-E-I-CT- TD broken and chipped teeth-cutters, in gauge, sealed bearing/ POOH x logging-TD	77/ 117/ 78,33/ 24,12/ 52,17/ 37,41	MWD LWD STAB	400 - 800 [gpm] n/a n/a	4,810 - 4,887/ 4,800 - 4,887/ 2.41 - 1.94/ 192.57 - 167.95

Source: (BDEP, 2010; CDC, 2015).

Table 39 - Drill-bit performance and record for the well # E - runs # 1, 2 and 3.

Run #	Drill-bit					BHA		Interval
	Size [in]/ length [m]	**TFA [in²]/ nozzles [in]**	**Type/ IADC code/ Vendor nomeclature**	**Dull grading/ observation/ POOH motive**	**Footage [m]/ rev [k-rev]/ TBRT [h]/ tripping/ [h]/ pumping [h]/ rotary [h]**	**Tools**	**Boundary [lower-upper]**	**MD [m]/ TVD [m]/ INC [º]/ AZIM [º]**
1	10.63/ 0.31	0.8498/ 3 * 12, 4 * 13	PDC/ M333/ MDSi716	4-2-CR-C,N-X-I-BT-CP/ cored properties in medium level, in gauge/ POOH x coring	32/ 97/ 88/ 26.5/ 53.93/ 26.9	MWD LWD RSS	400 - 800 [gpm] n/a n/a	4,665 - 4,697/ 4,505 - 4,534/ 22.45 - 22.45/ 342.83 - 342.24
Coring								4,697 - 4,701
2	10.63/ 0.31	0.9204/ 3 * 0	TCI/ 617/ HE44D3MRZ	1-1-WT-A-E-I-NO-CP/ worn and broken teeth-cutters in all area, in gauge/ POOH x coring	54/ 333/ 86.5/ 26.45/ 59.7/ 50.03	MWD LWD HI-STAB	600 - 1,200 [gpm] n/a n/a	4,701 - 4,755/ 4,538 - 4,588/ 22.45 - 22.4/ 342.24 - 342.2
Coring								
3	Clear information not provided.							4,755 - 4,906
Coring								

Source: (BDEP, 2010; CDC, 2015).

Table 40 - Drill-bit performance and record for the well # E - runs # 4, 5 and 6.

Run #	Drill-bit					BHA		Interval
	Size [in]/ length [m]	**TFA [in²]/ nozzles [in]**	**Type/ IADC code/ Vendor nomeclature**	**Dull grading/ observation/ POOH motive**	**Footage [m]/ rev [k-rev]/ TBRT [h]/ tripping/ [h]/ pumping [h]/ rotary [h]**	**Tools**	**Boundary [lower-upper]**	**MD [m]/ TVD [m]/ INC [º]/ AZIM [º]**
4	10.63/ 0.31	0.9204/ 3 * 20	TCI/ 617/ HE44D3MRZ	1-1-WT-A-E-I-NO-PR/ worn teeth-cutters in all area, in gauge/ POOH x ROP	61/ 540/ 50.5/ n/a/ 34.6/ 29.5	MWD LWD HI-STAB	600 - 1,200 [gpm] n/a n/a	4,906 - 4,967/ 4,732 - 4,744/ 18.12 - 17.43/ 334.02 - 330.22
5	10.63/ 0.27	0.9204/ 3 * 20	TCI/ 517/ F15HUB-PX1153	4-2-BT-A-N-1-LT-PR broken and lost teeth-cutters in all area, 0,0625 [in] under gauge/ POOH x ROP	23/ 540/ 53/ n/a/ n/a/ 23.23	MWD LWD HI-STAB	600 - 1,200 [gpm] n/a n/a	4,967 - 4,989/ 4,744 - 4,802/ 17.43 - 17.42/ 330.22 - 328.58
6	10.63/ 0.27	n/a/ n/a	TCI/ 617/ HE44D3MRZ	8-1-CR-N-F-I-LT-PR bearing seals failed and with fourteen missing TCI teeth in the nose part of the bit/ POOH x ROP	75/ 487/ 101/ n/a/ n/a/ 68.9	MWD LWD HI-STAB	600 - 1,200 [gpm] n/a n/a	4,989 - 5,064/ 4,802 - 4,870/ 17.42 - 17.04/ 328.58 - 324

Source: (BDEP, 2010; CDC, 2015).

Table 41 - Drill-bit performance and record for the well # E - runs # 7, 8, 9 and 10.

Run #	Drill-bit					BHA		Interval
	Size [in]/ length [m]	**TFA [in²]/ nozzles [in]**	**Type/ IADC code/ Vendor nomeclature**	**Dull grading/ observation/ POOH motive**	**Footage [m]/ rev [k-rev]/ TBRT [h]/ tripping/ [h]/ pumping [h]/ rotary [h]**	**Tools**	**Boundary [lower-upper]**	**MD [m]/ TVD [m]/ INC [º]/ AZIM [º]**
7	10.63/ 0.31	0.9204/ 3 * 20	TCI/ 617/ HE44D3MRZ	2-1-BT-G-E-I-NO-HR/ broken teeth-cutters, in gauge/ POOH x drill-bit hours	63/ 397/ 86/ n/a/ n/a/ 52.07	MWD LWD HI STAB	400 - 800 [gpm] n/a n/a	5,064 - 5,127/ 4,870 - 4,959/ 17.04 - 17.15/ 324 - 319/
8	10.63/ 0.31	0.9204/ 3 * 20	TCI/ 617/ HE44D3MRZ	1-1-CT-M-E-I-NO-HR/ chipped teeth-cutters, in gauge/ POOH x drill-bit hours	96/ 627/ 152/ n/a/ n/a/ 83.48	MWD LWD HI-STAB	400 - 800 [gpm] n/a n/a	5,127 - 5,223/ 4,959 - 5,031/ 17.15 - 17.38/ 319 - 318.3
9	10.63/ 0.28	0.9204/ 3 * 20	TCI/ 517/ MX-20GDX	8-8-BT-A-E-I-CT-PR/ broken and chipped teeth-cutter with severe damage and a lot of broken teeth in inner three rows, being two teeth lost, in gauge/ POOH x ROP	44/ 330/ 95/ n/a/ n/a/ 48.89	MWD LWD HI-STAB	400 - 800 [gpm] n/a n/a	5,223 - 5,267/ 5,031 - 5,075/ 17.38 - 17.59/ 318.3 - 317.25
10	10.63/ 0.34	n/a/ n/a	PDC/ M4333/ HCM408Z	2-1-WT-C-X-I-BT-TD/ worn and broken teeth-cutters, in gauge/ POOH x Well TD	208/ 1,435/ 95.17/ 29.1/ 66/ 51.91	MWD LWD HI-STAB	400 - 800 [gpm] n/a n/a	5,267 - 5,475/ 5,075 - 5,273/ 17.59 - 19.63/ 317.25 - 312.19

Source: (BDEP, 2010; CDC, 2015).

Table 42 - Drill-bit performance and record for the well # F - runs # 1 and 2.

Run #	Drill-bit					BHA		Interval
	Size [in]/ length [m]	**TFA [in²]/ nozzles [in]**	**Type/ IADC code/ Vendor nomeclature**	**Dull grading/ observation/ POOH motive**	**Footage [m]/ rev [k-rev]/ TBRT [h]/ tripping/ [h]/ pumping [h]/ rotary [h]**	**Tools**	**Boundary [lower-upper]**	**MD [m]/ TVD [m]/ INC [º]/ AZIM [º]**
1	12.25/ 0.44	1.037/ 8 * 13	PDC/ M111/ 508FHX	n/a/ n/a/ n/a	248/ 1,786/ 155.17/ 40.05/ 102.52/ 68.62	MWD LWD RSS	600 - 1,200 [gpm] n/a 460 - 1,600 [gpm]	4,899 - 5,147/ 4,696 - 4,927/ 23.45 - 21.78/ 205.16 - 207.38
2	12.25/ 0.28	1.011/ 2 * 13, 5 * 14	PDC/ M223/ MDSi2716	1-2-WT-T-NO-I-NO-TD/ worn teeth-cutters, sealed bearings, in gauge/ POOH x Well TD	95/ 627/ 172.72/ 43.43/ 98.22/ 82	MWD LWD RSS	600 - 1,200 [gpm] n/a 600 - 1,200 [gpm]	5,147 - 5,739/ 4,927 - 5,478/ 21.78 - 21.24/ 207.38 - 206.34

Source: (BDEP, 2010; CDC, 2015).

Table 43 - Drill-bit performance and record for the well # G.

Run #	Drill-bit					BHA		Interval
	Size [in]/ length [m]	**TFA [in²]/ nozzles [in]**	**Type/ IADC code/ Vendor nomeclature**	**Dull grading/ observation/ POOH motive**	**Footage [m]/ rev [k-rev]/ TBRT [h]/ tripping/ [h]/ pumping [h]/ rotary [h]**	**Tools**	**Boundary [lower-upper]**	**MD [m]/ TVD [m]/ INC [º]/ AZIM [º]**
n/a	12.25/ 0.41	13/ 3 * 14, 5 * 12	Hybrid (PDC-TCI)/ M423/ MDSi816-LBPX, KM633X	n/a/ n/a/ n/a	n/a/ n/a/ n/a/ n/a/ n/a/ n/a	LWD MWD LWD RSS	20 - 150 [rpm] n/a n/a 400 - 1,500 [gpm]	5,255 - 5,600/ 5,234 - 5,560/ 1.01 - 2.05/ 217.92 - 247

Source: (BDEP, 2010; CDC, 2015).

Table 44 - Drill-bit performance and record for the well # H - runs # 1, 2 and 3.

	Drill-bit					BHA		Interval
Run #	**Size [in]/ length [m]**	**TFA [in²]/ nozzles [in]**	**Type/ IADC code/ Vendor nomeclature**	**Dull grading/ observation/ POOH motive**	**Footage [m]/ rev [k-rev]/ TBRT [h]/ tripping/ [h]/ pumping [h]/ rotary [h]**	**Tools**	**Boundary [lower-upper]**	**MD [m]/ TVD [m]/ INC [º]/ AZIM [º]**
1	12.25/ 0.32	1.227/ 4 * 20	TCI/ 537X/ GFi30B	2-7-BT-G-E-1-WT-CP/ broken and worn teeth-cutters, 0.0625 [in] under gauge/ POOH x coring	32/ 93.02/ n/a/ 35.33/ n/a/ 19.38	MWD LWD LWD STAB	600 - 1,200 [gpm] n/a n/a n/a	5,050 - 5,082/ 5,050 - 5,082/ 0.06 - 0.32/ 43.2 - 43.28
Coring								5,082 - 5,084
Coring								5,084 - 5,123
2	12.25/ 0.3	1.203/ 8 * 14	PDC/ M323/ MDSi816	0-2-BT-T-X-I-NO-LOG/ broken teeth-cutters, in gauge/ POOH x logging	75/ 110.25/ 116.08/ 36.78/ 36.54/ 14.7	LWD MWD LWD STAB	20 - 150 [rpm] 600 - 1,200 [gpm] n/a n/a	5,123 - 5,198/ 5,123 - 5,198/ 0.41 - 0.49/ 41.5 - 32.6
3	12.25/ 0.3	1.203/ 8 * 14	PDC/ M323/ MDSi816	8-8-RO-N-X-1-CR-PR/ ring-out and coring characteristics, 0.0625 [in] under gauge/ POOH x ROP	89/ 253.5/ 190.5/ 48/ 89.24/ 42.25	LWD MWD LWD STAB	20 - 150 [rpm] 600 - 1,200 [gpm] n/a n/a	5,198 - 5,287/ 5,198 - 5,287/ 0.49 - 0.81/ 32.6 - 10.85

Source: (BDEP, 2010; CDC, 2015).

Table 45 - Drill-bit performance and record for the well # H - runs # 4, 5 and 6.

Run #	Drill-bit					BHA		Interval
	Size [in]/ length [m]	**TFA [in²]/ nozzles [in]**	**Type/ IADC code/ Vendor nomeclature**	**Dull grading/ observation/ POOH motive**	**Footage [m]/ rev [k-rev]/ TBRT [h]/ tripping/ [h]/ pumping [h]/ rotary [h]**	**Tools**	**Boundary [lower-upper]**	**MD [m]/ TVD [m]/ INC [º]/ AZIM [º]**
4	12.25/ 0.29	0.963/ 6 * 12, 2 * 14	PDC/ M333/ MDSi813	7-5-WT-T-X-1-BT-PR/ worn and broken teeth-cutters, 0.0625 [in] under gauge/ POOH x ROP	39/ 136.34/ 82/ 38.14/ 42.35/ 17.48	LWD MWD LWD STAB	20 - 150 [rpm] 600 - 1,200 [gpm] n/a n/a	5,287 - 5,326/ 5,287 - 5,326/ 0.81 - 1.48/ 10.85 - 275
5	12.25/ 0.32	1.227/ 4 * 20	TCI/ 617Y/ GF47Y	3-8-BT-A-E-4-WT-PR/ broken and worn teeth-cutters, 0.25 [in] under gauge/ POOH x ROP	114/ n/a/ n/a/ 44.1/ n/a/ 2.3	LWD MWD LWD STAB	20 - 150 [rpm] 600 - 1,200 [gpm] n/a n/a	5,326 - 5,440/ 5,326 - 5,440/ 1.48 - 1.91/ 275 - 252.92
6	12.25/ 0.31	1.227/ 4 * 20	TCI/ 617Y/ GF47Y	2-7-BT-G-E-1-CT-PR/ broken and chipped teeth-cutters, 0.0625 [in] under gauge/ POOH x ROP	39/ 226.85/ 95.45/ 36/ 69.83/ 42.01	LWD MWD LWD STAB	20 - 150 [rpm] 600 - 1,200 [gpm] n/a n/a	5,440 - 5,479/ 5,440 - 5,468/ 1.91 - 2.10/ 252.92 - 257.08

Source: (BDEP, 2010; CDC, 2015).

Table 46 - Drill-bit performance and record for the well # H - runs # 7, 8 and 9.

Run #	Drill-bit					BHA		Interval
	Size [in]/ length [m]	**TFA [in²]/ nozzles [in]**	**Type/ IADC code/ Vendor nomeclature**	**Dull grading/ observation/ POOH motive**	**Footage [m]/ rev [k-rev]/ TBRT [h]/ tripping/ [h]/ pumping [h]/ rotary [h]**	**Tools**	**Boundary [lower-upper]**	**MD [m]/ TVD [m]/ INC [º]/ AZIM [º]**
7	12.25/ 0.29	n/a/ n/a	PDC/ n/a/ MDSi816	5-4-CT-S-X-1-WT-PR/ chipped and worn teeth-cutters, 0.0625 [in] under gauge/ POOH x ROP	56/ 306.85/ 102.25/ 54.32/ 56.44/ 39.34	LWD MWD LWD STAB	20 - 150 [rpm] 600 - 1,200 [gpm] n/a n/a	5,479 - 5,535/ 5,479 - 5,535/ 2.1 - 3.5/ 257.08 - 251.53
8	12.25/ 0.3	n/a/ n/a	PDC/ M323/ MDSi816-LEBPX	4-4-BT-A-X-1-WT-PR broken and worn teeth-cutters, 0.0625 [in] under gauge/ POOH x ROP	167/ 987.67/ 158.25/ 53.6/ 127.62/ 110.85	LWD MWD LWD STAB	20 - 150 [rpm] 600 - 1,200 [gpm] n/a n/a	5,535 - 5,702/ 5,535 - 5,701/ 3.5 - 7.72/ 251.53 - 271.31
9	12,25/ 0.31	0.9457/ 2 * 14, 5 * 12, 1 * 11	PDC/ M323/ MDSi816-LEBPX	1-3-CT-S-X-I-WT-TD/ chipped and worn teeth-cutters, in gauge/ POOH x Well TD	138/ 452.07/ 99.5/ 30.05/ 61.84/ 48.61	LWD MWD LWD STAB	20 - 150 [rpm] 600 - 1,200 [gpm] n/a n/a	5,702 - 5,840/ 5,701 - 5,838/ 7.72 - 7.15/ 271.31 - 265.03

Source: (BDEP, 2010; CDC, 2015).